UT GSBS Dissertations and Theses (Open Access) Graduate School of Biomedical Sciences

12-2011

FUNCTION OF ZNF668 IN CANCER DEVELOPMENT

Ruozhen Hu

Recommended Citation

FUNCTION OF ZNF668 IN CANCER DEVELOPMENT

By

Ruozhen Hu, M.S.

APPROVED:

_____

Supervisory Professor, Shiaw-Yih Lin, Ph.D.

_____

Michelle Barton, Ph.D.

_____

Chengming Zhu, Ph.D.

_____

Ju-Seog Lee, Ph.D.

_____

Randy Legerski, Ph.D.

APPROVED:

_____

Dean, The University of Texas
Graduate School of Biomedical Sciences at Houston

FUNCTION OF ZNF668 IN CANCER DEVELOPMENT

A

DISSERTATION

Presented to the Faculty of
The University of Texas
Health Science Center at Houston
and
The University of Texas
M.D. Anderson Cancer Center
Graduate School of Biomedical Sciences
In Partial Fulfillment

of the Requirements

for the Degree of

DOCTOR OF PHILOSOPHY

By

Ruozhen Hu, M.S.

Houston, Texas
December, 2011

ACKNOWLEDGEMENTS

FUNCTION OF ZNF668 IN CANCER DEVELOPMENT

Ruozhen Hu, M.S.

Supervisory Professor: Shiaw-Yih Lin, Ph.D.

Human cancer develops as a result of accumulation of mutations in oncogenes and tumor suppressor genes. *Zinc finger protein 668 (ZNF668)* has recently been identified and validated as one of the highly mutated genes in breast cancer, but its function is entirely unknown. Here, we report two major functions of ZNF668 in cancer development.

(1) ZNF668 functions as a tumor suppressor by regulating p53 protein stability and function. We demonstrate that ZNF668 is a nucleolar protein that physically interacts with both MDM2 and p53. By binding to MDM2, ZNF668 regulates MDM2 autoubiquitination and prevents MDM2-mediated p53 ubiquitination and degradation; ZNF668 deficiency impairs DNA damage-induced p53 stabilization. Notably, ZNF668 effectively suppresses breast cancer cell proliferation and transformation *in vitro* and tumorigenicity *in vivo*. Consistently, ZNF668 knockdown readily transforms normal mammary epithelial cells. Together, our studies identify *ZNF668* as a novel breast tumor suppressor gene that acts at least in part by regulating the stability and function of p53.

(2) ZNF668 functions as a DNA repair protein by regulating histone acetylation. DNA repair proteins need to access the chromatin by chromatin

modification or remodeling to use DNA template within chromatin. Dynamic posttranslational modifications of histones are critical for cells to relax chromatin in DNA repair. However, the precise underlying mechanism mediating enzymes responsible for these modifications and their recruitment to DNA lesions remains poorly understood. We observed ZNF668 depletion causes impaired chromatin relaxation as a result of impaired DNA-damage induced histone H2AX hyper-acetylation. This results in the decreased recruitment of repair proteins to DNA lesions, defective homologous recombination (HR) repair and impaired cell survival after DNA damage, albeit with the presence of a functional ATM/ATR dependent DNA-damage signaling cascade. Importantly, the impaired loading of repair proteins and the defect in DNA repair in ZNF668-deficient cells can be counteracted by chromatin relaxation, indicating that the DNA-repair defect that was observed in the absence of ZNF668 is due to impeded chromatin accessibility at sites of DNA breaks. Our findings therefore identify ZNF668 as a key molecule that links chromatin relaxation with response to DNA damage in the control of DNA repair.

FIGURES **PAGE**

PART I. ROLE OF ZNF668 IN P53 REGULATION AND BREAST CANCER TUMORIGENESIS

CHAPTER 1 INTRODUCTION

1.1 Breast Cancer and Genetic Aberrations

Breast cancer continues to be the leading cause of cancer death in women in the United States and worldwide (Jemal et al., 2010). It is expected to account for 15% of all female cancer deaths in United States in 2010 (Jemal et al., 2010). The main types of breast cancer are ductal carcinoma and lobular carcinoma. The development of breast cancer is often attributed to many risk factors including sex, age, higher hormone levels, race and family history of breast cancer (McPherson et al., 2000).

Breast cancer development, like other types of cancer, is the consequence of the accumulation of multiple gene mutations (Wooster et al., 2003). Breast cancer risk is typically increased in individuals with family history. Although researchers found that the mutations in high-penetrance *BRCA1* and *BRCA2* genes contribute to breast cancer development, these mutations only account for less than 20% of the patients with familial risk (Anglian Breast Cancer Study Group, 2000; Wooster et al., 2003). These findings suggest that additional genetic alterations are required for the development of breast cancer. Identifying these relatively low-penetrance genes will help people to better understand the implication of genetic alterations in breast cancer development.

The high-throughput genotyping analysis and understand of genetic variation patterns in human genome have advanced the research of genetic abberiations in human cancer. The availability of the human genome sequence highthroughput analysis of tumor genome, and powerful computational methods make it possible to identify new candidate cancer genes and somatic changes in human cancers. For example, researchers investigated the genetic alterations in the coding sequences of well annotated genes and they identified the regions of the genome that have the potential to cause cancer development (Sjoblom et al., 2006; Wood et al., 2007). These studies will facilitate the design of targeted therapeutic approaches and provide key insights into the mechanisms underlying tumorigenesis.

1.2 Zinc Finger Protein 668 and its somatic mutations in patient breast cancer samples

The accumulation of mutations in oncogenes and tumor suppressor genes accounts for human cancer development (Vogelstein and Kinzler 2004). Thus, understanding how these genetic alterations contribute to human cancer development is a powerful tool to study the mechanisms underlying tumorigenesis and to identify new targets for clinical intervention.

Estimated New Cases*

	Males				Females	
Prostate	217,730	28%		Breast	207,090	28%
Lung & bronchus	116,750	15%		Lung & bronchus	105,770	14%
Colon & rectum	72,090	9%		Colon & rectum	70,480	10%
Urinary bladder	52,760	7%		Uterine corpus	43,470	6%
Melanoma of the skin	38,870	5%		Thyroid	33,930	5%
Non-Hodgkin lymphoma	35,380	4%		Non-Hodgkin lymphoma	30,160	4%
Kidney & renal pelvis	35,370	4%		Melanoma of the skin	29,260	4%
Oral cavity & pharynx	25,420	3%		Kidney & renal pelvis	22,870	3%
Leukemia	24,690	3%		Ovary	21,880	3%
Pancreas	21,370	3%		Pancreas	21,770	3%
All Sites	**789,620**	**100%**		**All Sites**	**739,940**	**100%**

Estimated Deaths

	Males				Females	
Lung & bronchus	86,220	29%		Lung & bronchus	71,080	26%
Prostate	32,050	11%		Breast	39,840	15%
Colon & rectum	26,580	9%		Colon & rectum	24,790	9%
Pancreas	18,770	6%		Pancreas	18,030	7%
Liver & intrahepatic bile duct	12,720	4%		Ovary	13,850	5%
Leukemia	12,660	4%		Non-Hodgkin lymphoma	9,500	4%
Esophagus	11,650	4%		Leukemia	9,180	3%
Non-Hodgkin lymphoma	10,710	4%		Uterine Corpus	7,950	3%
Urinary bladder	10,410	3%		Liver & intrahepatic bile duct	6,190	2%
Kidney & renal pelvis	8,210	3%		Brain & other nervous system	5,720	2%
All Sites	**299,200**	**100%**		**All Sites**	**270,290**	**100%**

FIGURE 1. Ten Leading Cancer Types for the Estimated New Cancer Cases and Deaths by Sex, 2010.
*Excludes basal and squamous cell skin cancers and in situ carcinoma except urinary bladder. Estimates are rounded to the nearest 10.

Figure 1. Ten leading cancer types for the estimated new cancer cases and deaths by sex, 2010. (Jemal et al., 2010).

Through genomewide gene sequencing, many genes that are frequently mutated in breast tumor samples have been discovered (Sjoblom et al., 2006). Among these mutated genes, a hypothetical protein (FLJ13479) later named zinc finger protein 668 (ZNF668) was identified, and validated as a frequently mutated gene in breast cancer (Sjoblom et al., 2006). ZNF668 gene mutations were found in four out of thirty-five breast cancer samples analyzed (11.4%) (Sjoblom et al., 2006). Since ZNF668 is frequently mutated in breast cancer, we

suspect that ZNF668 might be an important breast cancer gene that contributes to breast cancer development.
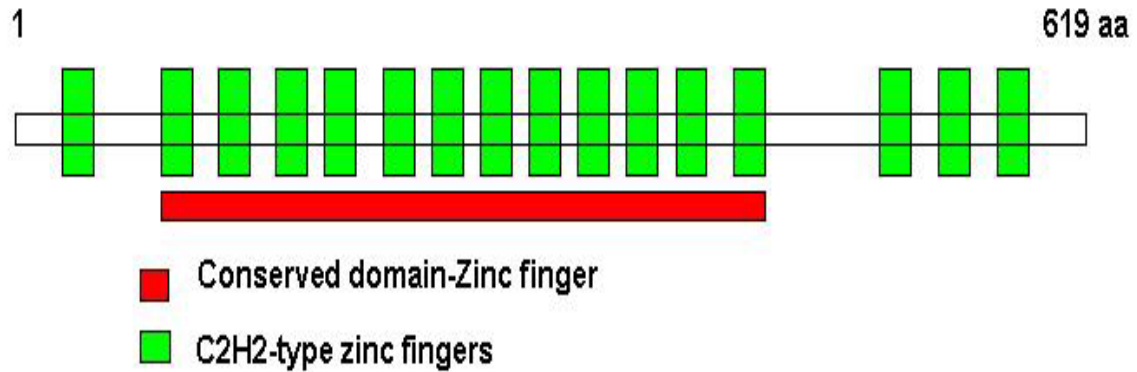
Figure 2. Conserved domain in zinc finger protein 668.

ZNF668 belongs to the kruppel C2H2-type zinc-finger protein family and contains 16 C2H2-type zinc fingers (Figure 2). So far, the function of ZNF668 has remained entirely unexplored. To understand the role of ZNF668 in breast cancer development, we used a proteomics-based approach to systematically identify ZNF668-binding proteins (Figure 3). A nucleolar protein, nucleophosmin (NPM, B23), was pulled down by ZNF668 (Figure 3), and interaction between ZNF668 and NPM was confirmed by immunoprecipitation analysis later.
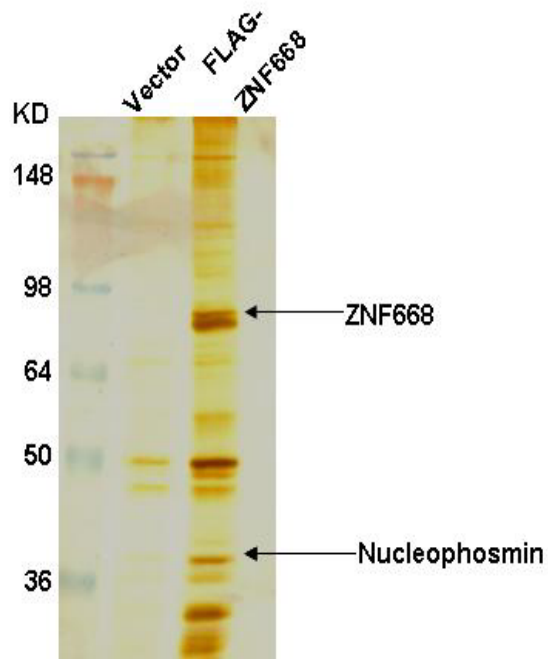
Figure 3. Silver staining of the ZNF668 complex separated by SDS-PAGE. The whole cell extracts were prepared from U2OS cells transiently transfected with empty vector or Flag-ZNF668. Cell lysates were mixed with M2-Flag agrose beads and the protein complex was pulled down and eluted with M2-Flag peptide. Flag-ZNF668 and nucleophosmin are indicated.

1.3 Role of nucleolus and nucleolar proteins in p53 regulation and tumorigenesis.

The connection between nucleolus function and tumorigenesis is now being appreciated. Although nucleolus is well known as the site for production and assembly of ribosome components, recent studies suggested that nucleolar components were also involved in cancer development events such as p53 stabilization and p53 induced cell cycle arrest (Lohrum et al., 2003; Dai et al., 2006 and Pestov et al., 2001).

NPM is a nucleolar phosphoprotein that constantly shuttles between the nucleus and cytoplasm (Yun et al., 2003; Grisendi et al., 2006). It is involved in ribosome biogenesis and can function as either an oncogene or a tumor suppressor depending on the context (Grisendi et al., 2006). Recent studies showed that NPM was involved in regulation of the p53 tumor suppressor protein function (Colombo et al., 2002; Kurki et al., 2004). NPM binds MDM2 and protects p53 from MDM2-mediated degradation (Kurki et al., 2004). The nucleolus, where most NPM resides, functions as a cellular stress sensor that integrates a variety of cellular stresses to trigger p53 responses and regulate the role of p53 in tumor suppression (Pestov et al., 2001; Rubbi and Milner 2003; Horn and Vousden 2004); the nucleolus plays an important role in p53 stabilization under stress conditions (Pestov et al., 2001). Indeed, subcellular redistribution of NPM and other nucleolar proteins, such as ARF, has regulated p53 function (Itahana et al., 2003; Bertwistle et al., 2004; Kurki et al., 2004; Korgaonkar et al., 2005; Grisendi et al., 2006).

The nucleolar ARF-MDM2-p53 feedback loop regulation also represents another example to explain the connection between nucleolar stress and tumorigenesis. Tumor suppressor ARF is a nucleolar protein and its association with MDM2 could contribute to the localization and retention of MDM2 to the nucleolus thereby sequester MDM2 activity and stabilize p53 (Zhang et al., 1998; Sherr et al., 2000; Honda et al., 1999; Kamijo et al., 1999; Stott et al., 1998 and Pomerantz et al., 1998). Under cellular stress, disruption of the nucleolar function is responsible for the redistribution of nucleolar proteins to stabilize and

regulate p53 function (Rubbi et al., 2003). Therefore, the nucleolus is proposed to be a sensor for integrating variety of cellular stresses together to trigger p53 responses and regulate its role in tumorigenesis (Pestov et al., 2001; Rubbi et al., 2003 and Horn et al., 2004).

Thus, the connection between nucleolus and regulation of p53 is highly implicated in tumorigenesis. The interaction between ZNF668 and NPM and the nucleolar localization of ZNF668 (see Figure 4) suggested that ZNF668 might be involved in p53 regulation.

1.4   p53 and tumor suppression

The tumor suppressor protein p53 was first identified in 1979 as a cellular protein that bound to the simian virus (SV40) large T antigen and accumulated in the nuclei of cancer cells (Lane et al., 1979). The real role of p53 was uncovered until 10 years after its discovery. At first, p53 was thought to be an oncogene because it present at increased levels in transformed cells (Vogelstein, 2001). However, later it was found that the p53 people were studying was in fact a mutant form because the p53 cDNA was cloned from cancer sample and it contained missense mutations. Since 1989, research into p53 supported that one of the major function of wild type p53 was tumor suppression.

In normal cells, p53 level is tightly controlled by its negative regulator, the E3 ubiquitin ligase MDM2 (Haupt et al., 1997; Kubbutat et al., 1997; Nampoothiri 1998; Kubbutat, et al. 1999). Ubiquitination of p53 by MDM2 leads to export of p53 from the nucleus to the cytoplasm followed by proteasomal degradation

(Boyd et al., 2000; Geyer et al., 2000). Under cellular stresses—such as genetic alterations, DNA damage stress, oncogene activation, and hypoxia—dissociation of MDM2 and p53 stabilizes p53 protein, and stabilization of p53 in turn leads to various cellular responses, including cell apoptosis, cell cycle arrest, cell senescence and DNA damage repair (Vousden and Lu 2002).

p53 plays a critical role in preventing damaged cells from transforming into malignant cells (Ryan et al., 2001). The most important pathways involved in tumor suppression that are activated by p53 include apoptosis, cell-cycle arrest, senescence and DNA repair.

If the DNA damage is too severe to be repaired, the activated p53 can initiate cell apoptosis, the programmed cell death (Jian et al., 2003). The p53 induced apoptosis can be explained by its activation of expression of various downstream target genes including p53AIP, bax, Fas/APO1, Tsp1, IGF-BP3, PUMA and others (Hickman et al., 2002). The activated p53 activates expression of p21 which is an inhibitor of cyclin-dependent kinases (CDKs). p21 binds to G1-to-S CDK complexes and inhibits G1-to-S transition (Harper et al., 1993). p53 may also inhibit G2-to-M transition by regulation of protein 14-3-3σ, which sequesters cyclin B1–CDK1 complexes outside the nucleus and stop cells in G2 phase (Hermeking et al., 1997). In tumors, mutant p53 can no longer bind DNA in an effective way and the downstream regulation of p21 failed to stop cell division, thus contributed to tumor formation by the uncontrolled cells division.

DNA damage, oncogene activation or telomere dysfunction can lead to the activation of p53 (Deng et al., 2008). Activated p53 can trigger senescence,

a permanent cell cycle arrest, and inhibit tumor progression. Senescence is likely to result from changes in the expression of a number of proteins such as the plasminogen activator inhibitor 1 (PAI-1) (Kortlever et al., 2006). p21 is another important player in response to p53-mediated senescence (Harper et al., 1993). In mouse models, reactivation of p53 in carcinomas and sarcomas triggers senescence rather than apoptosis (Artandi et al., 2005). In vivo study indicated that p53 induced senescence caused the subsequent engagement of the immune system and could result in tumor clearance (Xue et al., 2007).

The p53 protein is important in maintaining genetic stability. It may involve the induction of genes that regulate nucleotide-excision repair of DNA (Seo et al., 2002), chromosomal recombination and chromosome segregation. Further evidence for a role for p53 in DNA repair comes from the induction of a specific ribonucleotide reductase gene (p53R2) by p53 after DNA damage (Xue et al., 2007). p53 may also facilitate the homologous recombination repair of double strand breaks through the regulation of the fidelity of Rad51-dependent HR repair pathway (Bertrand et al., 2004).

1.5   Hypothesis and project goals

In our preliminary data, ZNF668 was associated with many nucleolar proteins including, nucleophosmin (NPM) and nucleostemin (NS), two proteins that bind and regulate p53 protein. We also identified ZNF668 as a novel p53 binding protein localized in the nucleoli of breast cancer cells. Therefore, we hypothesize that ZNF668 plays a critical role in regulation of p53 tumor

suppressor activity for breast tumor suppression. We suspect that ZNF668 may contribute to breast cancer suppression at least in part through regulation of p53.

In this part of study, we aim to demonstrate the functional interaction among ZNF668, p53, and MDM2. We will try to study the role of *ZNF668* as a novel tumor suppressor gene in breast cancer and reveal its mechanistic function in regulating the MDM2-p53 interaction.

CHAPTER 2 MATERIALS AND METHODS

2.1   Cell Culture and Transfection

U2OS cells and breast cancer cells were purchased from the American Type Culture Collection. U2OS cells were maintained in McCoy's 5A medium (Cellgro) supplemented with 10% fetal bovine serum (FBS) with glutamine, penicillin, and streptomycin. MCF7, MCF7-control, and MCF7-p53 knockdown cells were maintained in Dulbecco's modified Eagle's medium (DMEM) (Cellgro) supplemented with 10% FBS with glutamine, penicillin, and streptomycin. MCF10A cells were maintained in mammary epithelial growth medium (Clonetics), a proprietary serum-free medium containing insulin, hydrocortisone, epidermal growth factor, and bovine pituitary extract. HMECs were grown in mammary epithelial basal medium supplemented with MEGM SingleQuots growth factors (Lonza). Cells were incubated at 37°C in a humidified incubator with 5% CO_2 and transfected with Fugene 6 (Roche), Lipofectamine 2000 (Invitrogen) or Oligofectamine (Invitrogen).

2.2   Plasmids

To generate FLAG-ZNF668, V5-ZNF668, and GST-ZNF668 constructs, full-length ZNF668 cDNA was amplified by polymerase chain reaction (PCR) and subcloned into pCMV5-3 x FLAG vector (Sigma), pLenti4/TO/V5-DEST vector (Invitrogen), and pGEX-4T vector (Addgene). The R556Q (Mutant 1) and A66T (Mutant 2) point mutations were created from 3 x FLAG-ZNF668 using the

GeneTailor Site-Directed Mutagenesis System (Invitrogen). The FLAG-tagged ZNF668 deletion mutants ZNF668- Δ 1~ Δ 12 were generated by PCR and subcloned into 3 x FLAG vector. FLAG-p53 (108038, pcDNA3 FLAG-p53), GST-p53 (10852, p3113 GST-p53), and GST-MDM2 (16237, pGEX-4T MDM2 wild-type) were purchased from Addgene. MDM2 deletion plasmids Δ 58-89, Δ 212-296, Δ 222-437, Δ 296-437, and Δ 9 (RING finger domain deletion) were kind gifts from Dr. Karen Vousdens (The Beatson Institute for Cancer research). The identity of the plasmids was confirmed by sequencing at the MD Anderson Cancer Center DNA Analysis Core Facility.

2.3   Antibodies and Reagents

Nucleotides 548-1449 were subcloned into pGEX-4T with the sense primer 5′-TTTTGGATCCATGGAAGTGGAGGCTGCAGAG-3′ and the antisense primer 5′-TTTTGAATTCGCGCTGGTGGCGAGGGAAGCT-3′, and the protein product was used for immunization for rabbit polyclonal anti-ZNF668 antibody (Proteintech Group, Inc.). Anti-FLAG M2-agarose affinity gel was purchased from Sigma. Anti-p53 (FL-393), anti-MDM2 (SMP14), anti-NPM (C-19), anti-p53 (FL393), and anti-p21(C-19) were purchased from Santa Cruz Biotechnology. Anti-p53 (DO-1) was purchased from Calbiochem. Anti-phospho-p53–Ser 15 was purchased from Cell Signaling. Anti-ubiquitin (FK2) and an ubiquitinylation kit were purchased from BioMol. Anti-NS (MAB4311) was purchased from Chemicon. Anti-V5 (ab9116) and anti-NPM (ab10530) were purchased from Abcam. Fluorochrome-conjugated secondary antibodies were purchased from

Jackson ImmunoResearch Laboratories. A thrombine cleavage capture kit was purchased from Novagen. Cycloheximide was obtained from Sigma and used at 50 µg/ml (U2OS cells) or 20 µg/ml (MCF7 cells). MG132 (carbobenzoxy-L-leucyl-L-leucyl-L-leucine) was obtained from EMD Biosciences and used at 10 µM. Nutlin-3 was purchased from Cayman Chemical and used at 10 µM.

2.4　RNA Interference

ZNF668 knockdown was achieved by RNA interference using either siRNA (Dharmacon) or a lentiviral vector-based MISSION shRNA (Sigma). The ON-TARGETplus ZNF668 siRNA duplex and ON-TARGETplus SMARTpool HDM2 siRNA mix were purchased from Dharmacon Research, Inc. ON-TARGETplus nontargeting siRNA was used as a control for the siRNA reactions. RNA duplexes (final concentration 100 nM) were transfected into the cells using Oligofectmine (U2OS) or Lipofectamine 2000 (MCF7 & MCF10A) according to the manufacturer's protocol (Invitrogen). Cells transfected with ZNF668 siRNA duplexes were incubated for 2 and 3 days, respectively. A decrease in the respective protein levels was verified by Western blotting. Lentiviral particles corresponding to the MISSION shRNA ZNF668 target set were used, as well as the MISSION nontarget shRNA control. The specificity and efficacy of the shRNA ZNF668 procedure were controlled with Western blotting after transduction and puromycin selection in knockdown cells.

2.5　Immunofluorescent Microscopy

Cells were fixed with 4% paraformaldehyde and then permeabilized with 0.5% NP-40 and 1% Triton X-100. The primary antibodies were as follows: NPM, C-19; NS, MAB4311; V5-tag, ab9116; p53, FL393; and MDM2, SMP14. In coimmunostainings, donkey anti-rabbit conjugated Alexa 594, goat anti-rabbit conjugated Alexa 488, chicken anti-mouse conjugated Alexa 594, or goat anti-mouse conjugated Alexa 488 (Invitrogen) were used as fluorochromes, and DNA was stained with 4′,6-diamidino-2-phenylindole (DAPI, Vector Laboratories). Absence of cross-reactivity of the antibodies and conjugates was verified in separate experiments. Images were acquired using a Nikon Eclipse TE200-E microscope and processed with IPLab imaging software (BioVision Technologies).

2.6   Immunoblotting and Immunoprecipitation

Cells were washed in phosphate-buffered saline and lysed in modified RIPA buffer (50 mM Tris-HCl [pH 7.4], 1% NP-40, 10% sodium deoxycholate, 150 mM NaCl, 1 mM EDTA, 1 mM phenylmethylsulfonyl fluoride, 1 mM sodium orthovanadate, and 1 mM NaF). For nuclear extract preparation, cells were lysed in (10 mM HEPES [pH 8.0], 1.5 mM $MgCl_2$, 10 mM KCl, 0.5 mM dithiothreitol, and 0.5% NP-40), and nuclear extracts were prepared in nuclear extraction buffer (20 mmol/L HEPES [pH 7.9], 1.5 mM $MgCl_2$, 100 mM KCl, 420 mM NaCl, 0.2 mM EDTA, and 1 mM dithiothreitol). After clarification, cell lysates were immunoprecipitated with specific antibodies (NPM, ab10530; ZNF668, rabbit polyclonal anti-ZNF668 antibody; MDM2, SMP-14; and p53, DO-1). The

immunocomplexes were collected on Protein A/G plus-conjugated agarose beads (Santa Cruz Biotechnology). Cellular lysates or immunocomplexes were separated by 7% or 12% sodium dodecyl sulfate-polyacrylamide gel electrophoresis (SDS-PAGE) and transferred to Protran nitrocellulose membrane (Fisher Scientific). Membranes were blocked in Tris-buffered saline-0.1% Tween 20 (TBS-T)/5% (w/v) milk for 1 h at room temperature and were then incubated with primary antibodies diluted in TBS-T/5% (w/v) milk for 2 h at room temperature or overnight at 4°C. Subsequently, membranes were washed with TBS-T and incubated with horseradish peroxidase secondary antibody (1:5000) (Jackson ImmunoResearch) diluted in TBS-T/5% skim milk. Membranes were washed in TBS-T, and bound antibody was detected by enhanced chemiluminescence (GE Healthcare).

2.7 In Vivo Ubiquitination Assay

For the *in vivo* p53 ubiquitination assay, FLAG-tagged ZNF668 was transfected into U2OS cells using Fugene 6 (Roche). Forty-eight hours after transfection, cells were treated with MG132, harvested, washed with phosphate-buffered saline, pelleted, and lysed in RIPA buffer. The cell lysates were then subjected to SDS-PAGE, and p53 or MDM2 protein level was normalized so that there were equal levels of p53 or MDM2 in control cells and ZNF668-expressing cells. The proportional amounts of cell lysates were incubated with p53 or MDM2 antibody and pulled down using protein A/G beads. Beads were washed three

times and boiled for 5 min. The boiled samples were separated by SDS-PAGE, and protein was detected by immunoblotting with anti-ubiquitin antibody.

2.8   Preparation of Recombinant Proteins

The plasmids pGEX-4T-1-ZNF668, pGEX-4T-MDM2, and pGEX-2TK-p53 were used to express recombinant GST-ZNF668, GST-MDM2, and GST-p53 in *Escherichia coli* strain BL21 (GE Healthcare). The GST fusion proteins were expressed by induction for 12 h at 25°C with 0.1 mM isopropyl-1-thio-β-D-galactopyranoside in strain BL21 and purified using glutathione agarose (Sigma) according to the manufacturer's instructions. GST fusion proteins harboring p53, ZNF668, and MDM2 were cleaved and purified with a thrombin cleavage capture kit.

2.9   In Vitro GST-Protein Binding Assay

Cleaved p53 and MDM2 were purified as described in the preceding paragraph. GST-ZNF668 was not cleaved. Purified proteins were incubated in 300 ml of binding buffer (25 mM Tris-Cl [pH 7.2], 50 mM NaCl, and 0.2% NP-40) with continuous shaking. Proteins were recovered (2 h at 4°C) with glutathione agarose beads (Sigma). Beads were washed three times with 1 ml of washing buffer (100 mM Tris-Cl [pH 8.0], 100 mM NaCl, and 1% Nonidet P-40) four times and were eluted with 10 mg/ml fresh-made reduced glutathione (pH 8.0). Eluted proteins were subjected to SDS-PAGE and Western blotting analysis.

2.10   Reverse Transcriptase-PCR and PCR

cDNA was transcribed using SuperScript III (Invitrogen) following the manufacturer's instructions. ZNF668 was amplified by PCR using the primers 5′-GGAAGCCAGTGGGGAGAAGGTGTC-3′ and 5′-CGCTCGTGGCTCTGGTA GGAACTG-3′. For amplification of p53, the primers 5′-GCGCACAGA GGAAGAGAATC-3′ and 5′-CCTCATTCAGCTCTCGGAAC-3′ were used.

2.11   Luciferase Assay

U2OS cells were transfected with the pG13-LUC reporter vector in the absence or presence of expression vectors for the indicated proteins or empty expression vector (3 × FLAG). The total amount of expression vector was constant in all transfections. After 48 h, luciferase activities were determined in duplicate samples according to the manufacturer's instructions (Promega). The relative luciferase activity was assayed by cotransfection of a plasmid for the expression of renella and normalization for its activity. The fold increase in relative luciferase activity therefore represented the extent of p53 activation. Data were presented as the mean ± standard deviation (SD) of three independent experiments.

2.12   In Vitro Proliferation and Soft Agar Assay

To measure cell proliferation, cells were plated in 96-well plates (200-μl cell suspensions, 5×10^3 cells/ml) and allowed to grow for 1 to 4 days. Each day, 3-(4, 5-dimethylthiazol-2-yl)-2, 5-diphenyltetrazolium bromide (MTT; Sigma)

substrate (2 mg/ml) was added into the culture medium. Four hours later, the culture medium was removed, and dimethyl sulfoxide was added. The optical density was measured spectrophotometrically at 490 nm. Each experiment was repeated at least three times.

For soft agar assay, cells were resuspended in DMEM containing 0.35% agarose (ISC BioExpress, GenePure LE) and 10% FBS and seeded onto a coating of 0.5% agarose in DMEM containing 10% FBS. Colonies were counted 2 to 4 weeks after preparation.

2.13   Tumor Growth in Nude Mice

Six-week-old female nude mice were used for experiments. All animal studies were conducted in compliance with animal protocols approved by the MD Anderson Institutional Animal Care and Use Committee. Before injection of estrogen receptor-positive MCF7 cells, mice were implanted subcutaneously with 0.72 mg of 17-β-estradiol 60-day release pellets (E2 pellet; Innovative Research of America). Mice were injected in the mammary glands with 2×10^{6} cells from various cell lines in 100 µl of phosphate-buffered saline. After 1 week, tumors were measured every 3 days. Each cell line was tested in five different animals. Volume was calculated as $W^{2} \times L \times 0.52$.

CHAPTER 3 FUNCTION OF ZNF668 IN P53 AND TUMOR PROGRESS REGULATION

3.1 ZNF668 localizes in the nucleus, accumulates in the nucleolus, and interacts with NPM and nucleostemin

V5-tagged ZNF668 construct was induced to ectopically express ZNF668 protein in different breast epithelial cell lines, including MCF7 and MCF10A and human mammary epithelial cells (HMECs). Western blotting analysis revealed a 70- to 80-kD V5-tagged band in all ZNF668-overexpressing cell lines. Through motif analysis, two consensus nuclear localization sequences (R/K-R/K-X-R/K) were detected in the N-terminal of ZNF668 protein (Figure 4), suggesting that ZNF668 is a nuclear protein.

Figure 4. Sequence alignment of ZNF668 in different species. Boxed areas correspond to the consensus nuclear localization sequence. NPM (B23) and NS served as positive controls showing the consensus nuclear localization sequence in well-known nuclear proteins.

A rabbit polyclonal antibody was raised against a GST-ZNF668 fusion protein (aa 183-483) and used for Western blotting analysis. This ZNF668 antibody also detected a band between 70 and 80 kD with its expression enriched in the nuclear fraction (Figure 5). The specificity of our ZNF668 antibody was verified by small interfering RNA (siRNA) knockdown as well as overexpression of V5-tagged ZNF668 (data not shown).
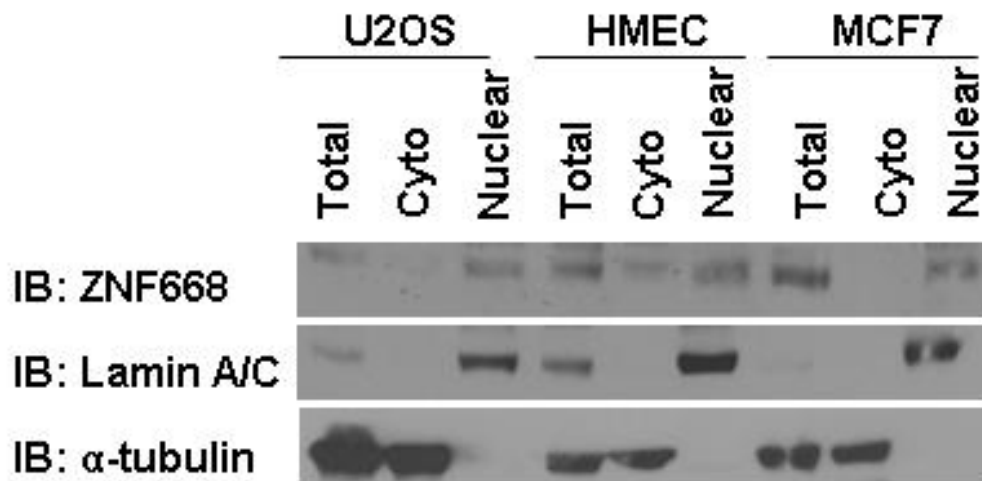
Figure 5. ZNF668 localizes predominantly in the nucleus. U2OS cells, HMECs, and MCF7 cells were lysed in RIPA buffer or nuclear extraction buffer. Lamin A/C and α-tubulin served as nuclear and cytoplasmic loading markers, respectively.

Immunofluorescence analysis revealed specific nuclear staining for ZNF668 with strong signals in one or more nucleolus-like nodular structures in both MCF7 and MDA-MB-468 cells (Figure 6, upper two rows). The specificity of the staining pattern was supported by V5 antibody staining in MCF7 cells and HMECs with overexpression of V5-tagged ZNF668 (Figure 6, lower two rows), and the nucleolar localization of ZNF668 was confirmed by ZNF668's

colocalization with two known nucleolar proteins, nucleostemin (NS) and NPM (Figure 6).
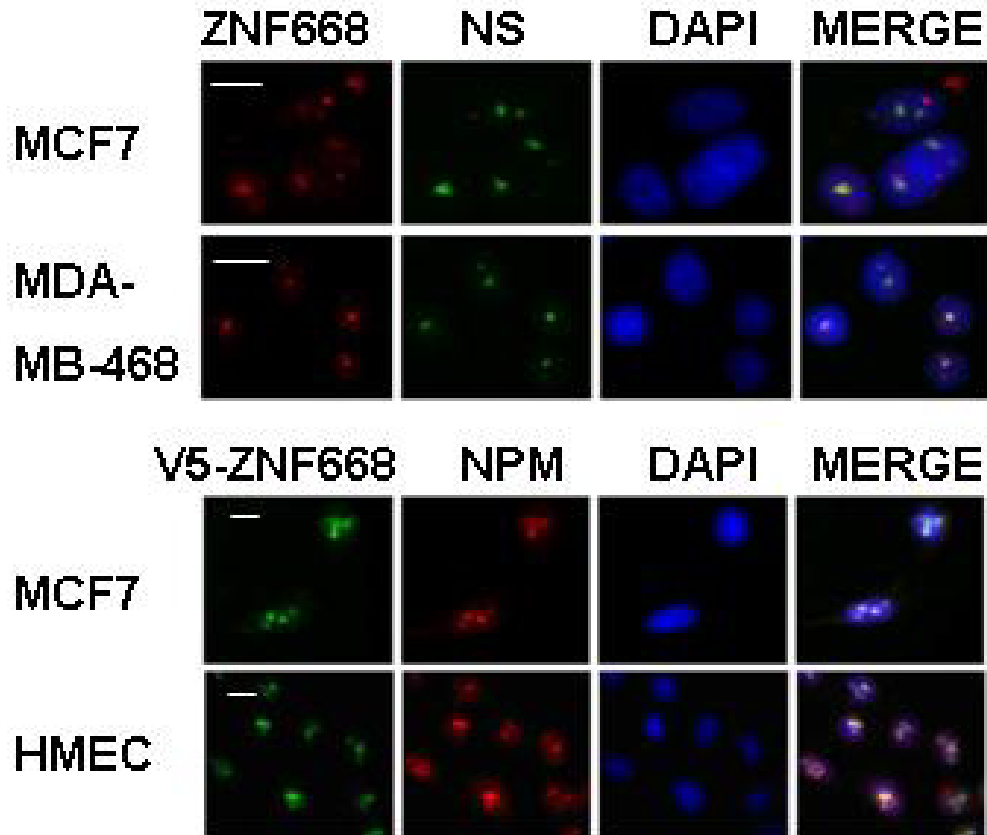
Figure 6. ZNF668 accumulates in the nucleolus. Upper panel: MCF7 and MDA-MB-468 cells were stained with antibodies against ZNF668 (red) and NS (green). Lower panel: Ectopic V5-tagged ZNF668 was induced in MCF7 cells and HMECs by doxycycline treatment. Cells were stained with V5 (green) and NPM (red). Nuclei were visualized with DAPI (blue). Scale bars: 20 μm.

To systematically identify proteins involved in ZNF668 function, we carried out immunoaffinity purification followed by mass spectrometry. We found that NPM was a major ZNF668-associated protein (Figure 3). To validate the mass spectrometry result, we performed immunoprecipitation/Western blotting analysis and found that ZNF668 co-precipitated with NPM and NS (Figure 7A).

The interaction between ZNF668 and NPM was further confirmed by reciprocal immunoprecipitation using ZNF668 or NPM antibody (Figure 7B). These results were consistent with results on immunofluorescent staining (Figure 6) and strongly suggested that ZNF668 localizes in the nucleus, accumulates in the nucleolus, and interacts with nucleolar proteins.
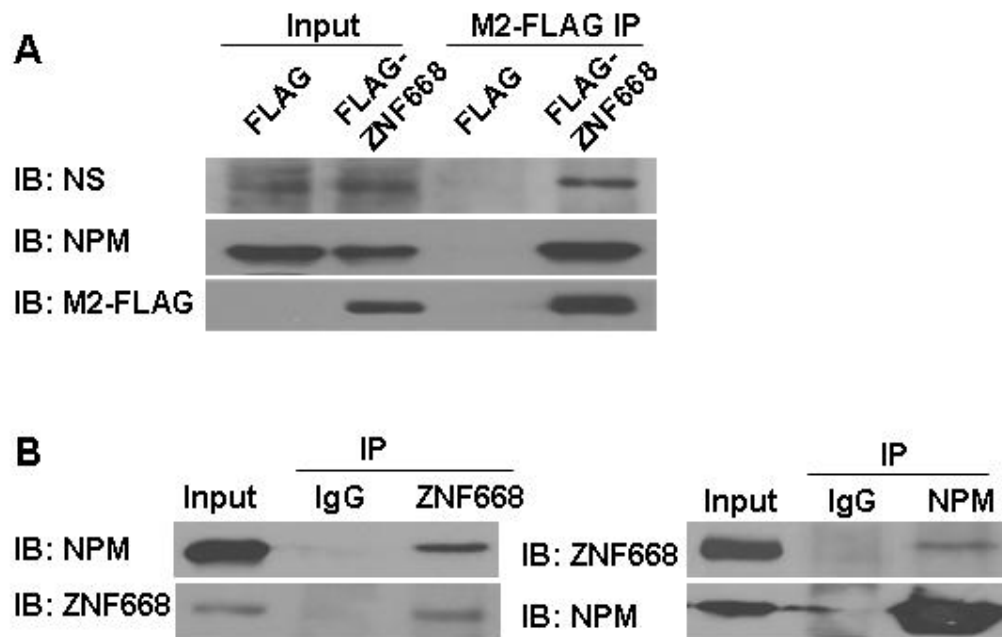
Figure 7. ZNF668 associates with NPM and NS. (A) U2OS cells were transfected with empty vector or Flag-ZNF668; 48 h later, cells lysates (3 mg) were immunoprecipitated and immunoblotted with antibodies against the indicated molecules. (B) Endogenous association between ZNF668 and NPM. Cell lysates from MCF7 cells were immunoprecipitated with anti-ZNF668, anti-NPM, or preimmune IgG and immunoblotted with anti-ZNF668 or anti-NPM antibody.

3.2   ZNF668 interacts with MDM2 and p53

It has been shown that NPM and NS bind to and regulate the protein stability and function of p53 (Colombo et al., 2002; Tsai and McKay 2002; Kurki et al., 2004; Ma and Pederson 2007). Therefore, we performed immunoprecipitation/Western blotting analysis to test whether ZNF668 also interacted with p53. We found that ZNF668 interacted with p53 when ZNF668 was ectopically expressed in U2OS human osteosarcoma cells (Figure 8A and B). Interestingly, ZNF668 also interacted with the negative regulator of p53, MDM2 (Figure 8A and B).
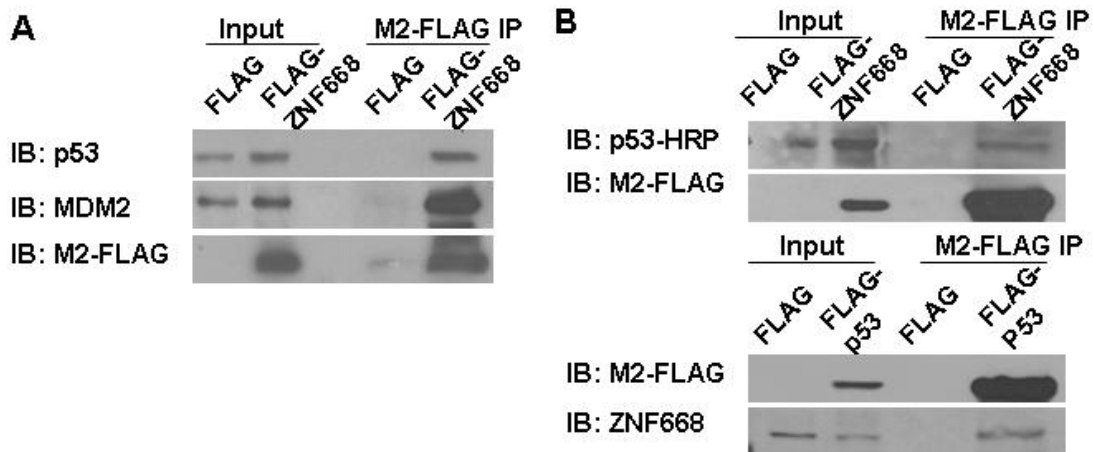
Figure 8. ZNF668 interacts with MDM2 and p53. (A) ZNF668 associates with MDM2 and p53 *in vivo*. U2OS cells were transfected with empty vector or Flag-ZNF668; 48 h later, cells lysates (3 mg) were immunoprecipitated and immunoblotted with antibodies against the indicated molecules. (B) Ectopically expressed p53 associates with ZNF668. U2OS cells were transfected with empty vector or Flag-p53; reciprocally, cells were transfected with empty vector or Flag-ZNF668. Forty-eight hours after transfection, cells lysates (3 mg) were immunoprecipitated with M2-Flag conjugated beads and immunoblotted with antibodies against the indicated molecules.

The interactions between ZNF668, p53, and MDM2 were further confirmed by reciprocal immunoprecipitation using ZNF668, p53, and MDM2 antibodies (Figure 9A), supporting the physical interactions among these three proteins in cells. *In vitro* GST-protein binding assay also confirmed the interactions among these three proteins (Figure 9B).
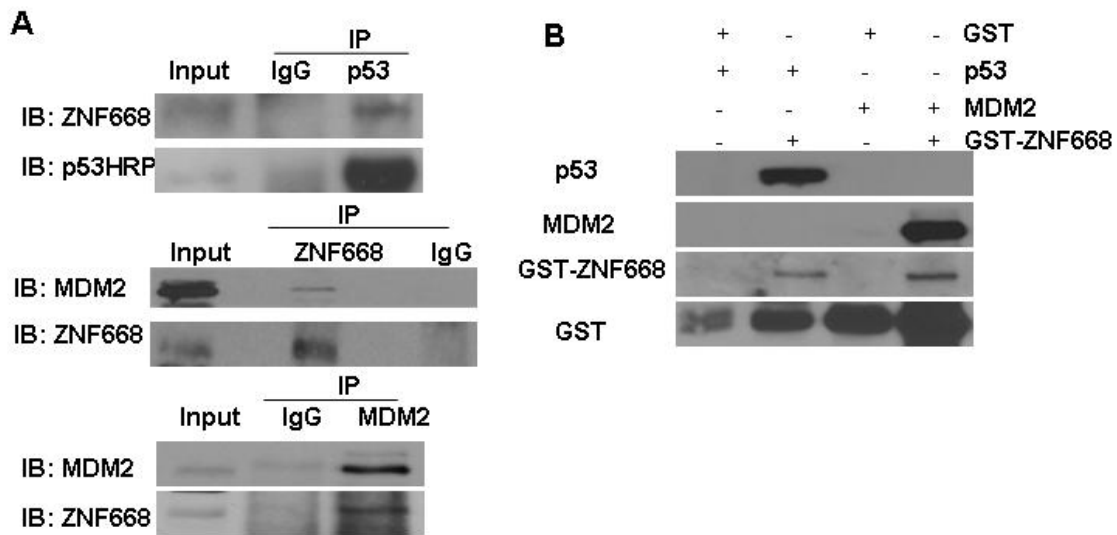
Figure 9. Endogenous ZNF668 interacts with MDM2 and p53. (A) Endogenous ZNF668 associates with p53 and MDM2. Cellular lysates of MCF10A cells were prepared by lysing the cells with RIPA buffer; immunoprecipitated with anti-ZNF668, anti-p53, anti-MDM2, or preimmune IgG; and immunoblotted with antibodies against the indicated molecules. (B) *In vitro* interaction between ZNF668, MDM2, and p53. GST-MDM2 and GST-p53 constructs were cleaved using a thrombin cleavage capture kit. Cleaved MDM2 or p53 was mixed with GST-ZNF668 in the binding buffer and incubated overnight at 4°C. Glutathione beads were added into the reaction and incubated for 2 h at 4°C; this was followed by extensive washing and analysis of the protein complexes by Western blotting for the indicated molecules.

To map the binding domain on ZNF668, we expressed FLAG-tagged wild-type ZNF668 and ZNF668 mutants lacking different parts of amino acid sequences in U2OS cells (Figure 10A). We found that both MDM2 and p53 could be co-precipitated with wild-type ZNF668, but their binding to ZNF668 with N-terminal deletions was much weaker than their binding to ZNF668 with C-terminal deletions (Figure 10B). Regions aa84-aa190 and aa268-aa367 were particularly important for the interaction between MDM2 and ZNF668: when these two regions were deleted, the MDM2-ZNF668 interaction was abolished. Interestingly, these two regions were also important for the interaction between p53 and ZNF668. Notably, immunofluorescent staining showed that the ZNF668 deletions lacking regions aa84-aa190 and aa268-aa367 were localized exclusively outside the nucleolar region, indicating that these two regions contain the nucleolar localization signals for ZNF668 (Figure 10C). These results identified the interaction domain of ZNF668 required for the interaction with MDM2 and p53 and indicated the importance of the nucleolar localization of ZNF668 for its interactions with MDM2 and p53.

A

ZNF668 aa	MDM2 binding	p53 binding	Nucleolar localization
WT 1-620	+	+	+
Δ1 84-620	+	+	+
Δ2 191-620	+	+	+
Δ3 268-620	+	+	+
Δ4 368-620	-	weak	-
Δ5 428-620	-	weak	-
Δ6 535-620	-	-	-
Δ7 1-83	-	-	-
Δ8 1-190	+	+	+
Δ9 1-267	+	+	+
Δ10 1-367	+	+	+
Δ11 1-427	+	+	+
Δ12 1-534	+	+	+

B

ZNF668 Deletions   M2-FLAG IP

C WT 1 2 3 4 5 6 7 8 9 10 11 12

p53-HRP

MDM2

Input

M2-FLAG

C

FLAG   NPM   DAPI   MERGE

Control
WT
D1
D2
D3
D4
D5
D6
D7
D8
D9
D10
D11
D12
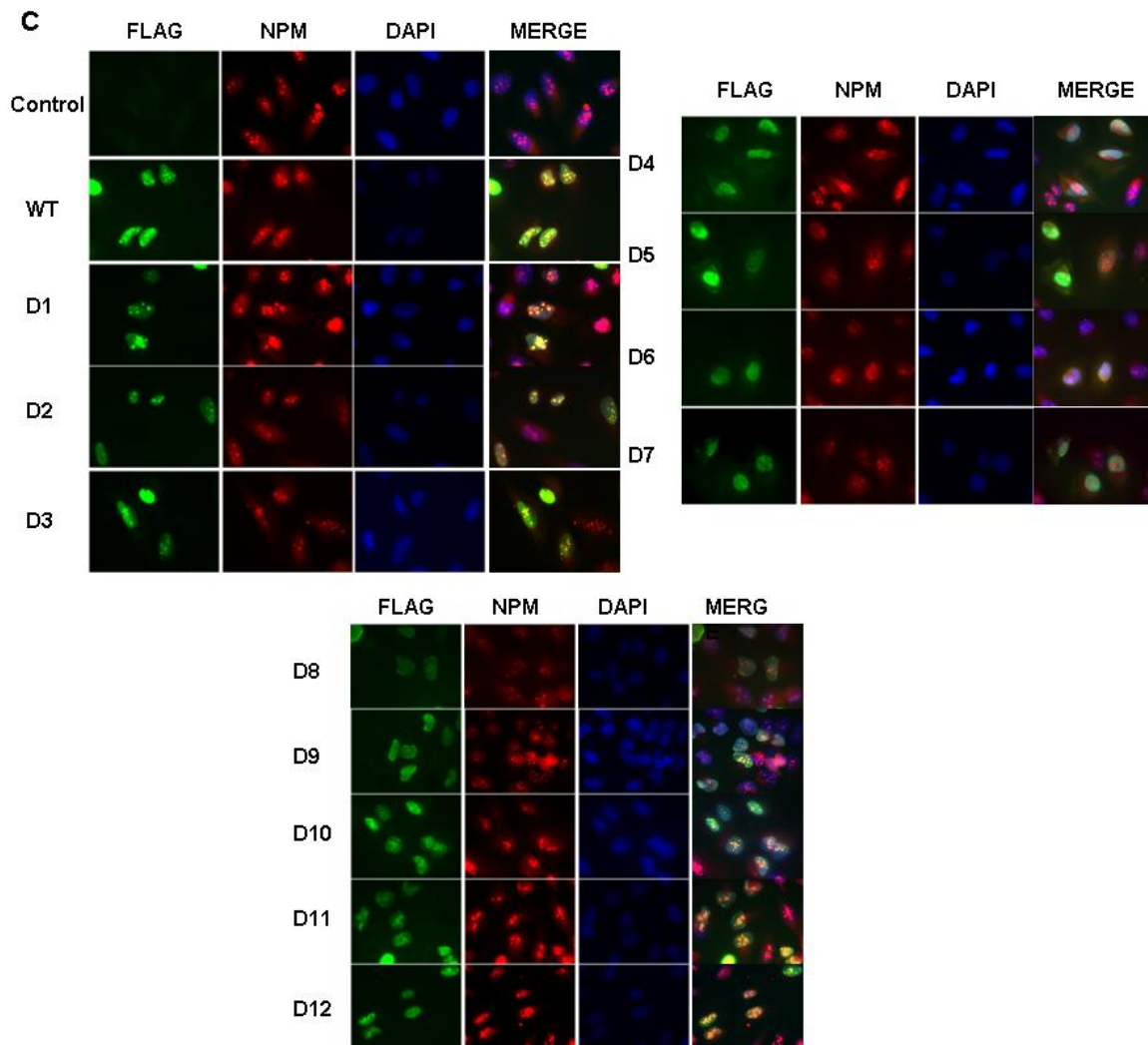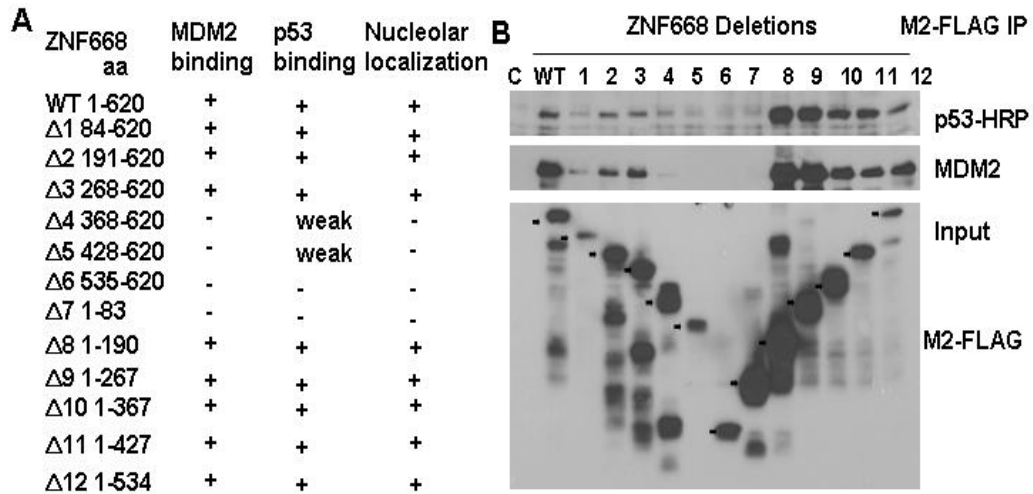
Figure 10. The interaction domain of ZNF668 with MDM2 and p53. (A) Summary of the binding of ZNF668 deletions with MDM2 and p53. (B) Mapping of the MDM2 and p53 binding domains of ZNF668. FLAG-tagged wild-type ZNF668 and deletion mutants of human ZNF668 were constructed and individually transfected into U2OS cells. After 2 days, the cells lysates (3 mg) were immunoprecipitated with M2-FLAG agarose beads and immunoblotted with antibodies against the indicated molecules. (C) Immunofluorescent staining of FLAG-tagged ZNF668 deletions. U2OS cells were overexpressed with FLAG-ZNF668 deletions and stained with antibodies against FLAG (green) and NPM (red).

Conversely, we also sought to map the MDM2 domains that are required for ZNF668 binding. We expressed MDM2 deletion proteins in U2OS cells that constantly expressed FLAG-ZNF668. MDM2 has been shown to bind to p53 through the N-terminal domain (Kubbutat et al., 1999). Although FLAG-tagged ZNF668 was co-precipitated with wild-type MDM2, an MDM2 protein carrying a p53 binding domain deletion (MDM2 Δ58-89), and an MDM2 protein carrying a C-terminal RING finger deletion (MDM2 Δ9), the interaction between ZNF668 and an MDM2 protein with the central region deleted (MDM2 Δ222-437) was defective (Figure 11A, B and C). In contrast, we confirmed that p53 could form a complex with wild-type MDM2, MDM2 Δ9, and MDM2 Δ222–437, but not MDM2 Δ58-89 (Figure 11C). These results indicated that p53 and ZNF668 bound to different regions on MDM2. Further analysis of mutations within the central region of MDM2 showed that deletion of aa212-aa296 significantly reduced the binding between ZNF668 and MDM2, although deletion of aa295-aa417 did not prevent their interaction (Figure 11B). Interestingly, a similar region of MDM2 is required for binding to ARF and ribosomal protein L11, suggesting a common

mechanism by which different molecules modulate the function of MDM2 (Bothner et al., 2001; Lohrum et al., 2003).
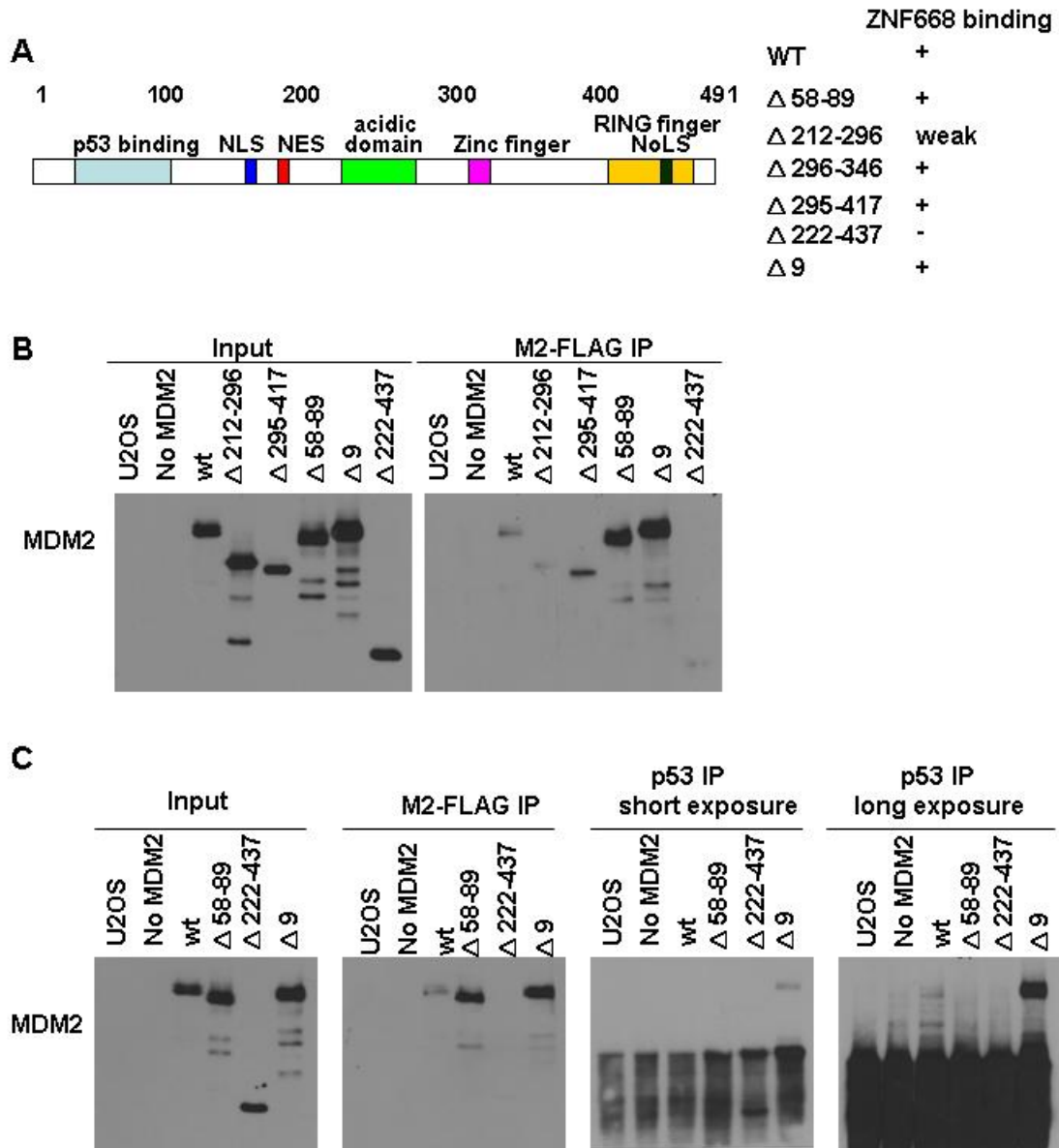
Figure 11. ZNF668 interacts with MDM2 in the central region. (A) Cartoon of the MDM2 protein, indicating the position of principal domains and summarizing the ZNF668 binding patterns. NLS: nuclear localization signal; NES: nuclear export signal; NoLS: nucleolar localization signal. (B) Mapping of the MDM2 binding domain of ZNF668. U2OS cells with constant Flag-ZNF668 overexpression were transfected with the indicated MDM2 deletion mutants. Twenty-four hours after transfection, the cells were lysed and immunoprecipitated with M2-Flag

28

conjugated beads. Associated MDM2 protein was detected by Western blotting. (C) Mapping of the MDM2 binding domain for p53 and ZNF668. U2OS cells with constant Flag-ZNF668 overexpression were transfected with the indicated MDM2 deletion proteins. Twenty-four hours after transfection, the cells were lysed and immunoprecipitated using M2-Flag beads or p53 antibody with protein A/G agarose beads. Associated MDM2 protein was detected by Western blotting.

3.3   ZNF668 regulates p53 stability and activity

Since ZNF668 binds to MDM2 and p53, we next sought to determine whether there is a causal relationship between ZNF668 status and p53 protein levels. As shown in Figure 12A, when FLAG-tagged ZNF668 was ectopically expressed in U2OS cells, we found increased p53 protein level as well as increased level of the p53 downstream target p21. p53 mRNA levels were not affected suggesting the effects were not on transcription or RNA stability. Increased p53 protein expression was also seen when we overexpressed ZNF668 in MCF7 cells and HMECs (Figure 12B).
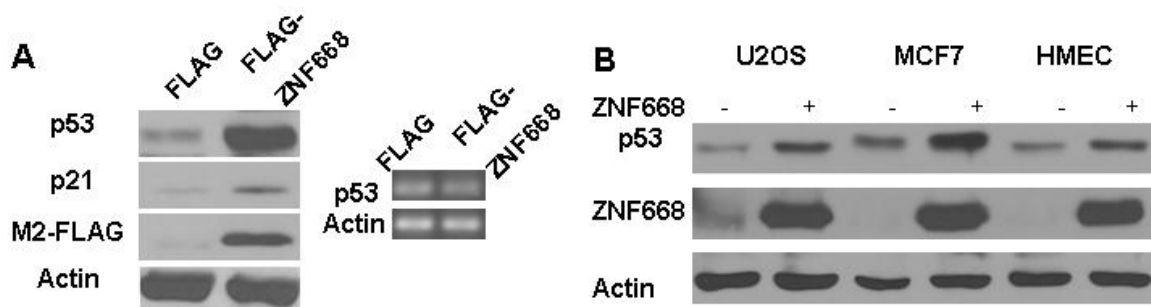
Figure 12. ZNF668 regulates p53 stability and activity. (A) ZNF668 positively regulates p53 protein expression without affecting p53 mRNA levels. U2OS cells were transfected with empty vector or Flag-ZNF668, and cell lysates were harvested and immunoblotted with antibodies against p53 and p21 (left panel) or subjected to RT-PCR of p53 (right panel). (B) ZNF668 positively regulates p53 protein expression in different cell lines. ZNF668 was overexpressed in U2OS and MCF7 cells and HMECs. Cell lysates were harvested and analyzed.

To determine whether the increase in the p53 level was regulated at the posttranslational level, we treated U2OS cells with cycloheximide to block de novo protein synthesis. In these cells, overexpression of ZNF668 increased the half-life of p53 protein from 1 h to more than 2 h (Figure 13A and B), suggesting a role of ZNF668 in stabilizing p53 protein. Inversely, knockdown of ZNF668 with siRNA in MCF7 cells resulted in a decrease of the p53 protein half-life from 2 h to 30 minutes (Figure 13C).
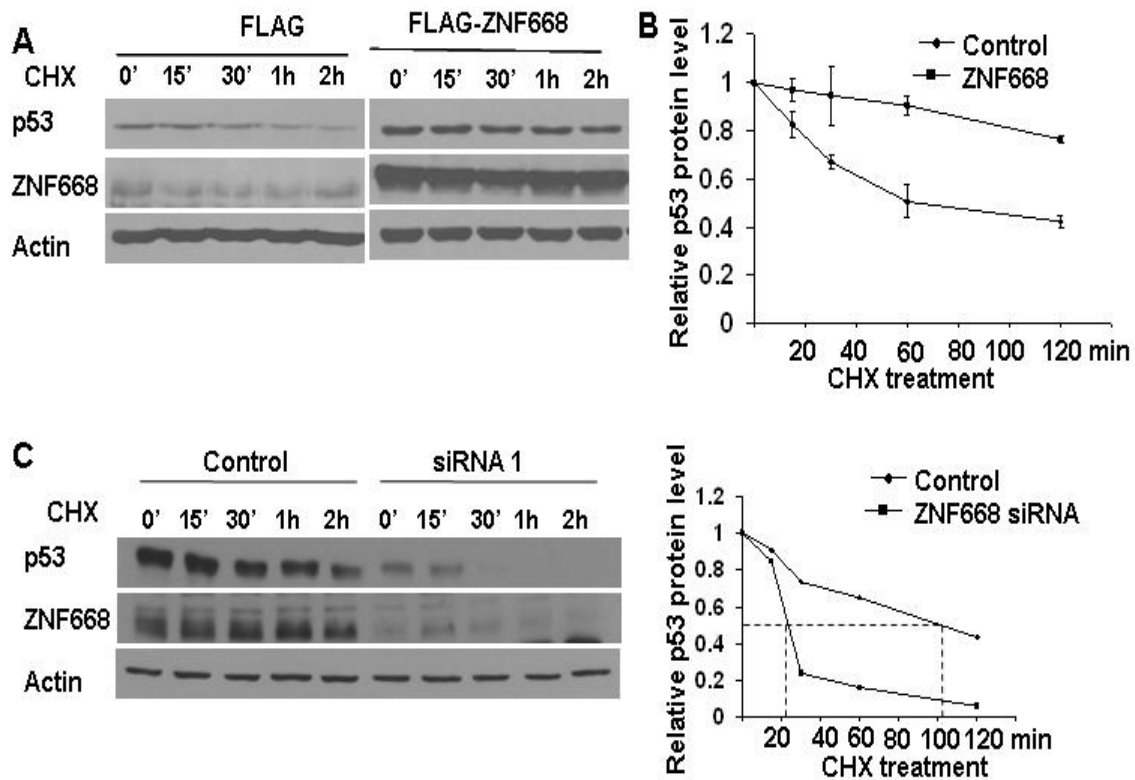
Figure 13. ZNF668 regulates p53 protein stability. (A) U2OS cells were transfected with empty vector or Flag-ZNF668. Cells were treated with cycloheximide (CHX) for the indicated times, and cell lysates were harvested and immunoblotted with antibodies against the indicated molecules. (B) Quantification (mean of three experiments) of p53 protein levels in control and ZNF668-overexpressing U2OS cells. (C) MCF7 cells were transfected with control or ZNF668 siRNA. Cells were treated with CHX for the indicated times,

and cell lysates were harvested and immunoblotted with antibodies against the indicated molecules. Right panel: Quantification of p53 protein levels in control and ZNF668-knockdown MCF7 cells.

To test whether ZNF668 regulates p53 activity, we transfected MCF10A, MCF7, and U2OS cells with siRNA targeting ZNF668 and then treated the cells with UV radiation (50 J/m^2) or γ radiation (10 Gy). Cell lysates were harvested 2 h later, and the changes in ZNF668 and p53 were analyzed. In U2OS cells, depletion of ZNF668 significantly reduced both stress-induced levels of p53 and p53 basal levels (Figure 14A). Similar results were observed in MCF10A and MCF7 cells (Figures 14B and C). The reduction in the level of p53 in response to DNA damage was paralleled by a reduction in phosphorylation of Ser15 of p53 (Figure 14A), a marker of stress-induced p53 activation. Furthermore, we observed a significant reduction in the expression of the p53 transcriptional target p21 (Figure 14D). These results demonstrated that in ZNF668-knockdown cells, the overall activation status of p53 and p53 downstream response after DNA damage is impaired.
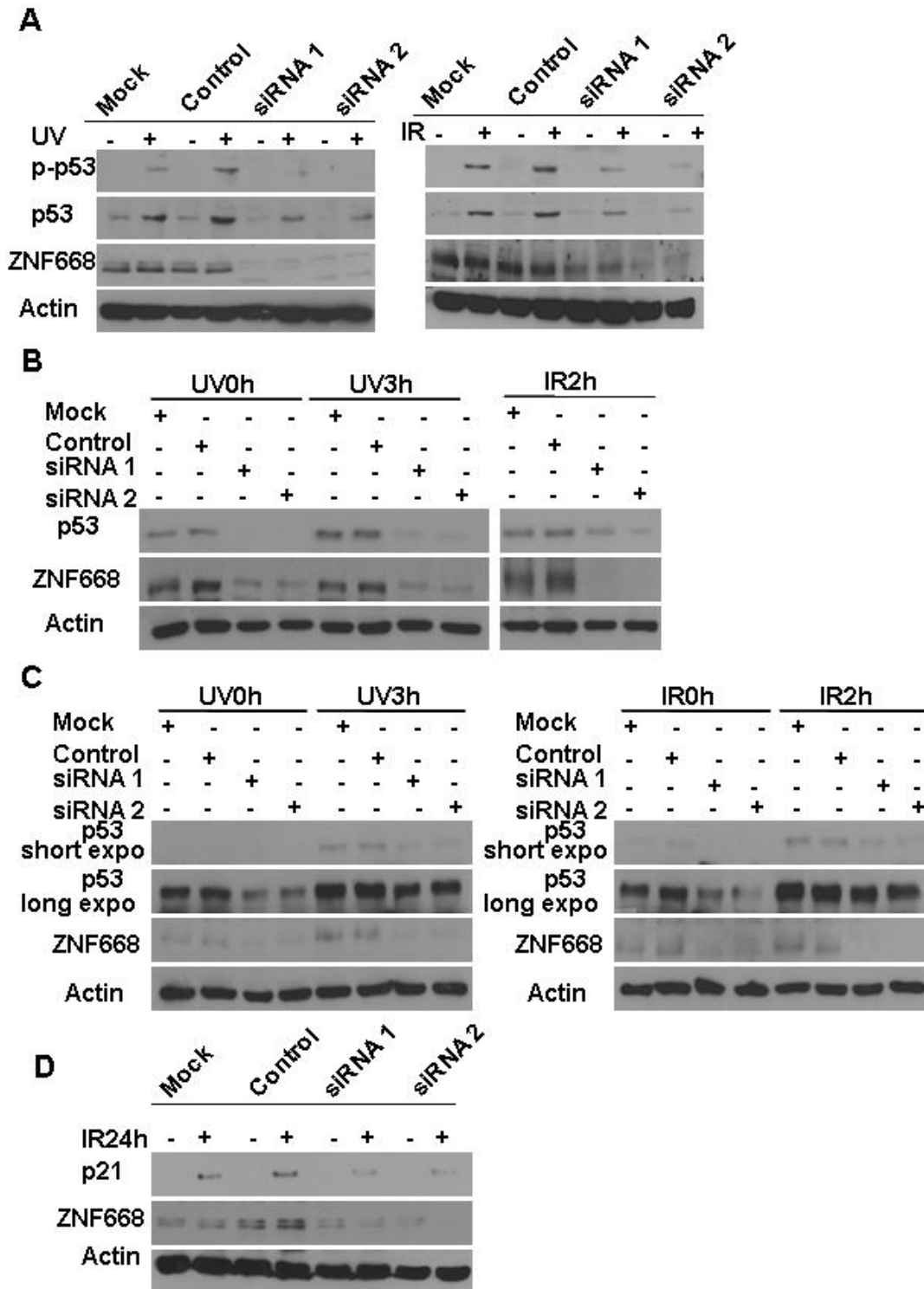
Figure 14. ZNF668 regulates both the maintenance and stress-induced stabilization of p53. (A) U2OS cells, (B) MCF10A cells and (C) MCF7 were transfected with siRNAs targeting ZNF668, and the knockdown cells were treated with UV radiation (50 J/m^2) or γ radiation (IR; 10 Gy). Cell lysates were

harvested 2 h later and immunoblotted with antibodies against the indicated molecules. (D) ZNF668 regulates p53-downstream p21 expression. U2OS cells were transfected with siRNAs targeting ZNF668, and the knockdown cells were treated with γ radiation (IR; 10 Gy). Cell lysates were harvested 24 h later and immunoblotted with antibodies against the indicated molecules.

Since *ZNF668* has been shown to be mutated in breast cancer, we next tested whether ZNF668 with mutations found in patient samples has the effect of ZNF668 on p53 activity. FLAG-tagged ZNF668 vectors that harbored mutations found in patient tumor samples were constructed through site-directed mutagenesis and expressed in U2OS cells. Importantly, we found that mutant ZNF668 could not stabilize p53 as efficiently as wild-type ZNF668 (Figure 15A). We also tested whether wild-type and mutant ZNF668 were similar in terms of regulating p53-dependent transcriptional activity. Analysis of p53 function using a p53-luciferase reporter showed that the ability of ZNF668 mutants to activate p53 was impaired compared to that of wild-type ZNF668 (Figure 15B). These results indicated that *ZNF668* mutations in patients may lead to impaired p53 activation, similarly to how *p53* mutations can lead to impaired p53 activation.
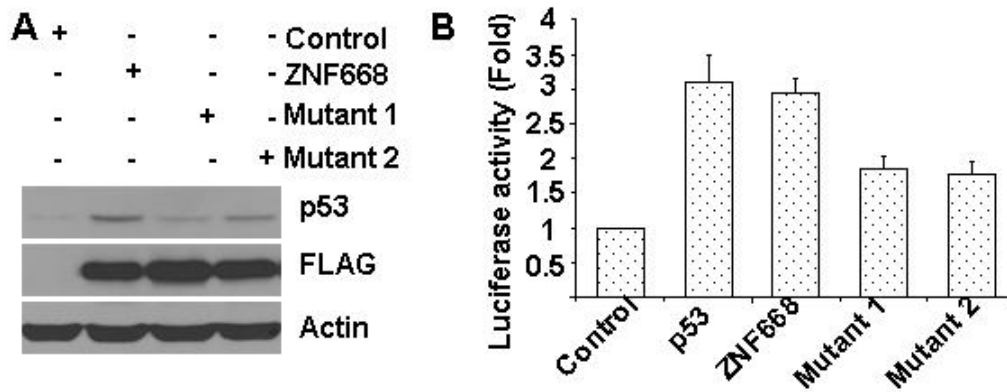
Figure 15. Mutant ZNF668 did not stabilize p53 as much as did wild-type ZNF668. (A) U2OS cells were transfected with wild-type or mutant Flag-tagged ZNF668. Forty-eight hours later, cell lysates were harvested and immunoblotted with antibodies against the indicated molecules. (B) Luciferase assay in U2OS cells transfected as indicated. Results represent the mean ± SD of three experiments.

3.4   ZNF668 facilitates p53 stabilization by disrupting MDM2-mediated ubiquitination and degradation

To determine whether ZNF668 regulates p53 protein stability through the MDM2-mediated proteasome pathway, we first tested whether ZNF668 could counteract the effect of MDM2 on p53. p53, MDM2, and ZNF668 were coexpressed in U2OS cells. MDM2 significantly decreased the p53 protein level, which could be restored, at least in part, by simultaneous expression of ZNF668 (Figure 16).
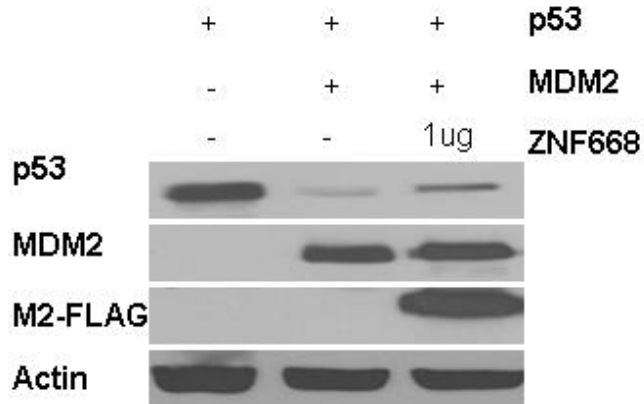
Figure 16. ZNF668 partially restores p53 protein level when ZNF668 is co-expressed with MDM2. U2OS cells were transfected with p53 (0.05 µg), MDM2 (1 µg), and ZNF668 (0~1 µg). Cell lysates were harvested 48 h later and immunoblotted with antibodies against the indicated molecules.

To test whether ZNF668 affects the interaction between MDM2 and p53, we performed an *in vitro* binding assay. Purified GST-ZNF668, MDM2, and p53 proteins were mixed and pulled down with MDM2 antibody. We found that addition of purified ZNF668 protein decreased MDM2-p53 binding in a dose-dependent manner (Figure 17). These data indicated that ZNF668 disrupts the interaction between MDM2 and p53.
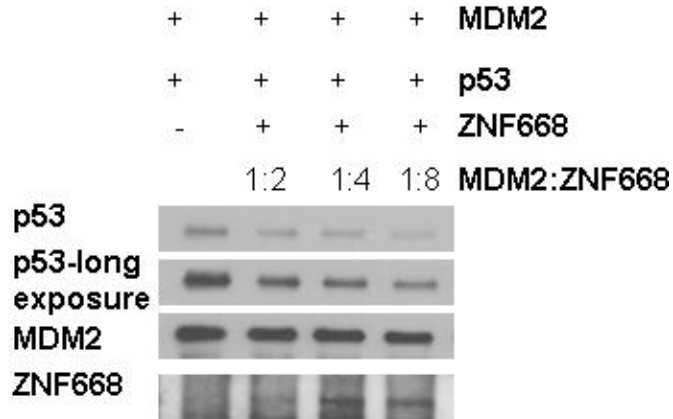
Figure 17. The presence of ZNF668 decreases the interaction between MDM2 and p53. Purified MDM2 and p53 were mixed in *in vitro* binding buffer, and GST-ZNF668 was added into the reaction at different GST-ZNF668:MDM2 ratios (0:1, 2:1, 4:1, and 8:1). Two hours later, the protein complex was immunoprecipitated with MDM2 antibody and immunoblotted with antibodies against the indicated molecules.

The presence of nutlin, which inhibits MDM2-p53 interaction, stabilizes and activates p53 (Vassilev et al., 2004; Colaluca et al., 2008). We found that nutlin treatment of ZNF668-knockdown cells reversed the effect of ZNF668 knockdown on DNA damage-induced p53 activation (Figure 18). These results further supported the MDM2-p53 interaction as the key target of by which ZNF668 induces p53 stabilization.
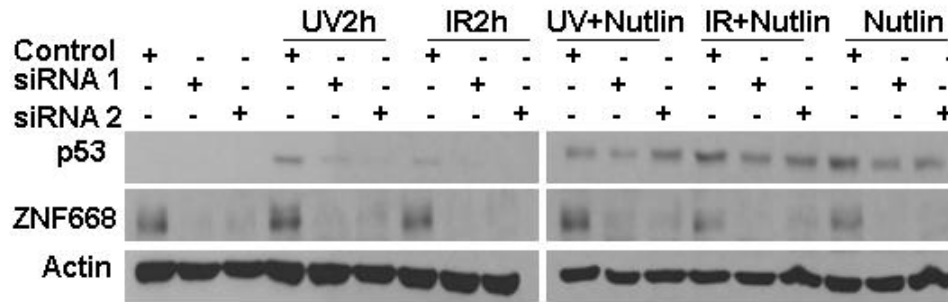
Figure 18. Nutlin restores ZNF668 knockdown effects on p53 response to DNA damage. U2OS cells were transfected with siRNA duplexes targeting ZNF668, and the ZNF668-knockdown cells were pretreated with or without nutlin. Two hours later, cells were treated with UV radiation (50 J/m^2) or γ radiation (IR; 10 Gy). Cell lysates were harvested 2 h later and immunoblotted with antibodies against the indicated molecules.

3.5   MDM2 regulates p53 protein turnover through its E3 activity

To test whether ZNF668 blocks MDM2-mediated p53 ubiquitination and degradation, cells were treated with the proteasome inhibitor MG132. As expected, MG132 treatment abolished the effect of ZNF668 on p53 level (Figure 19A, left). Moreover, we detected decreased ubiquitination of p53 when ZNF668 was overexpressed (Figure 19A, right), suggesting a role of ZNF668 in counteracting MDM2-mediated p53-ubiquitination. Interestingly, we also found that ZNF668 facilitated MDM2 autoubiquitination (Figure 19B). This observation was consistent with previous findings that L11 differentially regulates MDM2 and p53 ubiquitination (Dai et al., 2006). We speculate that in addition to directly blocking MDM2-p53 interaction (Figure 17), ZNF668 might also alter MDM2's

function by inducing autoubiquitination of MDM2 molecules. The dysregulated ubiquitination of MDM2 might further facilitate the stabilization of p53 by altering MDM2 E3 ligase activity or MDM2's binding affinity for its substrates.
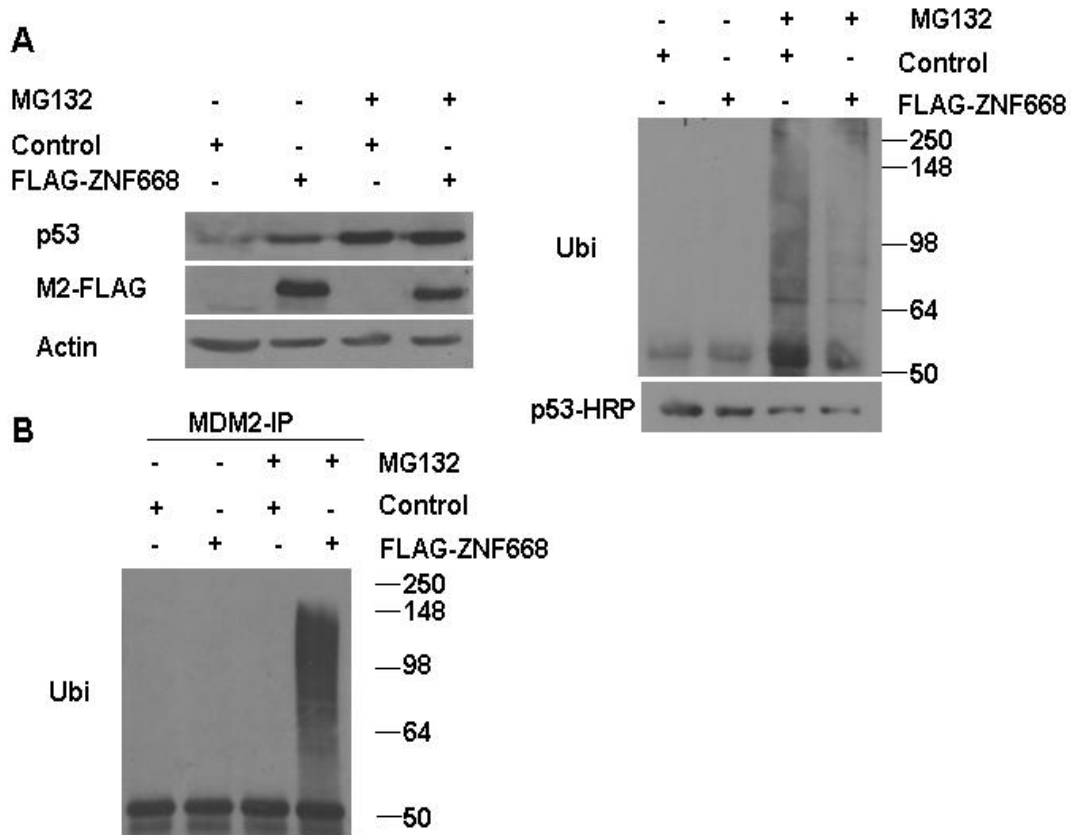
Figure 19. ZNF668 affects p53 and MDM2 ubiquitination. (A) ZNF668 decreases endogenous p53 ubiquitination. U2OS cells were transfected with Flag-ZNF668 and treated with or without 10 μM MG132 for 6 h. Cell lysates were harvested and analyzed. p53 levels were normalized by loading proportionally different amounts of cell extracts. Cell lysates were immunoprecipitated with p53 antibody and immunoblotted as indicated. (B) ZNF668 increases endogenous MDM2 ubiquitination. U2OS cells were transfected with Flag-ZNF668 and treated with or without 10 μM MG132 for 6 h. Cell lysates were harvested and analyzed. Cell lysates were immunoprecipitated with MDM2 antibody and immunoblotted as indicated.

3.6   ZNF668 suppresses tumorigenicity of human breast cancer cells

Since we found that ZNF668 regulates the stability of p53 protein, we posited that ZNF668 might itself function as a tumor suppressor gene. To test this possibility, we first examined the proliferation of cells ectopically expressing ZNF668. Overexpression of ZNF668 repressed proliferation of MCF7 cells (Figure 20A) and their ability to grow in soft agar (Figure 20B). In contrast, knockdown of ZNF668 increased soft agar colony formation in nontumorigenic MCF10A cells (Figure 20B).
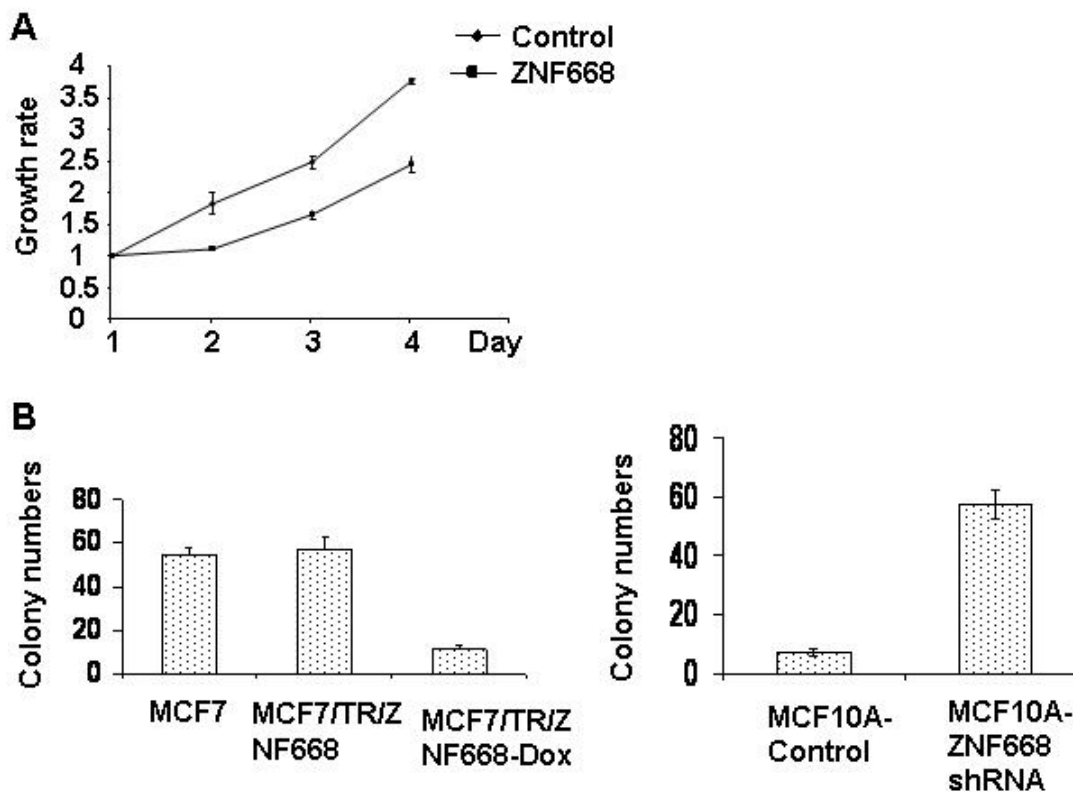
Figure 20. ZNF668 suppresses proliferation and transformation of human breast cancer cells. (A) Expression of ZNF668 reduces the proliferation of MCF7 cells. Control or ZNF668-overexpressing MCF7 cells were seeded in a 96-well plate at 5×10^3 cells per well. Cell proliferation was measured by MTT assay for 4 days. Results represent the mean ± SD of three independent experiments. (B) Expression of ZNF668 reduces the cell transformation of MCF7 cells. Knockdown of ZNF668 increases the transformation of MCF10A cells. ZNF668-expressing MCF7 cells or ZNF668-knockdown MCF10A cells were seeded in 0.35% agarose gel at 1×10^4 or 5×10^3 cells per plate. Viable colonies of MCF7 or MCF10A clones in three plates were counted; all soft agar assays were performed in triplicate. Results represent the mean ± SD of three independent experiments.

Given that ZNF668 effectively suppressed *in vitro* cellular transformation, we next tested whether ZNF668 suppressed tumorigenicity *in vivo*. Mice were injected in the mammary glands with ZNF668-overexpressing or vector-control MCF7 cells and monitored weekly for tumor formation. By week 8, all 10 mice injected with ZNF668-overexpressing clones remained tumor free, whereas all five of the control mice had developed tumors (Figure 21), indicating the ability of ZNF668 to suppress tumorigenicity *in vivo*.
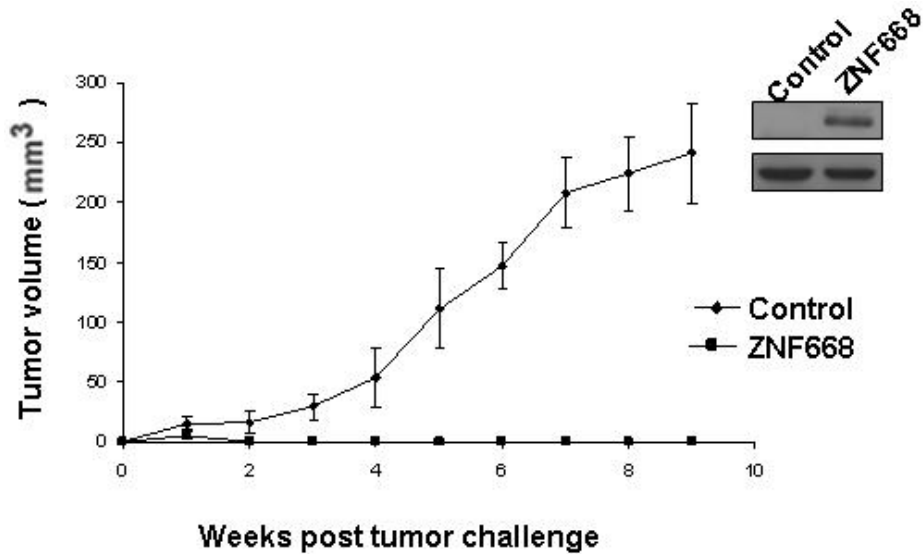
Figure 21. ZNF668 suppresses tumor growth. ZNF668-overexpressing or vector-control MCF7 cells were injected into the mammary glands of nude mice (5×10^6 cells per mouse), and tumor volumes were measured every 2 days. Results represent the mean ± SD of three independent experiments.

3.7 ZNF668 suppresses tumorigenicity in both p53-dependent and independent-manners

To determine whether p53 is the only target mediating ZNF668's activity in suppressing cellular transformation, we also performed *in vitro* cell proliferation and transformation assays using MCF7-p53-knockdown cells. Both MCF7-control and MCF7-p53-knockdown cells were transfected with FLAG-tagged ZNF668, and cells were selected with G418 for 10 days. Overexpression of ZNF668 was confirmed by Western blotting analysis (Figure 22A). ZNF668 suppressed the proliferation and transformation phenotype (Figure 22B and C) of MCF7-p53-knockdown cells, but to a lesser extent than it suppressed the proliferation and transformation phenotype of MCF7-control cells, indicating that

ZNF668 could suppress cell transformation through both p53-dependent and p53-independent pathways.
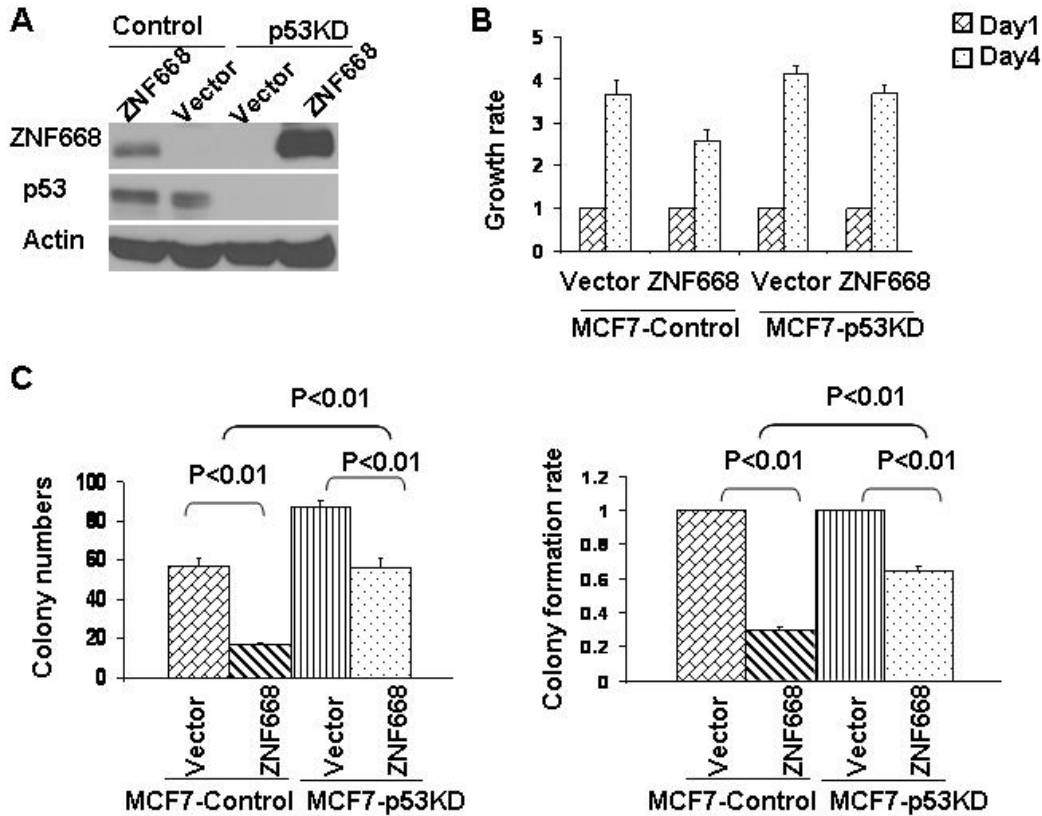
Figure 22. ZNF668 suppresses transformation phenotype of human breast cancer cells partially through p53. (A) Expression of Flag-ZNF668 in MCF7 control and MCF7-p53-knockdown (KD) cells. Cells were transfected with Flag-ZNF668. Two days later, cells were split and selected with G418 for another 10 days. Cell lysates were harvested and immunoblotted with antibodies against the indicated molecules. (B) Expression of ZNF668 reduces the proliferation of both MCF7 control and MCF7-p53-knockdown cells. Cells were transfected with Flag-ZNF668 and seeded in a 96-well plate at 5×10^3 cells per well. Cell proliferation was measured by MTT assay for 4 days. The growth rates of cells were calculated. Results represent the mean ± SD of three independent experiments. (C) ZNF668 suppresses cell transformation in both MCF7 control and MCF7-p53-knockdown cells. Cells were transfected with Flag-ZNF668 and seeded in 0.35% agarose gel at 5×10^3 cells per plate. Left: viable colonies in three plates were counted. Right: the colony formation rate was calculated; all soft agar assays were performed in triplicate. Results represent the mean ± SD of three independent experiments. Student's *t*-test.

3.8   Discussion

Our findings identify ZNF668 as a novel nucleolar protein that interacts with known nucleolar proteins NPM and NS. Recent studies have shown that the function of nucleolar proteins is not limited to participating in ribosomal biogenesis. Indeed, the nucleolus appears to be the site for convergence of the p53 pathway through regulation of different nucleolar proteins under various types of cellular stress (Kamijo et al., 1998; Colombo et al., 2002; Tsai and McKay 2002; Lohrum et al., 2003; Dai et al., 2006). Thus, the nucleolar localization of ZNF668 and its interaction with known nucleolar proteins suggested a potential role of ZNF668 in p53 regulation.

By forward and reverse genetic approaches, we clearly demonstrated a critical role of ZNF668 in p53 protein stabilization through inhibition of the p53 negative regulator, MDM2. Our findings further suggest that ZNF668 regulates MDM2 through a direct interaction between ZNF668 and MDM2-p53 complex since ZNF668 interacted with MDM2 and p53 *in vivo* and *in vitro* and since ZNF668 interfered with the MDM2-p53 interaction. It has been shown that physical interaction between MDM2 and p53 is a prerequisite for MDM2 to ubiquitinate p53 (Haupt et al., 1997; Kubbutat et al., 1997; Michael and Oren 2003). Therefore, our results strongly support alterations in direct protein-protein interactions as a mechanism by which ZNF668 regulates p53 and MDM2-mediated p53 ubiquitination *in vivo*. Our findings do not, however, exclude the possibility that ZNF668 could also regulate p53 through other pathways. For example, p53 can be regulated at the posttranslational level through

modifications such as phosphorylation and acetylation. ZNF668 could serve as a platform for assembly of complexes needed for p53 posttranslational modifications in response to cellular stress and thereby promote p53 activation and stabilization. Future experiments will be needed to determine whether other mechanisms besides direct protein-protein interactions may also be involved in ZNF668-mediated p53 regulation.

Recent reports indicate that the central acidic domain of MDM2 is important for controlling p53 activity (Ma et al., 2006; Wallace et al., 2006). Indeed, this domain was previously shown to be required for p53 ubiquitination and degradation (Argentini et al., 2001; Meulmeester et al., 2003). We found in the current study that deletion of residues 212-296 of MDM2 attenuated the interaction between ZNF668 and MDM2, indicating a mechanism by which ZNF668 could attenuate MDM2-mediated ubiquitination and degradation of p53. Indeed, it has previously been suggested that the ubiquitination of p53 is a stepwise process accompanied by a conformational alteration (Gu et al., 2001). Therefore, it is possible that binding of ZNF668 to the central domain of MDM2 induces a conformational change in both MDM2 and p53 that suppresses the ubiquitination of p53 but facilitates the autoubiquitination of MDM2 (Figure 23).
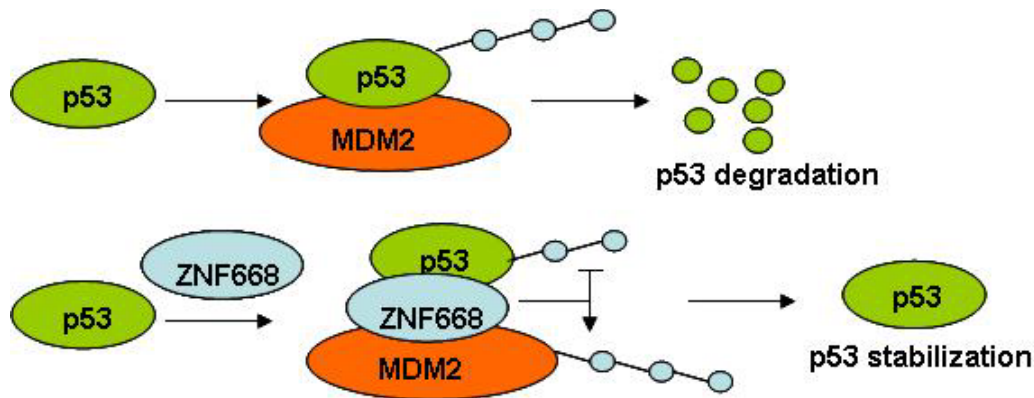
Figure 23. Schematic model of how ZNF668 interaction with MDM2 protects p53 from ubiquitin-mediated degradation. p53 is maintained at a low basal level in normal cells by MDM2-mediated degradation. When ZNF668 is present, it associates with both p53 and MDM2 and prevents MDM2-mediated degradation of p53 by disrupting the interaction between MDM2 and p53. The presence of ZNF668 leads to an increase of MDM2 auto-ubiquitination and decrease of p53 ubiquitination, which stabilizes p53.

Balancing MDM2 autoubiquination and ubiquination of its substrates such as p53 highly depends on the association between MDM2 with p53 (Stommel and Wahl 2004; Ronai 2006). DNA-damage induced phosphorylation of MDM2 results its dissociation with modified p53 and leads to accelerated MDM2 autoubiquitination and consequently, p53 stabilization and activation (Stommel and Wahl 2004). Our data indicated that ZNF668 could block the interaction between MDM2 and p53 (Figure 17), thus facilitated MDM2 autoubiquitination and p53 stabilization. Interestingly, it has been shown that L11 and ARF (Xirodimas et al., 2001; Brignone et al., 2004; Dai et al., 2006; Ronai 2006) can also facilitate autoubiquitination of MDM2 by preventing the recruitment of ubiquitinated MDM2 to the proteasome, either through potential adaptor proteins or by concealing MDM2 binding sites in the proteasome (Brignone et al., 2004;

Ronai 2006), thus inhibiting the postubiquitination pathway. It is therefore tempting to speculate that many p53 regulators, such as ARF and ZNF668, stabilize p53 protein both by directly interfering with MDM2-p53 interaction and by regulating MDM2 posttranslational modifications such as autoubiquitination to alter MDM2 E3 ligase activity or binding affinity toward its substrates.

Our studies also identified ZNF668 as a potential tumor suppressor in breast cancer. *ZNF668* was previously identified as a highly mutated gene in breast cancer. However, the implications of the mutation of *ZNF668* in breast cancer development are entirely unknown. Our studies strongly indicate p53 to be an important target of ZNF668. Indeed, the two ZNF668 mutants that we tested had impaired ability to stabilize p53 further support this notion. Of course, we cannot rule out impacts of ZNF668 on proteins other than p53. Indeed, the fact that ZNF668 also suppressed cell transformation in p53-mutated cells (Figure 22), albeit to a lesser degree than in cells with wild-type p53, indicates that ZNF668 can suppress cell transformation through both p53-dependent and p53-independent pathways. In future studies, we will identify the p53-independent ZNF668 targets and dissect the function of ZNF668 in both p53-dependent and p53-independent pathways.

PART II.   ROLE OF ZNF668 IN DNA REPAIR AND CHROMATIN REMODELING

CHAPTER 4 INTRODUCTION

4.1   Tumor suppressor and DNA repair

Tumor suppressor genes have diverse functions. The role of tumor suppressors in DNA damage response is well established. Many tumor suppressors, such as *ATM, BRCA1, BRCA2, NBS1, CHK2 and p53*, are involved in different steps of DNA damage response pathway, which leads to checkpoint response, increased DNA repair or cell apoptosis (Liang et al., 2009). Loss of the function of tumor suppressors leads to genetic instability, deficient DNA repair or impaired damaged cell death and results in tumor formation. For example, the tumor suppressor genes *BRCA1* and *BRCA2* play roles in DNA damage repair (Venkitaraman et al., 2001). *BRCA2* belongs to the tumor suppressor gene family and the protein encoded by this gene is involved in the repair of chromasomal damage with an important role in HR repair of DNA double strand breaks (Venkitaraman et al., 2001). Understanding the role of tumor suppressors in DNA damage response pathway provides an alternative opportunity for improving disease detection and management.

4.2   DNA damage response pathways

Cellular DNA is continuously exposed to various DNA damage signals (Hoeijmakers et al., 2009). Endogenous signals including spontaneous DNA alterations during replication, reactive oxygen species generated by cellular metabolism activity and intercross between DNA bases. Exogenous signals such as chemicals, UV radiation and ionizing radiation can cause different types of DNA lesions.

DNA damage response is a highly conserved but complicated process with multiple steps including the initial recognition and signaling of DNA lesions, the access of repair proteins to the damaged DNA and the restoration of the chromatin to its original state (Harper et al., 2007; Rouse et al., 2002). Although there are different types of DNA repair in response to different classes of DNA lesions, DNA damage responses usually occur by a common general process (Figure 24). Right after the DNA damage, DNA damage sensors detect the damage and recruit transducer kinases such as ATM/ATR/DNA-PK and mediators such as MDC1 to the damage sites. The kinases will activate downstream effectors with the coordination of mediators. Mediators mediate the signal from the transducer kinases to the effectors. Effectors execute the DNA damage response, which includes activation of cell cycle checkpoints, repair of the damage, transcriptional regulation and activation of apoptosis if the damage is too severe to be repaired (Bartkova, 2007).
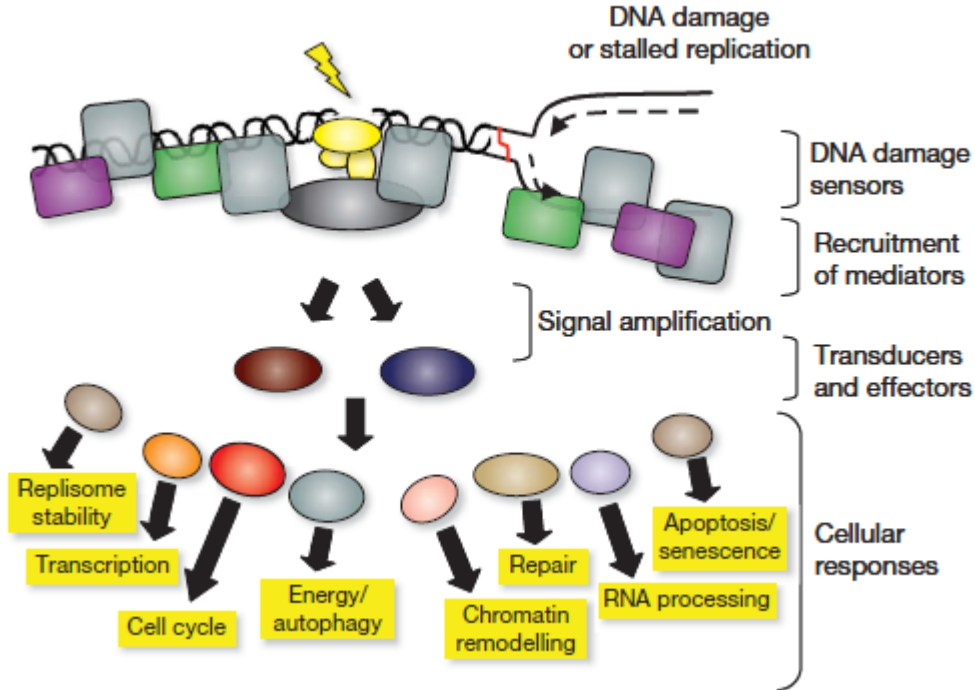
Figure 24. A common model for the DNA damage response. The presence of a lesion in the DNA, which can lead to replication stalling, is recognized by various sensor proteins. These sensors initiate signaling pathways that have an impact on a wide variety of cellular processes. (Stephen P. Jackson & Jiri Bartek, 2009)

4.3   DNA repair pathways

To preserve its genomic integrity, cells need to develop different types of repair pathways to fix the various types of DNA damage. For example, base-excision repair (BER) is important for the repair of DNA alterations caused by chemicals (Jiricny et al.,2006); mismatch repair (MMR) can replace the misrepaired DNA bases with correct bases; nucleotide excision repair (NER) repairs more complex lesions, such as pyrimidine dimers and intrastrand crosslinks; single-strand break repair (SSBR) repairs single strand breaks caused by UV irradiation; double strand breaks (DSBs) are mainly repaired by

homologous recombination (HR) and nonhomologous endjoining (NHEJ) (Caldecott, 2008; West, 2003).

For DNA double strand breaks, HR uses the undamaged sister chromatids as template to accurately restore the break. In contrast, NHEJ repairs the break by direct ligation of the two broken ends, which can result in inaccurate relegation of the breaks and cause DNA deletions. Cells activate different repair pathway in co-ordinance with specific cell cycle phase (Figure 25) (Branzei et al., 2008; Mandal et al., 2010).
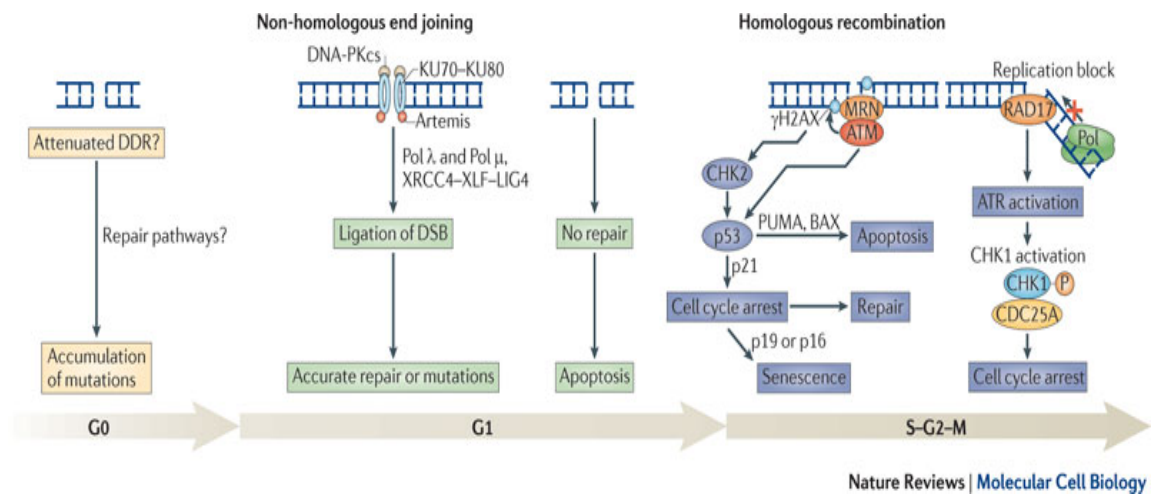
Figure 25. DNA double strand break repair during cell cycle. In G1, double strand breaks are recognized by the KU dimer to provide a scaffold and recruit the repair proteins to perform NHEJ repair. In S and G2 cells, DNA lesions are detected and processed by the MRE11–RAD50–NBS1 (MRN) complex. This leads to recruitment and activation of ataxia-telangiectasia mutated (ATM) signalling pathway and leads to transient cell cycle arrest for DNA repair. Replication blocks during S phase activate ataxia-telangiectasia- and RAD3-related (ATR) activation and lead to cell cycle arrest (Mandal et al., 2010). HR repair is the major repair pathway during G2/S phase.

4.4   Chromatin dynamics and gene regulation

In eukaryotic cells, genomic DNA is packed with histones to form the nucleosomes, which are further packaged into a condensed chromatin structure. Nucleosomes are comprised of 147 bp of DNA wrapped around a hetero-octamer of histones H2A, H2B, H3, and H4 (Khorasanizadeh, 2004). Generally, the condensed chromatin structure will suppress cellular processes that involve DNA transactions such as DNA replication, gene transcription and DNA double strand break repair (Felsenfeld et al., 2003).

Gene transcription initiation involves the opening of chromatin structure at the promoter region to allow access for transcription factors to bind DNA sequences (Wollffe 1998). In order to overcome the chromatin barrier, cells have developed several pathways to relax the chromatin structure. The ATP-dependent chromatin remodeling complexes utilize the energy from ATP hydrolysis to displace nucleosomes and induce conformational changes in chromatin (Lusser et al., 2002; Peterson et al., 2002; Flaus et al., 2004). The posttranslational modifications of the core histones, such as phosphorylation, methylation, ubiquitination and acetylation (Jenuwein et al., 2001; Turner, 2002; Kouzarides et al., 2007) have emerged as another important mechanism by which cells regulate the structure and accessibility of chromatin. Moreover, cells alter the composition of nucleosomes through the incorporation of histone variants that can directly or indirectly alter the accessibility of DNA within chromatin (Kamakaka et al., 2005; Henikoff et al., 2005).

4.5   Chromatin dynamics and DNA repair

The chromatin structure also has an impact on the DNA damage response because in the DNA damage pathway, the condensed chromatin structure blocks the DNA repair machinery to access the damaged chromosomal DNA lesions. The chromatin structure is modulated by several mechanisms in response to DNA damage.

ATP-dependent chromatin remodeling complexes regulate the chromatin structure in response to DNA damage signal. With the DNA damage signal, ATP-dependent chromatin remodelers such as INO80, SWR1 Swi2-family proteins and SWI/SNF chromatin remodeling factors are recruited to the double strand breaks (Narlikar et al. 2002; Morrison et al., 2004; van Attikum et al., 2004; Shim et al., 2005; Chai et al., 2005). These remodelers are responsible for efficient initiation of DNA damage response including the induction of histone phosphorylation. They are also responsible for the followed histone ubiquitination, nucleosome reassemble and the exchange of histones in the DNA damage breaks.

Combinations of the posttranslational modifications in the core histones will form so-called "histone code" to regulate different types of cellular process such as gene regulation, DNA repair and chromatin condensation (Strahl et al., 2000). The posttranslational modifications of the core histones can regulate the structure and accessibility of chromatin. The amino- and carboxy-terminal tails of histones are the regions that frequently be modified because of their location on the chromatin surface. In addition to histone modifications, there are different histone variants that consist of different sequence and play different roles from

canonical histones. For example, one of the major H2A variants, H2AX differs from H2A at various amino acid residues along the entire protein and in its C-terminal extensions. H2AX is phosphorylated in response to the introduction of DNA double-strand breaks, and the phosphorylated H2AX (γ-H2AX) participates in foci formation at sites of DNA damage and plays an important role in the recognition and signaling of DNA Damage. The phosphorylation of H2AX is mediated by ATM/DNA-PK/ATR. ATM and DNA-PK majorly function after ionizing radiation (IR), whereas ATR responds to replication stress and UV irradiation (Rogakou et al., 1998; Stiff et al., 2004; Czornak et al., 2008; Cimprich et al., 2008). Studies have shown that phosphorylated-H2AX (γ-H2AX) serves as a platform to recruit and retain DNA repair factors to the DNA damage sites without affecting chromatin organization (Celeste et al., 2003). After DNA damage, the γ-H2AX is expanded around the double strand break region and provides docking sites for other DNA damage and repair proteins such as 53BP1 and BRCA1.

The re-open of condensed chromatin structure for efficient DNA repair involves induced histone acetylation at the DSB sites. After the incorporation of γ-H2AX, other core histones such as H2A, H3 and H4 are modified by acetylation and contribute to the destabilization of the nucleosome and the opening of chromatin. Other histone modifications such as ubiquitylation and sumoylation also have roles in histone exchange and the recruitment of the chromatin remodeling complexes (Attikum et al., 2009).

After repair has been completed, γ-H2AX is eliminated from the chromatin surrounding the repaired DSB, by either replacement with H2AZ variant (Mizuguchi et al., 2004) or dephosphorylation by phosphatases such as hPP2A, hPP4C, hPP6 and hWip1 (Chowdhury et al., 2005; Chowdhury et al., 2008; Macurek et al., 2010; Douglas et al., 2010).

4.6 Histone acetylation and its role in transcription regulation

Among all the posttranslational modifications of histones, histone acetylation by histone acetyltransferase (HAT) complexes has been implicated in both transcriptional regulation and DNA damage repair.

HAT can catalyze the transfer of an acetyl group from acetyl-CoA to the lysine amino groups on the N-terminal tails of histones. In actively transcribed regions of chromatin histones tend to be hyperacetylated, whereas in transcriptionally silent regions histones are hypoacetylated. Histone acetylation can neutralize histone charge and weaken DNA-histone interaction. The acetyl-lysines on histone tails can provide recognition sites for transcription factors involved in either the activation or repression of gene expression. For example, lysine acetylation provides a stable epigenetic mark on chromatin for SWI/SNF and RSC chromatin remodeling complex or HAT complexes to dock and in turn regulate gene expression (Hassan et al., 2002).

In addition, other covalent modification of histones, which is called as histone code, will provide an epigenetic marker for gene expression (Strahl et al., 2000). The complexity of the histone code also influences recruitment of

HAT to promoters. For example, phosphorylation of histone H3 serine 10 can enhance the targeting of Gcn5 HAT to the INO1 promoter in yeast (Lo et al., 2001). In mammals, methylation of H3 lysine 9 inhibits HAT targeting and promoter acetylation (Rea et al., 2000). All of these histone modifications will coordinately provide a unique signal for specific gene activation or suppression.

4.7   Histone acetylation and DNA repair

Recent studies have implicated the role of chromatin acetylation by HAT complexes in DNA-damage detection and DNA repair (Ikura et al., 2000; Carrozza et al., 2003; Murr et al., 2006). For example, Tip60 is one of the HATs that acetylate H2A and its variant H2AX on lysine 5 (K5). In drosophila, Tip60's activity on H2Av acetylation is important for histone variant H2AZ exchange with phosphorylated-H2AX, which is important for DNA repair (Kusch et al., 2004). Acetylation of H2AX (Kusch et al., 2004; Downs et al., 2004) and histone H4 (Murr et al,. 2006; Bird et al., 2002; Downs et al., 2004) is required for the formation of open chromatin structures at DSBs and is critical for the access of the DNA repair machinery to DSBs (Murr et al., 2006; Bird et al., 2002; Kusch et al., 2004; Jha et al., 2008). Recent studies also showed that H3 acetylation on lysine 56 (K56) is required for the appropriate nucleosome assembly and facilitates DNA double strand break repair (Li et al., 2008; Chen et al., 2008). Therefore, the increased acetylation of histones at DNA lesions after DNA damage can contribute to DNA double strand break repair by regulating histone variant exchange, remodeling chromatin structure and recruiting DNA repair proteins to the sites of DNA damage. However, the precise underlying

mechanism mediating enzymes responsible for the histone modifications and their recruitment to DNA lesions remains poorly understood.

4.8 Hypothesis and project goals

ZNF668 (zinc finger protein 668) was initially identified and validated as a highly mutated gene in breast cancer (Sjoblom et al., 2006). Our preliminary data showed that *ZNF668* functions as a potential tumor suppressor and it is involved in p53 regulation. Since tumor suppressors play an important role in DNA damage response, we hypothesize that, as a novel tumor suppressor and a key regulator of p53, ZNF668 might participate in DNA damage response.

In this part of the study, we aim to demonstrate the functional interaction among ZNF668, histones, and chromatin. We study the role of *ZNF668* as a novel tumor suppressor gene in regulation of histone acetylation and chromatin structure after DNA damage and reveal its mechanistic function in regulating DNA damage repair.

CHAPTER 5 MATERIALS AND METHODS

5.1 Cell Culture and Transfection

U2OS cells were purchased from the American Type Culture Collection. U2OS cells were maintained in McCoy's 5A medium (Cellgro) supplemented with 10% fetal bovine serum (FBS) with glutamine, penicillin, and streptomycin.

Cells were incubated at 37°C in a humidified incubator with 5% CO_2 and transfected with Fugene 6 (Roche), or Oligofectamine (Invitrogen).

5.2 Plasmids and small interfering RNAs (siRNAs)

To generate FLAG-ZNF668, full-length ZNF668 cDNA was amplified by polymerase chain reaction (PCR) and subcloned into pCMV5-3 x FLAG vector (Sigma). The siRNA-resistant ZNF668 was created from 3 x FLAG-ZNF668 using the QuickChange II Site-Directed Mutagenesis Kit (Stratagene). FLAG-H2AX plasmid was a gift from Dr. Jiri Lukas. ZNF668 knockdown was achieved by RNA interference using siRNA (Dharmacon). The ON-TARGETplus ZNF668 siRNA duplex and ON-TARGETplus SMARTpool ZNF668 siRNA mix were purchased from Dharmacon Research, Inc. ON-TARGETplus nontargeting siRNA was used as a control for the siRNA reactions. RNA duplexes or SMARTpool (final concentration 100 nM) were transfected into the U2OS cells using Oligofectmine according to the manufacturer's protocol (Invitrogen). Cells transfected with ZNF668 siRNA were incubated for 2 or 3 days. A decrease in the respective protein levels was verified by Western blotting.

5.3 Antibodies and Reagents

Rabbit polyclonal anti-ZNF668 antibody (Proteintech Group, Inc.) was generated as described in Chapter 2.3. Anti-FLAG M2-agarose affinity gel was purchased from Sigma. RPA antibody was purchased from NeoMarkers. Phospho-RPA32 (S4/S8) antibody was purchased from Bethyl. Rad51 was

purchased from Calbiochem, ATM, phospho-H2AX were purchased from Cell Signaling. Histone H2A (acetyl K5) antibody was from Abcam. Anti-Tip60 and phospho-ATM were purchased from Millipore. Fluorochrome-conjugated secondary antibodies were purchased from Jackson ImmunoResearch Laboratories. Cisplatin was purchased from Sigma. Sodium butyrate and trichostatin were obtained from Sigma and used at 5 mM or 200 ng/mL respectively.

5.4   Affinity purification of ZNF668 and H2AX protein complex

U2OS cells were transiently transfected with empty FLAG plasmid, FLAG-ZNF668 or FLAG-H2AX plasmid. Forty-eight hours later, whole cellular extracts were prepared with RIPA buffer (50 mM Tris-HCl pH 7.4, 1% NP-40, 10% sodium deoxycholate, 150 mM NaCl, 1 mM EDTA, 1 mM phenylmethylsulfonyl fluoride, 1 mM sodium orthovanadate, and 1 mM NaF) and immunoprecipitated with anti-FLAG M2 affinity gel (Sigma) overnight. Bead-bound immunocomplexes were eluted with 3XFLAG peptide (Sigma). Immunocomplexes were separated by 7% or 12% sodium dodecyl sulfate-polyacrylamide gel electrophoresis (SDS-PAGE) and transferred to Protran nitrocellulose membrane (Fisher Scientific). Membranes were blocked in Tris-buffered saline-0.1% Tween 20 (TBS-T)/5% (w/v) milk for 1 h at room temperature and were then incubated with primary antibodies diluted in TBS-T/5% (w/v) milk for 2 h at room temperature or overnight at 4°C. Subsequently, membranes were washed with TBS-T and incubated with horseradish

peroxidase secondary antibody (1:5000) (Jackson ImmunoResearch) diluted in TBS-T/5% skim milk. Membranes were washed in TBS-T, and bound antibody was detected by enhanced chemiluminescence (GE Healthcare).

5.5   Immunofluorescent Microscopy

For detection of DNA damage induced foci of p-RPA34, RPA34 and Rad51, cells were treated with cytoskeleton and stripping buffer, fixed with 4% paraformaldehyde and then permeabilized with 0.5% NP-40 and 1% Triton X-100. The primary antibodies were as follows: mouse anti-RPA (1:1000), rabbit anti-pRPA (1:1000) and rabbit anti-Rad51 (1:500). Primary antibodies were incubated for 2h at room temperature (RT) and secondary antibodies donkey anti-rabbit conjugated Alexa 594 and goat anti-rabbit conjugated Alexa 488 were incubated for 1 h at RT. Slides were mounted in medium containing DAPI (Vector laboratories, Burlingame, CA) and analyzed under a fluorescence microscope. The number of foci per cell was scored for at least 50 cells per sample. For chromatin remodeling, cells were incubated in the presence of sodium butyrate (5 mM) after ultraviolet (UV) or ionized radiation (IR) exposure before staining for DNA damage foci was performed.

5.6   Immunoblotting, chromatin fractionation and Immunoprecipitation

Cells were washed in phosphate-buffered saline and lysed in urea buffer or modified RIPA buffer. For chromatin fractionation, cells were lysed in (10 mM HEPES pH 7.9, 1.5 mM $MgCl_2$, 10 mM KCl, 0.34 M sucrose, 10% Glycerol, 1

mM dithiothreitol, and 0.1% Tirton X-100), and nuclear extracts were lysed in buffer (3 mM EDTA, 0.2 mM EGTA and 1 mM dithiothreitol). After clarification, cell pellets were resuspended in SDS sample buffer. For immunoprecipitation, cells were lysed in RIPA buffer. After clarification, cell lyses were immunoprecipitated with specific antibodies (RPA or ZNF668). The immunocomplexes were collected on Protein A/G plus-conjugated agarose beads (Santa Cruz Biotechnology). Cellular lysates or immunocomplexes were subjected to SDS-PAGE analysis.

5.7   Cell survival and proliferation assays

U2OS cells were transfected with ZNF668 siRNAs and 72 h after the transfection, cells were plated at low density and irradiated with UV or IR. Cells were incubated for 2–3 weeks to allow colonies to form. Colonies were detected by staining with 2% methylene blue/50% ethanol. Colonies containing 50 or more cells were counted. For proliferation assay, cells transfected with ZNF668 siRNAs were seeded in 96 well plates and treated with various doses of cisplatin. 72 h after the treatment, MTT assay was performed to measure cell viability.

5.8   HR repair analysis

U2OS cells containing a single copy of the HR repair reporter substrate DR-GFP in a random locus were generated as previously described (Peng et al., 2009). U2OS-DR-GFP cells were transfected with ZNF668 siRNA with or without

siRNA-resistant FLAG-ZNF668. 48 hours after transfection, cells were transfected with pEGFP-C1 as for transfection efficiency control or pCBASce plasmid for detection of HR repair efficiency. 48 hours later, GFP positive cells were detected by flow cytometry analysis. Cellquest software (Becton Dickinson, San Jose, CA) is used for the acquisition and analysis of FACS data. For chromatin remodeling recovery experiments, cells were incubated for 16 hr in sodium butyrate (5 mM) or trichostatin (200 ng/mL) to induce chromatin remodeling before analysis by flow cytometry.

5.9   PCR analysis of I-SceI-induced DNA cutting

To assay the cutting efficiency of I-SceI in cells transfected with control or ZNF668 siRNA, genomic DNA was extracted at different time points after I-SceI transfection and adjusted to equal concentrations. Semi-quantitative PCR was carried out using the primers around the DSB site (30 cycles). Beta-actin primers (Applied biosystems) were used as an internal control (25 cycles).

5.10   Cell cycle analysis

Cells from HR repair analysis were fixed in 70% cold ethanol (-20°C) overnight. After washing with cold phosphate-buffered saline (PBS), cells were incubated in staining solution (40 µg/mL propidium iodide, 50 µg/mL RNAase A and 0.05% Triton X-100). Cell cycle analysis was performed at the M. D. Anderson Cancer Center Flow Cytometry Facility.

CHAPTER 6 FUNCTION OF ZNF668 IN DNA REPAIR, HISTONE ACETYLATION AND CHROMATIN STRUCTURE REGULATION

6.1 ZNF668 depletion causes prolonged DNA damage after IR.

To understand the role of ZNF668 in DNA damage response, we first measured cell survival following treatment with DNA damage agents. ZNF668 deficient cells showed an increased sensitivity to ionize irradiation and UV light by clonogenic survival assays (Figure 26A). In a cell proliferation assay, ZNF668 knockdown cells were also sensitive to DNA cross-linking agent cisplatin in a dose dependent manner (Figure 26B). These data indicate ZNF668 depletion cells are sensitive to DNA damage. Therefore, ZNF668 is needed for cell survival in response to a wide variety of DNA damaging agents.
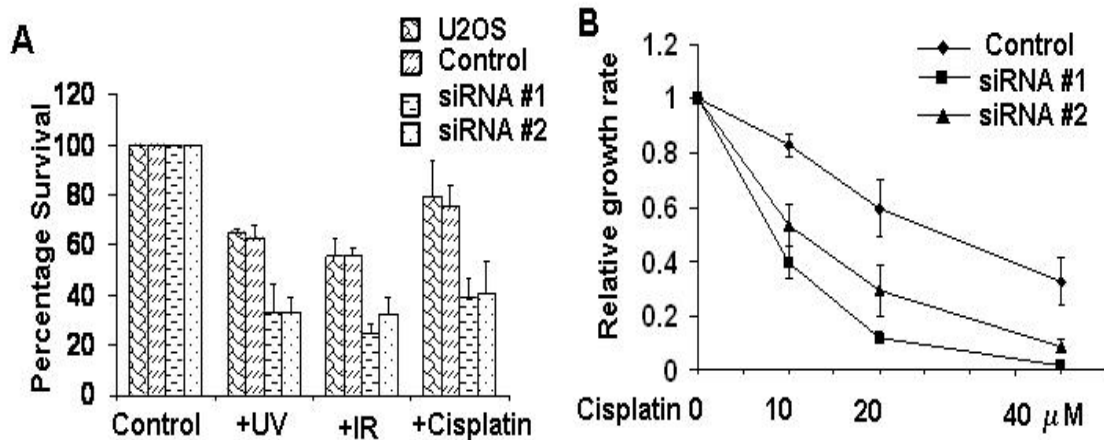
Figure 26. ZNF668 depletion impairs cell survival after DNA damage. (A) ZNF668-depletion impaired cell survival in U2OS cells exposed to UV or IR radiation. Control or ZNF668-depletion U2OS cells were seeded at low density and treated with UV or IR. Viable cell colonies in three plates were counted. The graphs represent the mean ± SD of three independent experiments. (B) ZNF668-depletion impaired cell proliferation in cells exposed to DNA damage

reagent (cisplatin). Control or ZNF668-depletion U2OS cells were seeded in a 96-well plate at 2×10^3 cells per well and treated with various doses of cisplatin. Cell proliferation was measured by MTT assay after 3 days. Results represent the mean ± SD of three independent experiments.

6.2   ZNF668 affects DNA damage repair.

Effective DNA repair of damaged DNA is essential to cell survival. To test

whether ZNF668 plays a role in DNA repair, we measured DNA repair efficiency

in ZNF668 knockdown cells using the neutral comet assay that specifically

measures double-strand breaks (DSB). Although induction of DNA breaks was

similar in ZNF668-containing and ZNF668-deficient cells, ZNF668-deficient cells

exhibited a lower repair efficiency compared to control, thereby indicating that

ZNF668 depletion compromised the repair of DNA breaks (Figure 27).
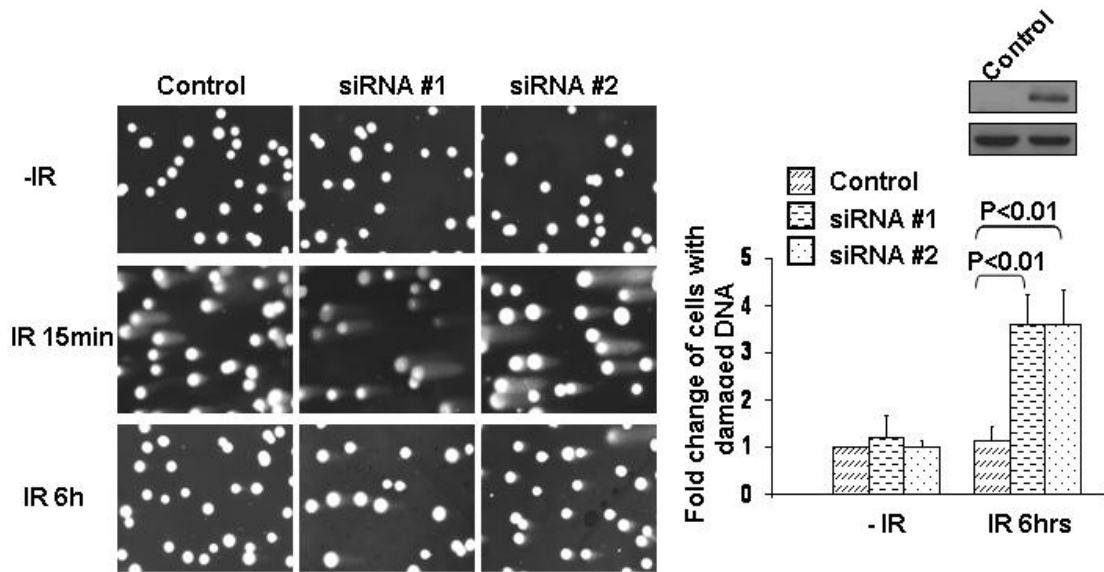
Figure 27. ZNF668-depletion impaires DNA repair. Comet analyses at the indicated time points after exposure of U2OS cells transfected with control siRNA, ZNF668 siRNA #1 or ZNF668 siRNA #2 to ionizing radiation (IR). (Left) Representative images. (Right) Quantitative analysis of three independent experiments and representative western blot analyses showing the knockdown of ZNF668. Percentage of cells with damaged DNA (tail moment greater than 1)

in control cells without IR exposure was set as 1. At least 100 cells were scored in each sample and each value represents the mean ± SD of three independent experiments; Student t-test.

6.3   ZNF668 affects HR repair of DNA double strand breaks.

In mammalian cells, homologous recombination (HR) is one of major conserved pathways involved in DSB repair. To confirm ZNF668's role in DSB repair, we analyzed ZNF668-deficient cells using an HR repair analysis system. In this system, DSB was generated by the introduction of *I-SceI* enzyme and the HR repair efficiency was reflected by the induced-GFP$^+$ signal. We found ZNF668 knockdown cells showed a significant decrease (30%) in HR repair induced-GFP$^+$ cells, indicating defective HR repair (Figure 28A). To rule out the possibility that ZNF668 status may affect the access of *I-SceI* to chromatin DNA, we detected *I-SceI*-induced cutting efficiency by semi-quantitative PCR analysis over a time course by using a primer pair to amplify only the uncut *I-SceI* locus. The *I-SceI* cutting efficiency was similar in ZNF668-containing and ZNF668-deficient cells (Figure 28B).
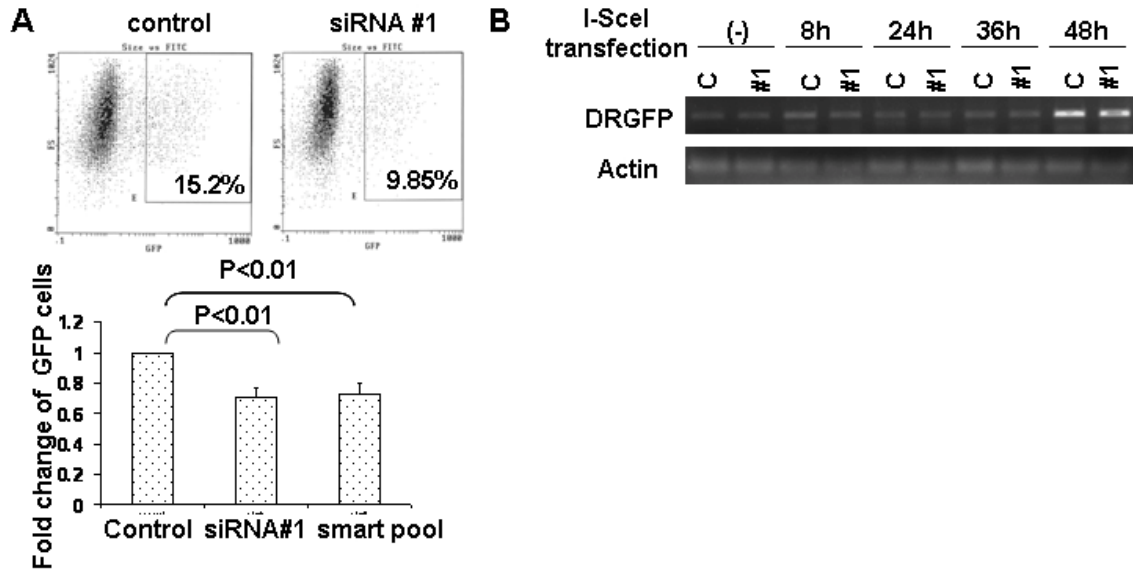
Figure 28. Impaired HR results from the loss of ZNF668. (A) ZNF668-depletion impaired HR repair. ZNF668-depleted cells transfected with ZNF668 siRNA #1 and siRNA smartpool were subjected to HR repair analysis. Each value is relative to the percentage of GFP$^+$ cells in *I-SceI*-transfected cells with control siRNA transfection, which was set to 1 and represents the mean ± SD of three independent experiments; Student's t-test. (B) Cutting efficiency of *I-SceI* was detected by semi-quantitative PCR using a primer pair flanking the DSB site. ZNF668 knockdown cells exhibited no differences in PCR products when compared to control cells at different time points, suggesting similar cutting efficiency of I-SceI in ZNF668 knockdown and control cells.

Furthermore, ZNF668-deficient and ZNF668-containing cells showed similar cell-cycle profiles (Figure 29A), indicating that loss of ZNF668 didn't alter cell-cycle position during *I-SceI* cleavage. Moreover, transfection of ZNF668-containing and ZNF668-deficient cells with a control GFP-expressing vector (pEGFP-C1) resulted in similar numbers of GFP-positive cells (Figure 29B), indicating that the lower frequency of repaired GFP$^+$ cells in ZNF668-deficient cells was not due to a lower transfection efficiency.
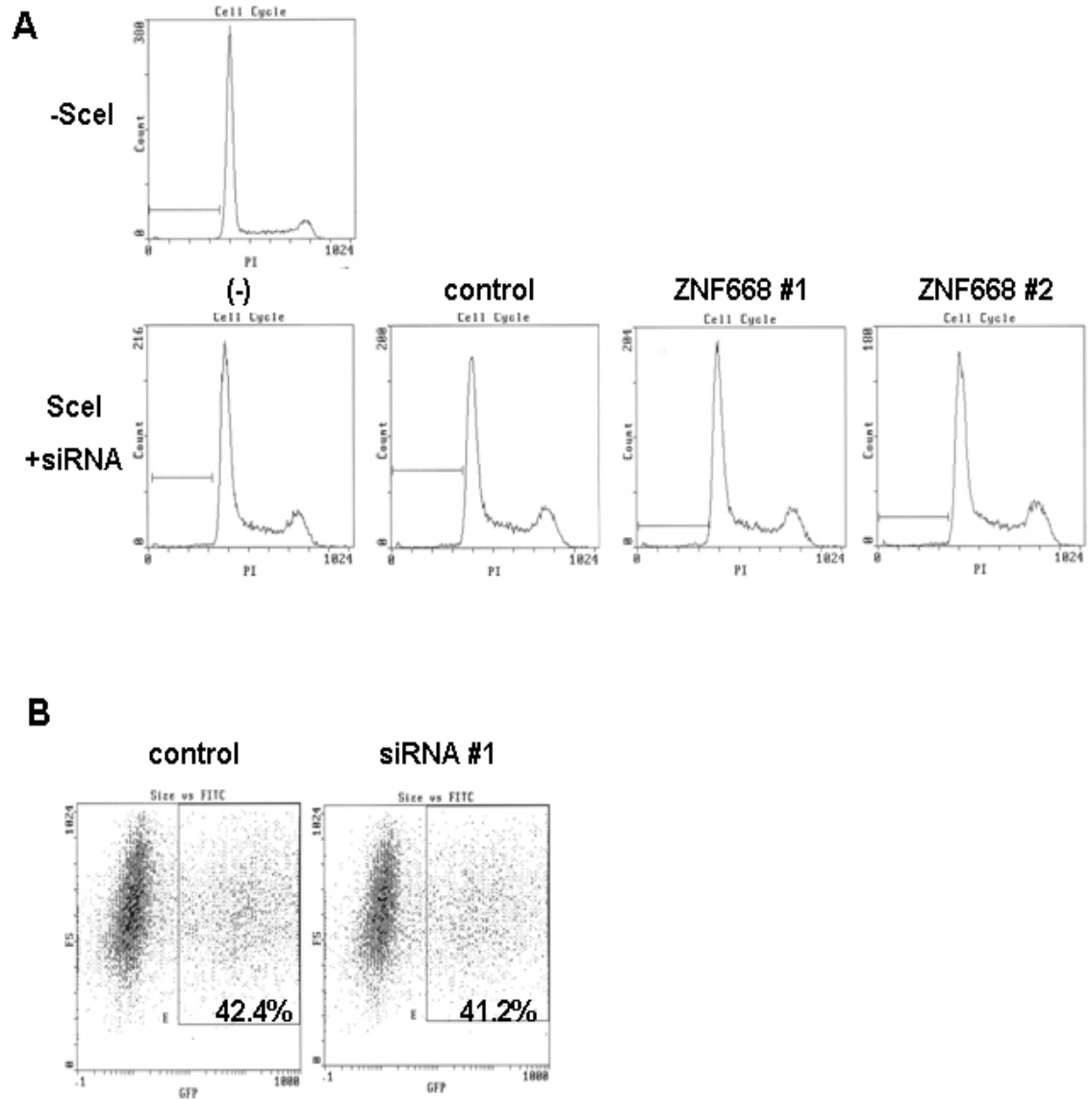
Figure 29. Cell cycle profiles and transfection efficiency of ZNF668-depletion cells with *I-SceI* transfection. (A) Cell cycle profiles of cells that were analyzed for HR repair efficiency. ZNF668 knockdown didn't affect cell cycle distribution. (B) Transfection efficiency was monitored by using a control GFP-expression vector (pEGFP-C1) in indicated cells. ZNF668 knockdown and control cells showed similar transfection efficiency (~40%).

To further test whether the defective HR repair in ZNF668 knockdown cells is specific due to the lack of ZNF668, ectopic siRNA-resistant FLAG-ZNF668 was introduced back to the ZNF668-depleted cells and it was able to restore the HR repair efficiency (Figure 30). All together, our data reveal a critical function of ZNF668 in HR repair.
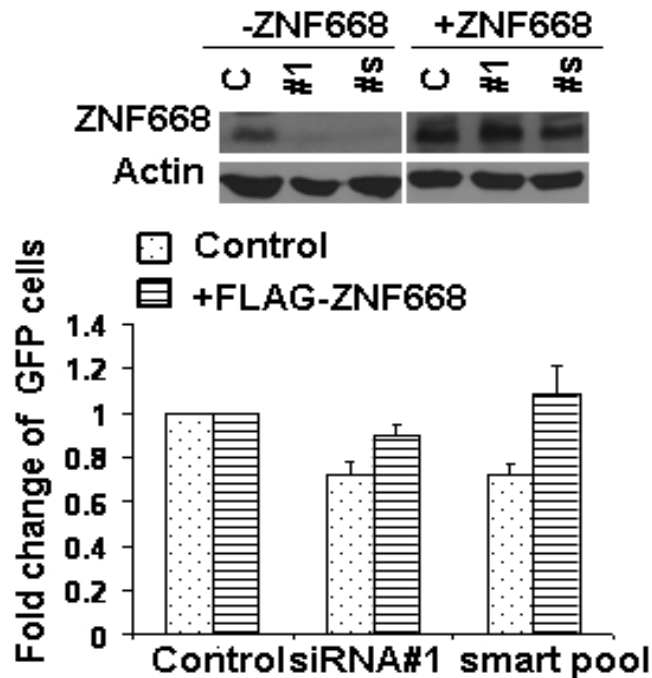
Figure 30. siRNA resistant Flag-ZNF668 restores the defective HR repair in ZNF668-depleted cells. Each value is relative to the percentage of GFP+ cells in I-SceI-transfected cells with control siRNA transfection, which was set to 1 and represents the mean ± SD of three independent experiments. Western blotting analyses to demonstrate the effective ZNF668 knockdown and Flag-ZNF668 overexpression were shown next to the graph.

6.4 ZNF668 doesn't affect ATM/ATR DNA damage detection and signaling.

To test whether DNA-damage detection and signaling is affected in cells lacking ZNF668, we investigated the ATM and ATR signaling pathway after IR or UV irradiation treatment. Treatment with IR induced ATM and Chk2 posphorylation at similar levels in ZNF668-containing and ZNF668-defecient cells (Figure 31A and B).
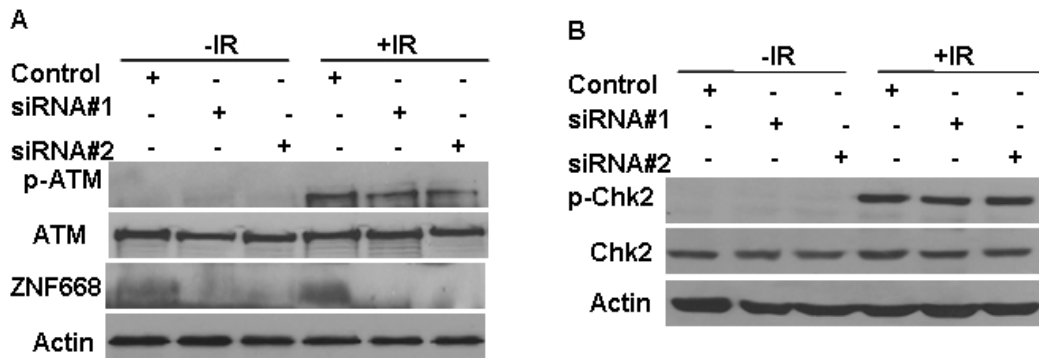
Figure 31. ZNF668-depletion doesn't affect DNA-damage sensing or signaling. (A and B) ZNF668-depletion didn't affect ATM/Chk2 activation. ZNF668-containing and ZNF668-depletion U2OS cells were exposed to IR irradiation (10Gy) and cell lyses were prepared at the indicated time points after treatment. Cell lyses were subjected to Western blot analyses and immunoblotted with antibodies against the indicated molecules. (A) ATM phosphorylation and (B) Chk2 phosphorylation were analyzed.

In parallel, IR induced phosphor-ATM foci were indistinguishable in ZNF668-containing and ZNF668-defecient cells (Figure 32A), indicating that ATM auto-activation and downstream events occur normally in cells lacking

ZNF668. In addition to ATM/Chk2 pathway, UV induced Chk1 phosphorylation showed similar levels in both ZNF668-containing and ZNF668-deficient cells (Figure 32B).
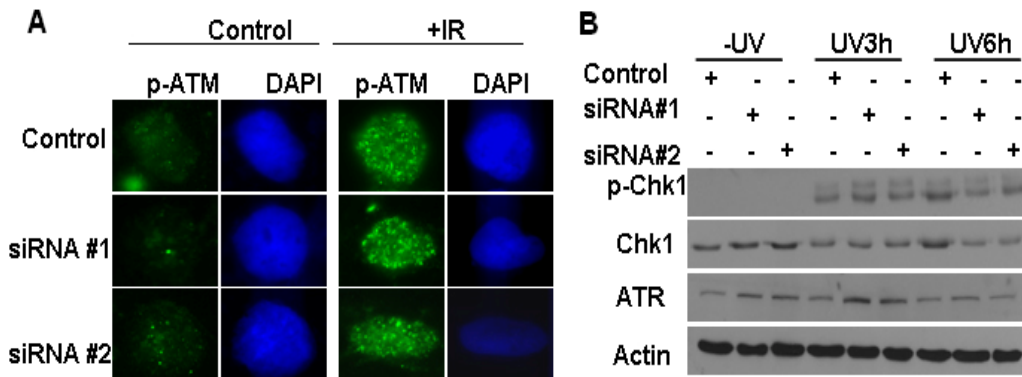
Figure 32. ZNF668-depletion doesn't affect ATM activation and ATR/Chk1 activation. (A) p-ATM foci formation after DNA damage treatment. ZNF668-containing and ZNF668-depletion U2OS cells were exposed to irradiation and stained with phoshoprylated ATM, counterstained with DAPI. (B) ZNF668-depletion didn't affect ATR/Chk1 activation. ZNF668-containing and ZNF668-depletion U2OS cells were exposed to UV irradiation ($50J/m^2$) and cell lyses were prepared at the indicated time points after treatment. Cell lyses were subjected to Western blot analyses and immunoblotted with antibodies against the indicated molecules.

Moreover, the phoshporylation of H2AX was similarly induced in ZNF668-deficient and ZNF668-containing cells after irradiation (Figure 33). These data suggest that the inefficient HR repair in ZNF668-deficient cells is probably not caused by the defects in the DNA-damage signaling cascade.
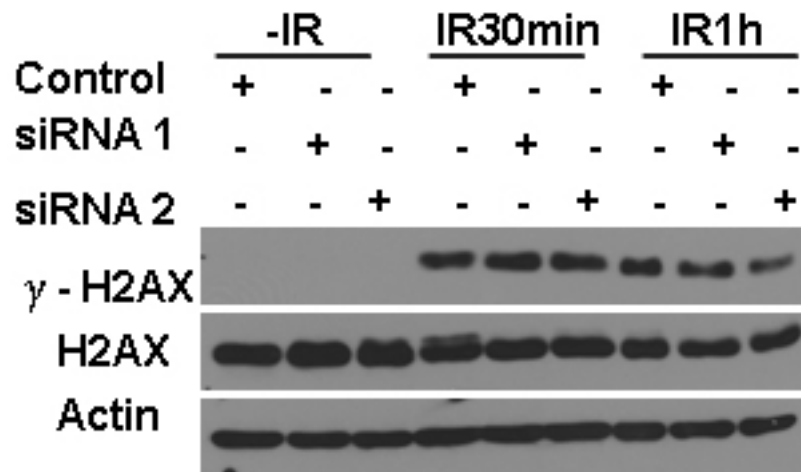
Figure 33. Analysis of histone H2AX phosphorylation following DNA damage in cells lacking ZNF668. ZNF668-containing and ZNF668-depletion U2OS cells were exposed to irradiation and cell lyses were prepared at the indicated time points after treatment. Cell lyses were subjected to Western blot analyses and immunoblotted with antibodies against the indicated molecules. H2AX phosphorylation was analyzed.

6.5 ZNF668 affects efficient activation and loading of repair proteins at sites of DNA damage.

Next, we tested whether ZNF668 depletion impair DNA repair proteins recruitment to DNA damage site. Replication protein A (RPA) is one of the key participants in DSB repair. The RPA phospholylation was significantly decreased in ZNF668 deficient cells without affecting the total RPA level (Figure 34A). In parallel, the foci formation of p-RPA decreased in ZNF668-deficient cells (Figure 34B).
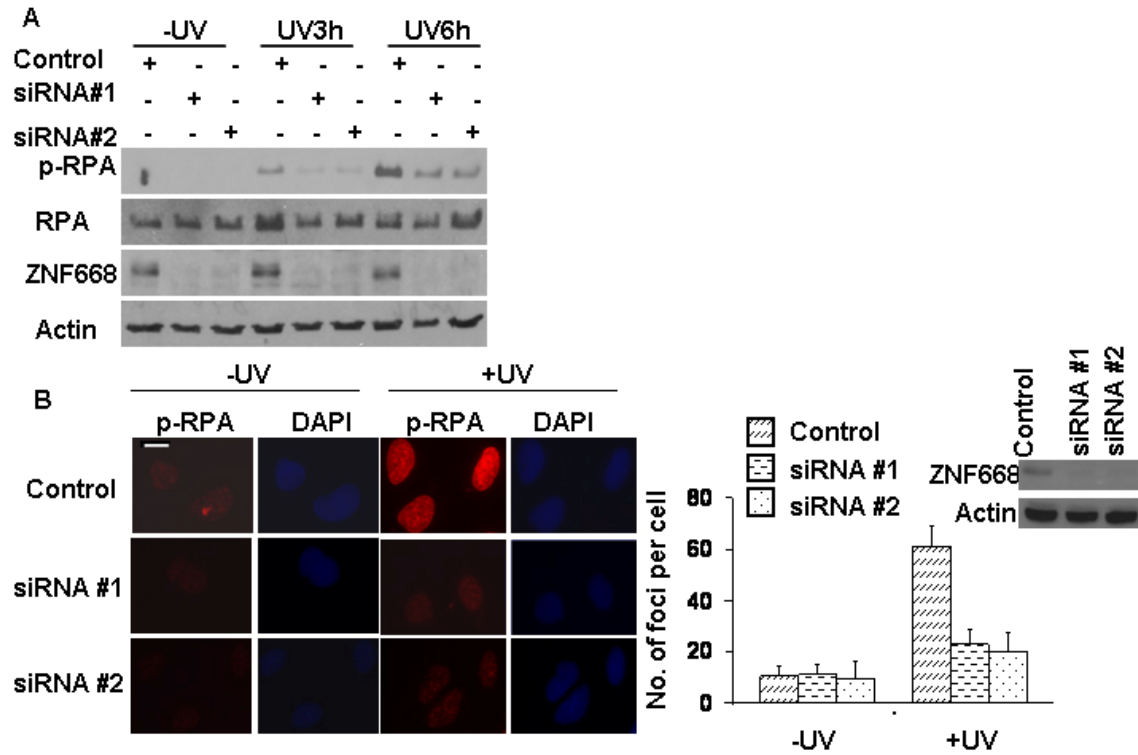
Figure 34. ZNF668 depletion impairs RPA34 phosphorylation. (A) ZNF668 depletion impairs RPA34 phosphorylation. U2OS cells were transfected with siRNAs targeting ZNF668, and the knockdown cells were treated with UV radiation (50 J/m^2). Cell lysates were harvested 3 h later and immunoblotted with antibodies against the indicated molecules. (B) ZNF668 is required for phospho-RPA34 foci formation. (Left) Representative immunostaining images. Scale bar is 10 µM. (Right) The bar graph represents the mean ± SD of three independent experiments; Student's t-test. At least 50 cells were scored in each sample. Western blot analyses to demonstrate the effective ZNF668 knockdown were shown next to the graph.

We also found that the foci formation of both RPA and Rad51 were decreased (Figure 35A and B), indicating ZNF668 contributes to DNA repair protein activation and recruitments to DNA damage site to perform repair function.
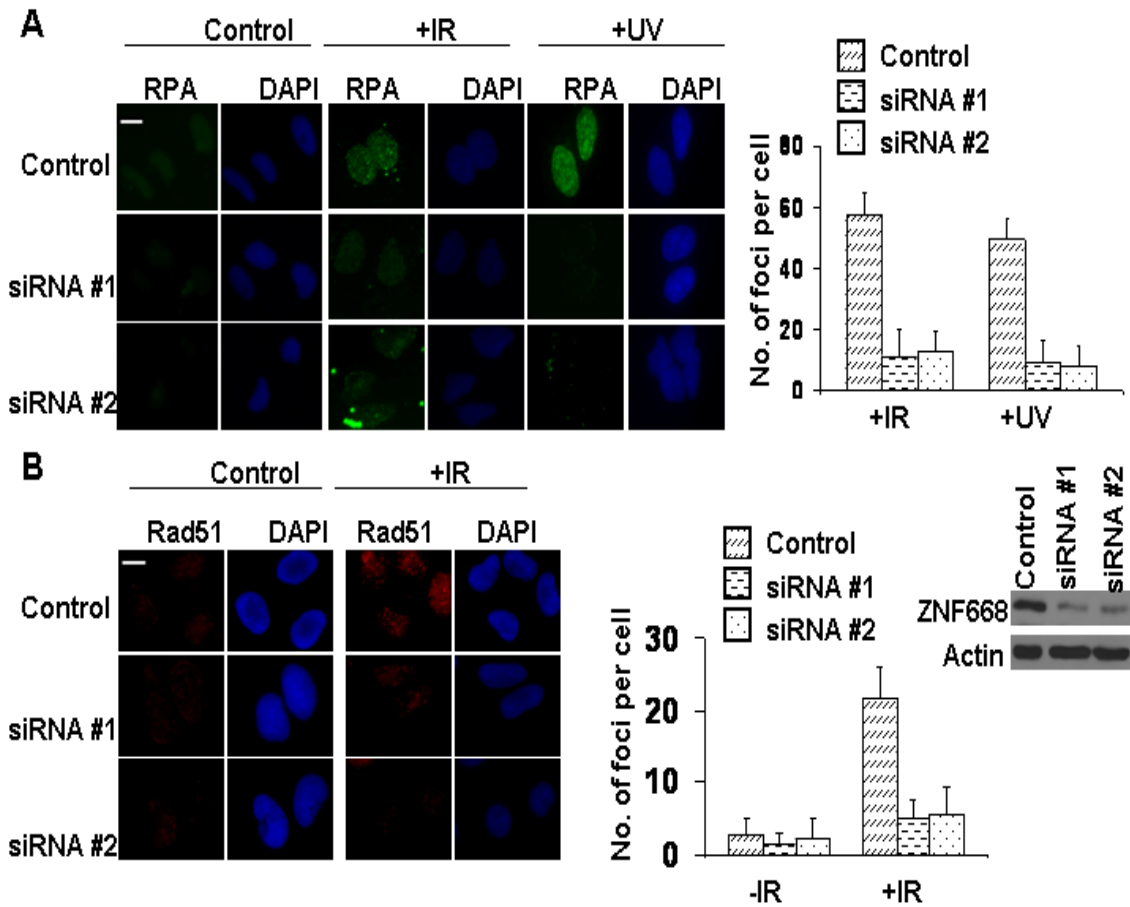
Figure 35. ZNF668 depletion impairs DNA repair protein foci formation. (A) ZNF668 is required for RPA34 foci formation. (Left) Representative immunostaining images. Scale bar is 10 μM. (Right) The bar graph represents the mean ± SD of three independent experiments; Student's t-test. At least 50 cells were scored in each sample. (B) ZNF668 is required for Rad51 foci formation. (Left) Representative immunostaining images. Scale bar is 10 μM. (Right) The bar graph represents the mean ± SD of three independent experiments; Student's t-test. At least 50 cells were scored in each sample. Western blot analyses to demonstrate the effective ZNF668 knockdown were shown next to the graph.

6.6   ZNF668 affects association of DNA repair proteins with chromatin.

To test whether ZNF668 itself is a chromatin associating protein, chromatin fraction was extracted and tested. As shown by Figure 36A, endogenous ZNF668 was enriched in chromatin fractionation. Moreover, the recruitment of DNA repair proteins to chromatin was also impaired. The chromatin binding of p-RPA and RPA were impaired in ZNF668-deficient cells (Figure 36B). Interestingly, endogenous ZNF668 associated with RPA34, indicating ZNF668 might serve as a platform to recruit DNA repair proteins to chromatin (Figure 36C).
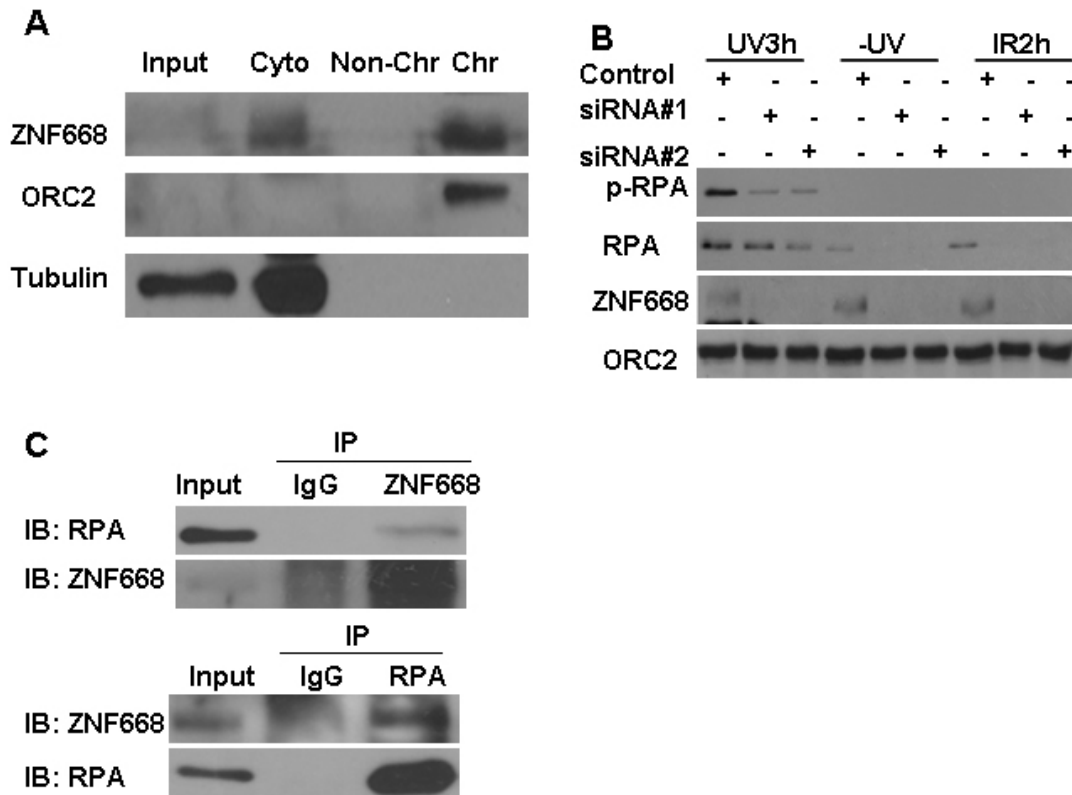
Figure 36. ZNF668 depletion impairs association of DNA repair proteins with chromatin. (A) ZNF668 is a chromatin association protein. Chromatin fractionation was extracted from U2OS cells and cell lysate was subjected to Western blot analyses. (Input) total cell lysate in Urea buffer; (Cyto) cytosolic fraction; (Non-Chr) Non-chromatin association fraction; (Chr) Chromatin fraction.

(B) ZNF668 depletion impaired recruitment of DNA repair proteins to chromatin. ZNF668-containing and ZNF668-depletion U2OS cells were exposed to UV or IR. The chromatin fraction was prepared at the indicated time post-irradiation and subjected to Western blot analyses. (C) Endogenous ZNF668 associates with RPA34. Cellular lysates of U2OS cells were prepared by lysing the cells with RIPA buffer; immunoprecipitated with anti-ZNF668, anti-RPA34 or preimmune IgG; and immunoblotted with antibodies against the indicated molecules.

6.7   Chromatin modification agents improve activation of DNA repair proteins.

Since chromatin modification is important for the recruitment of DNA repair proteins to the DNA damage site, we suspect that the impaired recruitment of DNA repair proteins to DSB sites in ZNF668 depletion cells is due to the lack of efficient chromatin modification. To test this hypothesis, firstly, we tested whether chromatin modification reagents (sodium butyrate, NaB or trichostatin A, TSA) can reverse the effects of ZNF668 depletion on DNA repair protein activation and recruitments to DNA damage sites. The treatment of chromatin modification agents significantly reversed the effects of ZNF668 depletion on RPA phosphorylation and foci formation (Figure 37A, B and C).
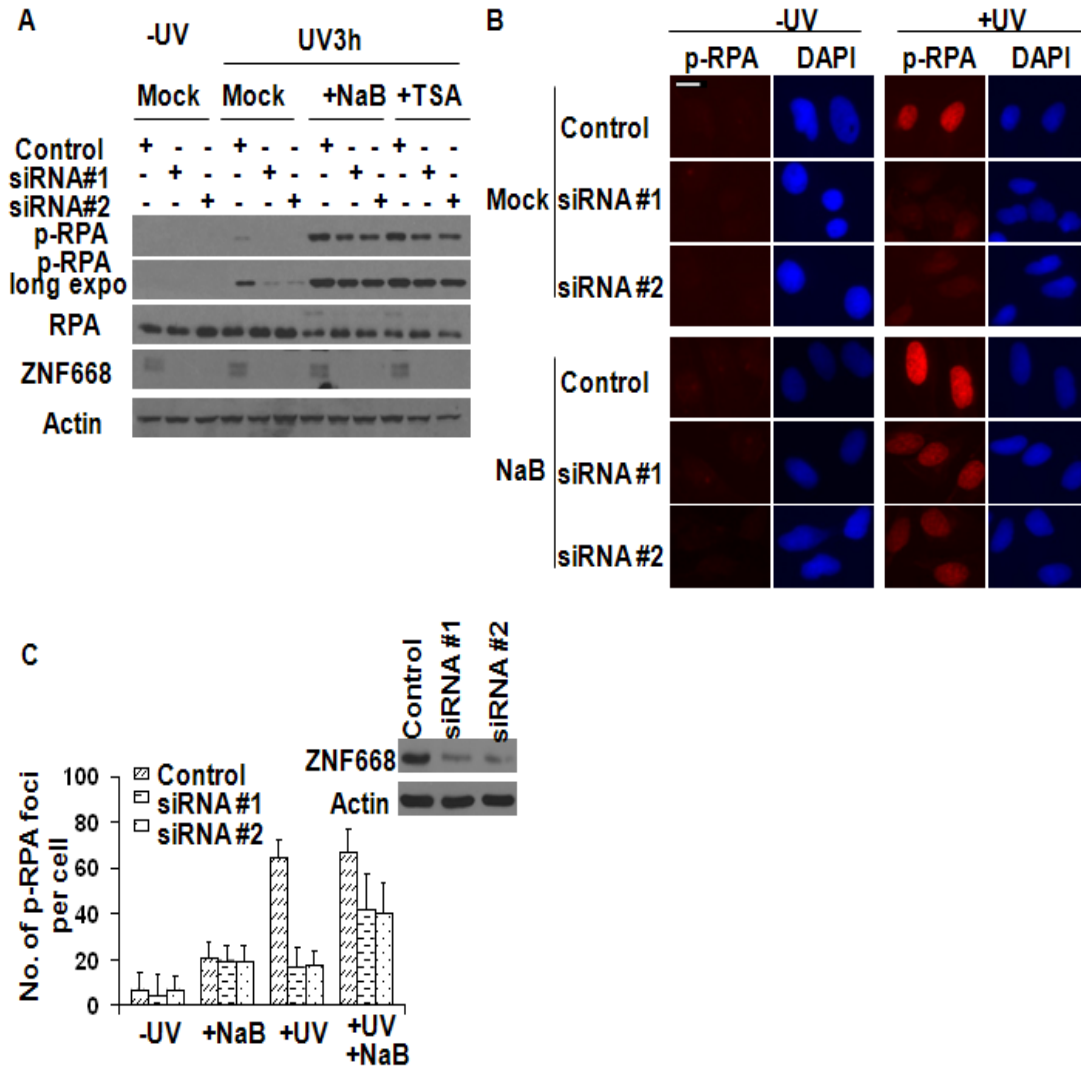
Figure 37. Chromatin modification agents improve activation DNA repair protein RPA. (A) Sodium butyrate (NaB) or trichostatin A (TSA) -induced chromatin modification restored the effect of ZNF668-depletion on RPA phosphorylation. ZNF668 knockdown cells were exposed to 50 J/m^2 of UV irradiation in the presence or absence of chromatin modification reagents (NaB, 5 Mm; TSA, 200 ng/ml). Cell lysates were prepared and subjected to Western blotting analysis 3 hr after irradiation. (B) Sodium butyrate (NaB)-induced chromatin modification improved p-RPA34 foci formation in ZNF668-depletion cells. ZNF668 knockdown cells were exposed to 50 J/m^2 of UV irradiation in the presence or absence of NaB. Cells were prepared and subjected to immunostaining 3 hr after irradiation. Representative immunostaining images. Scale bar is 10 μM. (C) Quantitative analysis of p-RPA34 foci induced in ZNF668-depletion cells from multiple experiments. At least 50 cells were scored in each sample. Western blotting analysis showed the effective ZNF668 knockdown in the cells was shown above the graph.

Consistently, the treatment of chromatin modification agents also significantly reversed the effects of ZNF668 depletion on Rad51 foci formation (Figure 38A and B).
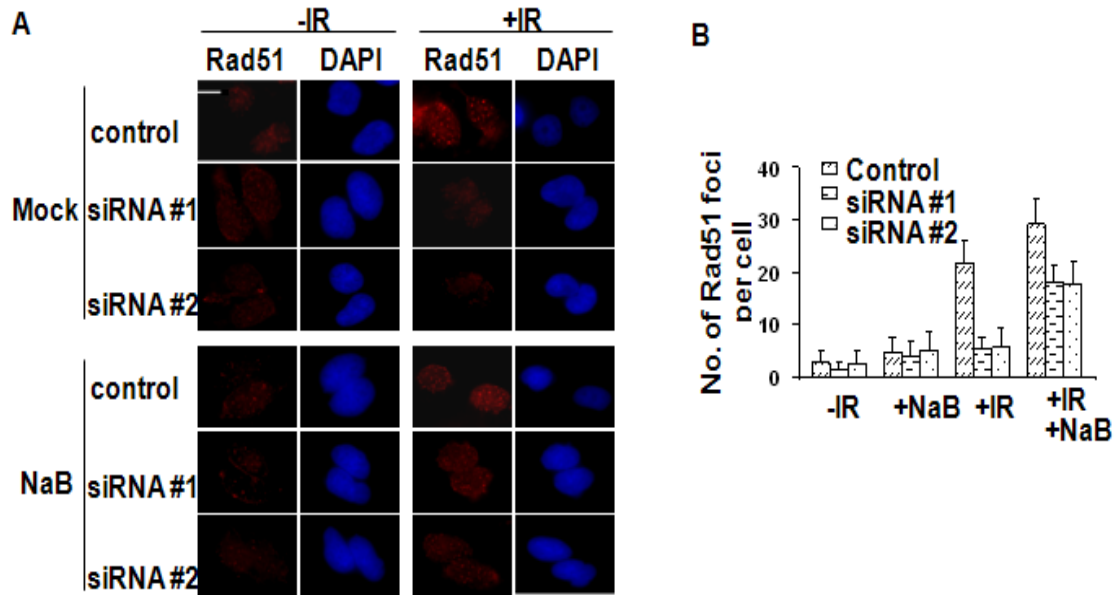
Figure 38. Chromatin modification agents improve activation of DNA repair protein RAD51. (A) Sodium butyrate (NaB)-induced chromatin modification improved Rad51 foci formation in ZNF668-depletion cells. ZNF668 knockdown cells were exposed to 10Gy of IR irradiation in the presence or absence of NaB. Cells were prepared and subjected to immunostaining 3 hr after irradiation. Representative immunostaining images. Scale bar is 10 µM. (B) Quantitative analysis of Rad51 foci induced in ZNF668-depletion cells from multiple experiments. At least 50 cells were scored in each sample.

Furthermore, the treatment of chromatin modification agents recovered RPA and p-RPA recruitment to the chromatin (Figure 39A). The reduced HR repair efficiency in ZNF668 knockdown cells was reversed in the presence of

chromatin modification agents (Figure 39B). These data indicate that the impaired HR repair and compromised recruitment of DNA repair proteins is a direct consequence of impaired access to chromatin in ZNF668-deficient cells.
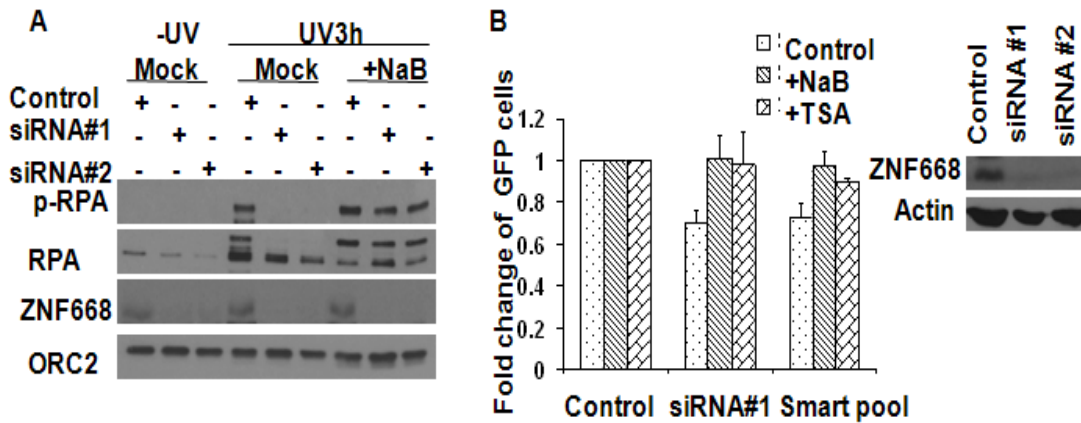
Figure 39. Chromatin modification agents improve recruitment of DNA repair proteins to chromatin and recover HR repair. (A) Sodium butyrate (NaB)-induced chromatin modification improved chromatin-associated p-RPA34 and RPA34 in ZNF668-depletion cells. ZNF668 knockdown cells were treated with 50 J/m^2 of UV irradiation in the presence or absence of sodium butyrate (5mM). Three hours after treatment, chromatin-enriched fractions were subjected to Western blot analysis. (B) Sodium butyrate (NaB) or trichostatin A (TSA) -induced chromatin modification restored the impaired HR repair in ZNF668-depletion cells. ZNF668-depleted cells were subjected to HR repair analysis in the presence or absence of chromatin modification reagents. Each value is relative to the percentage of GFP$^+$ cells in *I-SceI*-transfected cells with control siRNA transfection, which was set to 1 and represents the mean ± SD of three independent experiments; Student's t-test.

6.8   ZNF668 depletion impairs histone H2A acetylation

Histone acetylation is important for chromatin modification after DNA damage response. Since we observed that the compromised HR repair in ZNF668 deficient cells was associated with impaired chromatin access for repair proteins, we reasoned that this may be due to impaired regulation of histone acetylation in the absence of ZNF668.

To test this, we examined the histone acetylation in ZNF668 depletion cells. We found that both the overall and IR-induced H2A K5 acetylation in whole cell lysates (extracted by SDS sample buffer) were affected by ZNF668 depletion (Figure 40), which indicated that ZNF668-mediated H2A acetylation may have a role in DSB repair.
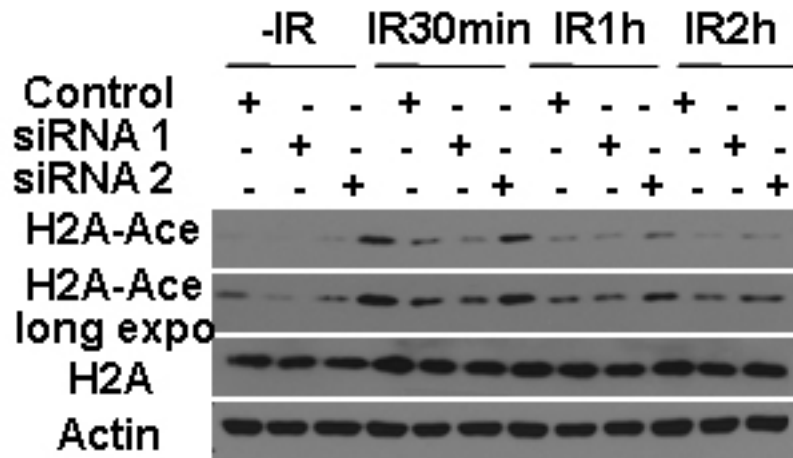
Figure 40. Analysis of histone H2A acetylation following DNA damage in cells lacking ZNF668. ZNF668-containing and ZNF668-depletion U2OS cells were exposed to irradiation and cell lyses were prepared at the indicated time points after treatment. Cell lyses were subjected to Western blot analyses and immunoblotted with antibodies against the indicated molecules. H2A acetylation was analyzed.

Next, we examined whether the chromatin modification reagents can recover ZNF668's effect on the impaired H2A acetylation at K5 site. The treatment of chromatin modification agents significantly reversed the effects of ZNF668 depletion on H2A acetylation at the K5 site after IR treatment (Figure 41).
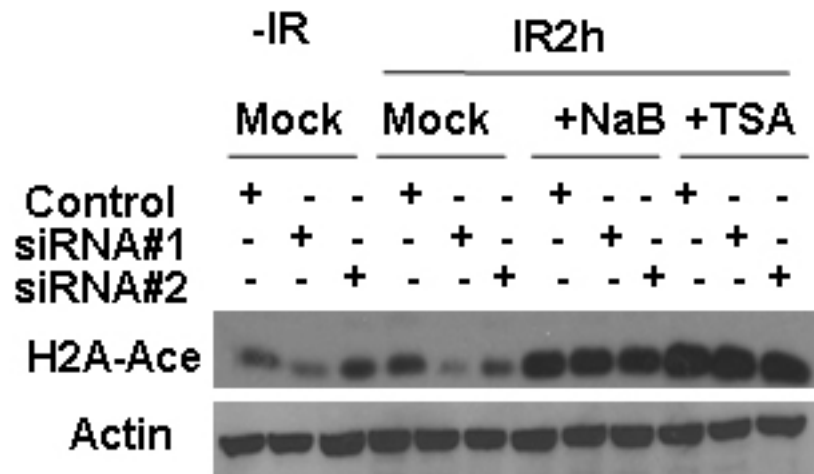
Figure 41. Chromatin modification reagents sodium butyrate (NaB) or trichostatin A (TSA) -induced chromatin modification restored the effect of ZNF668-depletion on H2A acetylation after IR. ZNF668 knockdown cells were exposed to 10Gy of IR irradiation in the presence or absence of chromatin modification reagents (NaB, 5 Mm; TSA, 200 ng/ml). Cell lysates were prepared and subjected to Western blotting analysis 2 hr after irradiation.

The acetylation site K5 is conserved in H2A and its viarant H2AX. Previous studies showed H2AX K5 is the target of acetylation upon DSBs in the chromatin because the IR-induced acetylation was abolished by the H2AX (K5R) mutation (Ikura et al., 2007). To clarify whether H2AX acetylation is the target of ZNF668 regulated acetylation process, we overexpressed Flag-H2AX in U2OS

cells and pull down the Flag-H2AX protein complex by immunoprecipitation. The

Flag-H2AX acetylation was detected with K5 acetylation antibody. As shown in

Figure 42, we found that H2AX K5 acetylation was induced by IR treatment and

in ZNF668 depletion cells, the K5 acetylation of H2AX was significantly reduced.

These data are consistent with the previous finding and indicate that ZNF668 is

important for efficient H2AX K5 acetylation after IR DNA damage.
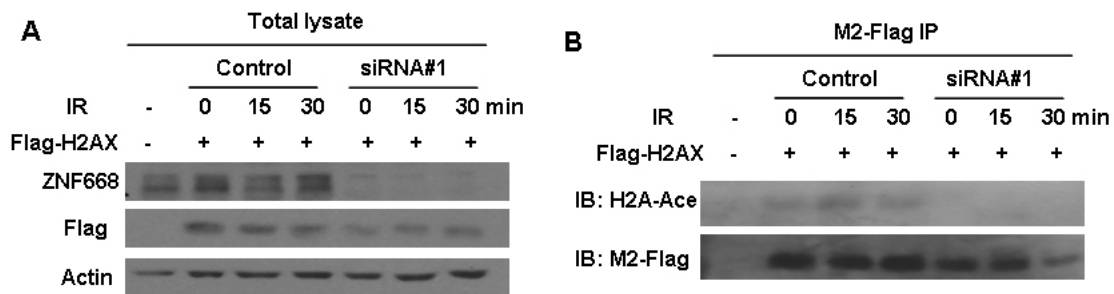
Figure 42. ZNF668 depletion impairs IR induced H2AX acetylation. U2OS cells were transfected with control or ZNF668 siRNA; 24h later, cells were transfected with empty vector or Flag-H2AX; 48 h later, cells were exposed to IR treatment and cells were harvest at indicated time post-IR treatment. (A) Total cell lysates were subjected to western blotting analysis to confirm efficient ZNF668 knockdown. (B) The cell lysates (1.5 mg) were immunoprecipitated and immunoblotted with antibodies against the indicated molecules.

6.9   ZNF668 depletion impairs histone H2AX acetylation by regulating Tip60-H2AX interaction.

Histone H2AX acetylation plays a role in the selective histone variant

exchange, which is important for chromatin structure regulation at DNA damage

sites (Kusch et al., 2004). Since we observed decreased histone H2AX

acetylation in ZNF668-depletion cells, we suspect that ZNF668 is important for histone H2AX acetylation and chromatin structure regulation.

To test how ZNF668 regulates H2AX acetylation, firstly we tested whether ZNF668 interacted with H2AX. As shown in Figure 43, immunoprecipitation analysis showed that H2AX interacted with ZNF668.
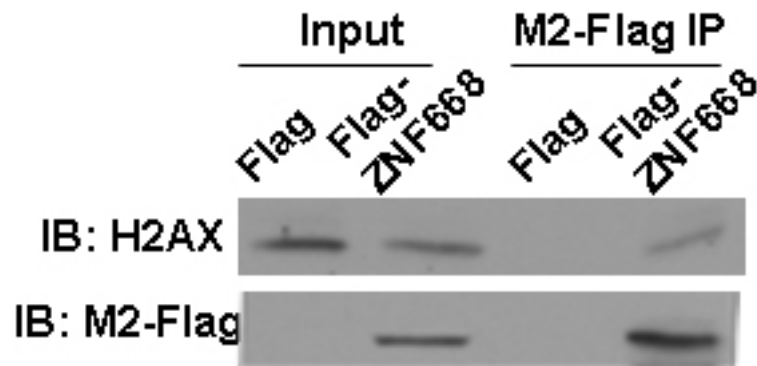
Figure 43. ZNF668 associates with H2AX. U2OS cells were transfected with empty vector or Flag-ZNF668; 48 h later, cells lysates (3 mg) were immunoprecipitated and immunoblotted with antibodies against the indicated molecules.

Previous studies have shown that K5 of histone H2A is acetylated by Tip60 in vitro (Kimura et al., 1998). The interaction between Tip60 and H2AX is IR-induced. After IR treatment, Tip60 specifically binds to H2AX but not H2A and facilitates H2AX K5 acetylation (Ikura et al., 2000). Since we observed decreased acetylation of H2AX K5 in ZNF668 depletion cells after IR, we suspect that ZNF668 regulates H2AX acetylation through the regulation of Tip60-H2AX protein complex. To test this, firstly, we tested whether ZNF668 regulates Tip60 expression. As shown in Figure 44A, Tip60 protein level didn't

change in ZNF668-depletion cells with or without IR treatment. Chromatin

fractionation analysis also showed that the chromatin associated Tip60 didn't

change with ZNF668 knockdown and IR treatment (Figure 44B).
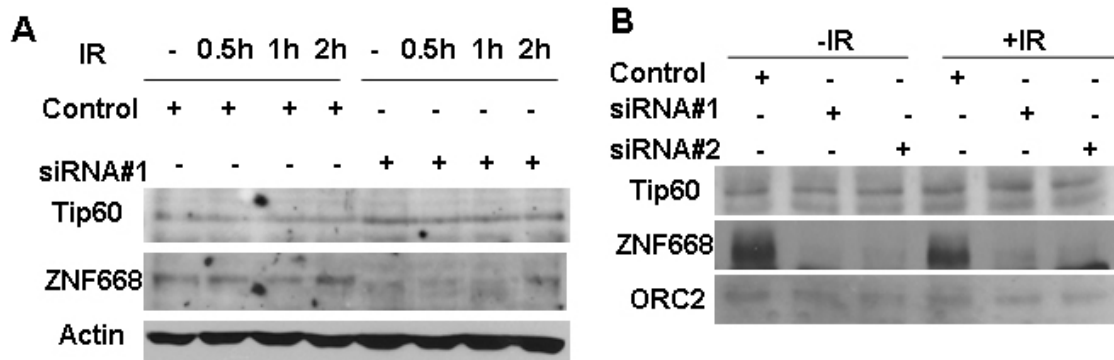
Figure 44. Tip60 expression and chromatin association in ZNF668-depletion cells. (A) ZNF668 depletion didn't impair Tip60 expression with or without IR. ZNF668-containing and ZNF668-depletion U2OS cells were exposed to IR. Total cell lysate were harvested in urea buffer at the indicated time points and subjected to Western blot analyses. (B) Tip60's association with chromatin were similar in control and ZNF668-depletion cells. ZNF668-containing and ZNF668-depletion U2OS cells were exposed to IR. The chromatin fraction was prepared and subjected to Western blot analyses.

To test whether the reduced H2AX acetylation in ZNF668-deficient cells is

due to the decreased interaction between Tip60 and H2AX proteins, we did

immunoprecipitation assay of FLAG-H2AX protein complex. As shown in Figure

45A, the interaction between H2AX and Tip60 was induced by IR treatment in

control cells, which was consistent with previous finding (Ikura et al., 2007).

However, ZNF668-depletion impaired the IR-induced interaction between Tip60

and H2AX, indicating ZNF668 is required for facilitating Tip60 interaction with

H2AX to acetylate H2AX after DNA damage treatment (Figure 45B).
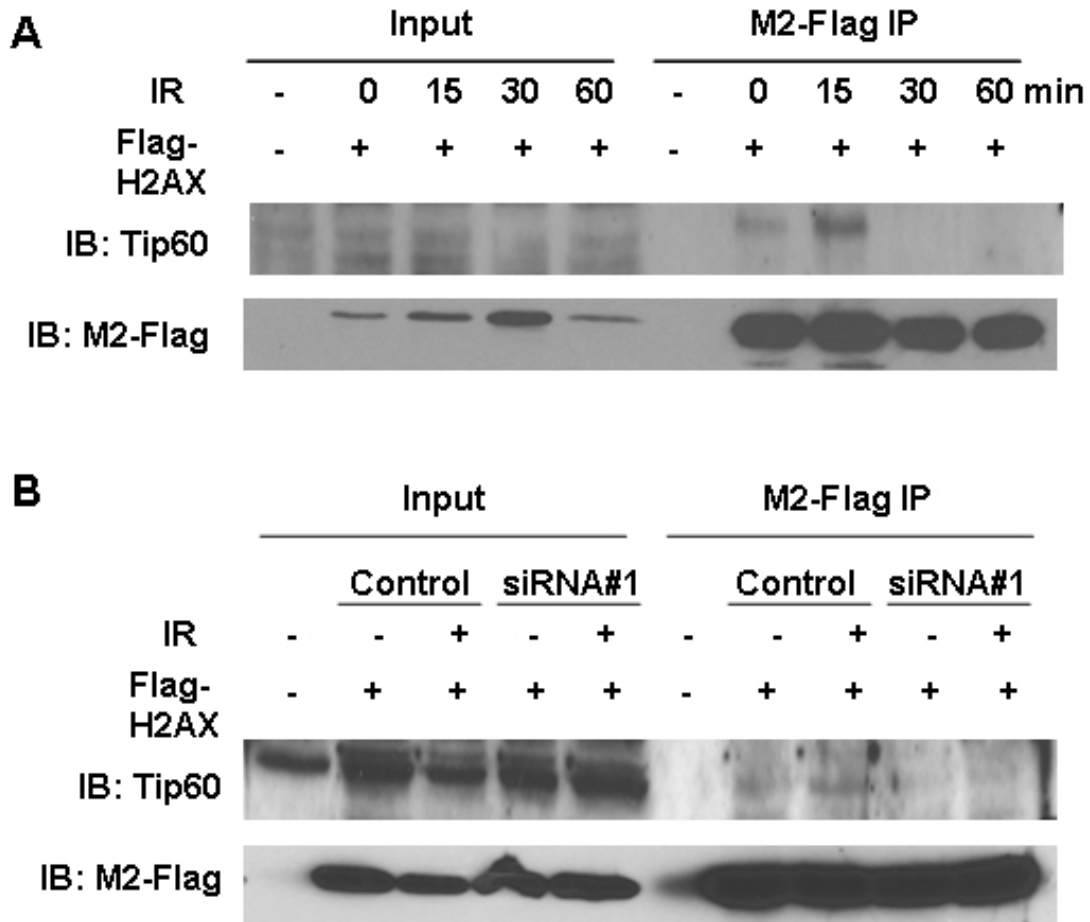
Figure 45. ZNF668 depletion impairs IR induced Tip60-H2AX interaction. (A) U2OS cells were transfected with Flag-H2AX and exposed to IR treatment 48 hours after transfection. Cell lysates were harvested at indicated time post-IR treatment and subjected to immunoprecipitation and immunoblotting. (B) U2OS cells were transfected with control or ZNF668 siRNA; 24h later, cells were transfected with empty vector or Flag-H2AX; 48 h later, cells were exposed to IR treatment and cells were harvest at 30 minutes post-IR treatment. The cell lysates (1.5 mg) were immunoprecipitated and immunoblotted with antibodies against the indicated molecules.

6.10 Discussion

In this part of study, we studied the function of ZNF668 in DNA damage response pathways. Our data indicated that ZNF668 didn't affect the initiation and signaling cascade of DNA damage pathway. However, ZNF668 participated in DNA damage repair. The inefficient DNA repair in ZNF668 depletion cells caused prolonged DNA damage and genetic instability.

Chromatin modification is important for efficient DNA damage repair proteins' recruitment to the damage sites. Our data showed that ZNF668 is a chromatin associating protein (Figure 36A) and it interacts with histone variant H2AX (Figure 43). ZNF668 didn't affect H2AX activation but it affects histone H2AX acetylation upon DNA damage treatment, which is important for the open of chromatin structure upon DNA damage treatment and the access of repair proteins to the damaged DNA. Therefore, our results suggest a model for ZNF668 function in double strand break repair. ZNF668 promotes chromatin modification and in turn facilitates the recruitment of DNA repair proteins to DNA lesions for efficient repair. Loss of ZNF668 would lead to impaired chromatin modification and DNA DSB repair, which may contribute to the development of cancer.

Our findings also reveal a mechanism by which ZNF668 regulates chromatin modification. Different types of histone acetylase are responsible for the acetylation of different histones (Tsukuda et al., 2005; Ziv et al., 2006; Peterson et al., 2000). With DNA damage, the Tip60 acetylase is recruited to DNA lesions by other molecules to recognize histone H2AX and induce H2AX

modifications. Our studies demonstrate that ZNF668 is necessary for the recruitment of Tip60 to the DNA damage site to perform its function on H2AX acetylation. Therefore it will be of future interests to address the underlying mechanism of ZNF668 regulation on Tip60-H2AX complex and illustrate the additional roles of ZNF668 in the regulation of Tip60-H2AX complex in response to DNA double strand breaks induced by DNA damage.

The present study shows that ZNF668 participates in homologous recombination repair by regulating histone modification and chromatin remodeling. We propose a model (Figure 46) to explain the mechanism of ZNF668 in regulation of DNA repair. ZNF668 is a chromatin association protein. When the double strand breaks are induced by DNA damage treatment, ZNF668 binds to histone H2AX around the DSBs. The protein complex of ZNF668-H2AX serves as a platform to recruit HAT-Tip60 to the DSBs. Then Tip60 acetylates H2A that surrounds DNA breaks. Acetylated histones facilitate access and binding of DNA repair proteins to chromatin DNA. After DNA repair is completed, the chromatin is reassembled. It has been shown that HAT complexes are related to cancer development because they are important for transcription regulation and regulation of DNA damage response (Cairns et al., 2001; Yang et al., 2004). Therefore, our studies identify a novel factor with the potential to regulate histone acetylation and chromatin remodelling during DNA repair and to maintain genomic stability.
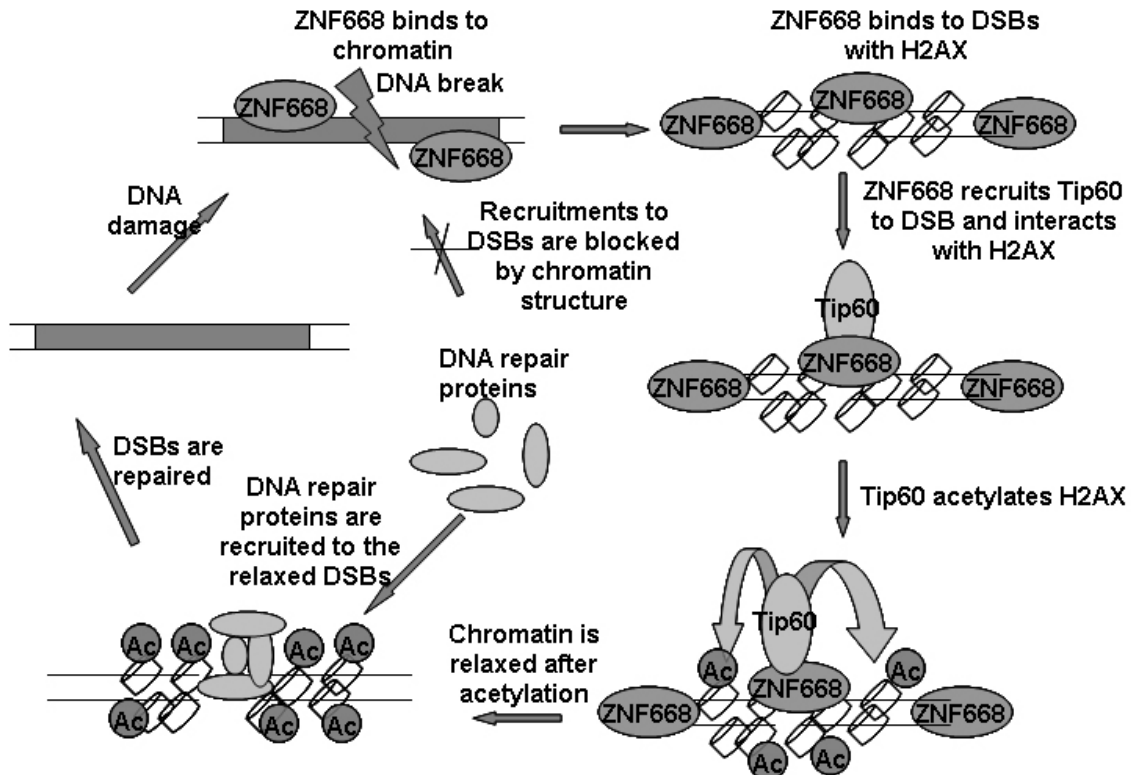
Figure 46. A schematic model for the role of ZNF668-mediated histone acetylation and chromatin reconfiguration in DNA repair.

Together, these results indicate that ZNF668 participates in chromatin

modification and reconfiguration, which facilitate access of the repair machinery

to the site of DNA breaks. However, further experiments will be needed to

emphasize the role of ZNF668 in DNA double strand break repair. In addition to

the DNA damage induced H2A acetylation, we also observed an overall

decrease of H2A acetylation in ZNF668 deficient cells without DNA damage,

indicating ZNF668 may also participate in the regulation of global acetylation. To

further clarify the role of ZNF668 in DNA Damage site modification or global

modification, chromatin immunoprecipitation (ChIP) and PCR techniques can be

used to determine the recruitment of specific molecules such as Tip60,

acetylated H2AX, acetylated H3 and H4 to the double strand break sites. The

U2OS cells that used in our study to study the HR repair provides us a useful tool to investigate the status of specific proteins in DSB sites. The DSB can be induced by I-SCE enzyme transfection and the primers flanking the DSB sites can be used to analyze the recruitment of proteins to the DSB sites after ChIP.

In this study, we emphasized on the acetylation status of K5 site in H2AX in ZNF668 deficient cells because the role of H2AX K5 acetylation in DNA repair has been reported previously. However, there are other acetylation sites in H2AX such as K9. It is important to determine whether ZNF668 affects other sites of H2AX acetylation. This ambiguity can be resolved by examining site-specific mutants in the histone proteins themselves. For example, K5 or K9 site-specific H2AX mutants can be generated through site-directed mutagenesis and the acetylation status of mutant H2AX can be studied under DNA damage treatment with or without ZNF668 expression.

In addition, our study doesn't rule out the possible role of ZNF668 on other core histones' acetylation. Many histone modifying enzymes have broad substrate specificities. For example, Tip60 can acetylate both H2A and H4. Due to this reason, it is difficult to discern the contributions of other histone acetylation to DNA repair. It is unclear whether ZNF668 regulates DNA repair through the regulation of Tip60's acetylation effects on H2A or other histones. Antibodies specific to site-specific modifications of each core histone can be used to perform ChIP and PCR analyses to clarify the recruitment of histones to the DSB sites in ZNF668 deficient cells. Moreover, future experiments will be

needed to identify the possibility of ZNF668's effect on other type of histone modifications.

Tumorigenesis is driven by the direct or indirect effects from the genetic alterations in oncogenes and tumor suppressor genes. Our studies indicate ZNF668 is a potential tumor suppressor. In addition to the mutation inside ZNF668, it can also regulate other important genes involved in multiple pathways which are necessary for normal cell growth. These results make ZNF668 a potential therapeutic target for human breast cancer. Therefore, the novel findings from this project have both the potential to improve our understanding of genetic mechanisms underlying breast cancer and also the likelihood of novel approaches to the treatment of breast cancer.

CHAPTER 7 REFERENCE

Argentini, M., Barboule, N., and Wasylyk, B. 2001. The contribution of the acidic domain of MDM2 to p53 and MDM2 stability. Oncogene 20:1267-1275.

Artandi, S. E., and Attardi, L. D. 2005. Pathways connecting telomeres and p53 in senescence, apoptosis, and cancer. Biochemical and Biophysical Research Communications 331:881-890.

Barak, Y., Juven, T., Haffner, R., and Oren, M. 1993. Mdm2 Expression Is Induced by Wild Type-P53 Activity. Embo Journal 12:461-468.

Bartkova, J., Horejsi, Z., Sehested, M., Nesland, J. M., Rajpert-De Meyts, E., Skakkebaek, N. E., Stucki, M., Jackson, S., Lukas, J., and Bartek, J. 2007. DNA damage response mediators MDC1 and 53BP1: constitutive activation and aberrant loss in breast and lung cancer, but not in testicular germ cell tumours. Oncogene 26:7414-7422.

Bertrand, P., Saintigny, Y., and Lopez, B. S. 2004. P53 ' s double life: transactivation-independent repression of homologous recombination. Trends in Genetics 20:235-243.

Bertwistle, D., Sugimoto, M., and Sherr, C. J. 2004. Physical and functional interactions of the Arf tumor suppressor protein with nucleophosmin/B23. Mol Cell Biol 24:985-996.

Bird, A. W., Yu, D. Y., Pray-Grant, M. G., Qiu, Q. F., Harmon, K. E., Megee, P. C., Grant, P. A., Smith, M. M., and Christman, M. F. 2002. Acetylation of histone H4 by Esa1 is required for DNA double-strand break repair. Nature 419:411-415.

Bothner, B., Lewis, W. S., Di Giammarino, E. L., Weber, J. D., Bothner, S. J., and Kriwacki, R. W. 2001. Defining the molecular basis of Arf and Hdm2 interactions. Journal of Molecular Biology 314:263-277.

Boyd, S. D., Tsai, K. Y., and Jacks, T. 2000. An intact HDM2 RING-finger domain is required for nuclear exclusion of p53. Nature Cell Biology 2:563-568.

Branzei, D., and Foiani, M. 2008. Regulation of DNA repair throughout the cell cycle. Nat Rev Mol Cell Biol 9:297-308.

Brignone, C., Bradley, K. E., Kisselev, A. F., and Grossman, S. R. 2004. A post-ubiquitination role for MDM2 and hHR23A in the p53 degradation pathway. Oncogene 23:4121-4129.

Cairns, B. R. 2001. Emerging roles for chromatin remodeling in cancer biology. Trends Cell Biol 11:S15-21.

Carrozza, M. J., Utley, R. T., Workman, J. L., and Cote, J. 2003. The diverse functions of histone acetyltransferase complexes. Trends Genet 19:321-329.

Celeste, A., Fernandez-Capetillo, O., Kruhlak, M. J., Pilch, D. R., Staudt, D. W., Lee, A., Bonner, R. F., Bonner, W. M., and Nussenzweig, A. 2003. Histone H2AX phosphorylation is dispensable for the initial recognition of DNA breaks. Nature Cell Biology 5:675-U651.

Chai, B., Huang, J., Cairns, B. R., and Laurent, B. C. 2005. Distinct roles for the RSC and Swi/Snf ATP-dependent chromatin remodelers in DNA double-strand break repair. Genes Dev 19:1656-1661.

Chen, C. C., Carson, J. J., Feser, J., Tamburini, B., Zabaronick, S., Linger, J., and Tyler, J. K. 2008. Acetylated lysine 56 on histone H3 drives chromatin assembly after repair and signals for the completion of repair. Cell 134:231-243.

Cimprich, K. A., and Cortez, D. 2008. ATR: an essential regulator of genome integrity. Nat Rev Mol Cell Biol 9:616-627.

Colaluca, I. N., Tosoni, D., Nuciforo, P., Senic-Matuglia, F., Galimberti, V., Viale, G., Pece, S., and Di Fiore, P. P. 2008. NUMB controls p53 tumour suppressor activity. Nature 451:76-80.

Colombo, E., Marine, J. C., Danovi, D., Falini, B., and Pelicci, P. G. 2002. Nucleophosmin regulates the stability and transcriptional activity of p53. Nat Cell Biol 4:529-533.

Czornak, K., Chughtai, S., and Chrzanowska, K. H. 2008. Mystery of DNA repair: the role of the MRN complex and ATM kinase in DNA damage repair. J Appl Genet 49:383-396.

Dai, M. S., Shi, D., Jin, Y., Sun, X. X., Zhang, Y., Grossman, S. R., and Lu, H. 2006. Regulation of the MDM2-p53 pathway by ribosomal protein L11 involves a post-ubiquitination mechanism. J Biol Chem 281:24304-24313.

Deng, Y. B., Chan, S. S., and Chang, S. 2008. Telomere dysfunction and tumour suppression: the senescence connection. Nature Reviews Cancer 8:450-458.

Felsenfeld, G., and Groudine, M. 2003. Controlling the double helix. Nature 421:448-453.

Flaus, A., and Owen-Hughes, T. 2004. Mechanisms for ATP-dependent chromatin remodelling: farewell to the tuna-can octamer? Curr Opin Genet Dev 14:165-173.

Geyer, R. K., Yu, Z. K., and Maki, C. G. 2000. The MDM2 RING-finger domain is required to promote p53 nuclear export. Nature Cell Biology 2:569-573.

Grisendi, S., Mecucci, C., Falini, B., and Pandolfi, P. P. 2006. Nucleophosmin and cancer. Nat Rev Cancer 6:493-505.

Gu, J. J., Nie, L. H., Wiederschain, D., and Yuan, Z. M. 2001. Identification of p53 sequence elements that are required for MDM2-mediated nuclear export. Molecular and Cellular Biology 21:8533-8546.

Harper, J. W., Adami, G. R., Wei, N., Keyomarsi, K., and Elledge, S. J. 1993. The p21 Cdk-interacting protein Cip1 is a potent inhibitor of G1 cyclin-dependent kinases. Cell 75:805-816.

Harper, J. W., and Elledge, S. J. 2007. The DNA damage response: ten years after. Mol Cell 28:739-745.

Haupt, Y., Maya, R., Kazaz, A., and Oren, M. 1997. Mdm2 promotes the rapid degradation of p53. Nature 387:296-299.

Henikoff, S., and Ahmad, K. 2005. Assembly of variant histones into chromatin. Annual Review of Cell and Developmental Biology 21:133-153

Hermeking, H., Lengauer, C., Polyak, K., He, T. C., Zhang, L., Thiagalingam, S., Kinzler, K. W., and Vogelstein, B. 1997. 14-3-3 sigma is a p53-regulated inhibitor of G2/M progression. Molecular Cell 1:3-11.

Hickman, E. S., Moroni, M. C., and Helin, K. 2002. The role of p53 and pRB in apoptosis and cancer. Current Opinion in Genetics & Development 12:60-66.

Hoeijmakers, J. H. J. 2009. DNA Damage, Aging, and Cancer. New England Journal of Medicine 361:1914-1914.

Honda, R., Tanaka, H., and Yasuda, H. 1997. Oncoprotein MDM2 is a ubiquitin ligase E3 for tumor suppressor p53. Febs Letters 420:25-27.

Honda, R., and Yasuda, H. 1999. Association of p19 (ARF) with Mdm2 inhibits ubiquitin ligase activity of Mdm2 for tumor suppressor p53. Embo Journal 18:22-27.

Horn, H. F., and Vousden, K. H. 2004. Cancer: guarding the guardian? Nature 427:110-111.

Ikura, T., Ogryzko, V. V., Grigoriev, M., Groisman, R., Wang, J., Horikoshi, M., Scully, R., Qin, J., and Nakatani, Y. 2000. Involvement of the TIP60 histone acetylase complex in DNA repair and apoptosis. Cell 102:463-473.

Itahana, K., Bhat, K. P., Jin, A., Itahana, Y., Hawke, D., Kobayashi, R., and Zhang, Y. 2003. Tumor suppressor ARF degrades B23, a nucleolar protein involved in ribosome biogenesis and cell proliferation. Mol Cell 12:1151-1164.

Jemal, A., Siegel, R., Xu, J. Q., and Ward, E. 2010. Cancer Statistics, 2010. Ca-a Cancer Journal for Clinicians 60:277-300.

Jenuwein, T., and Allis, C. D. 2001. Translating the histone code. Science 293:1074-1080.

Jha, S., Shibata, E., and Dutta, A. 2008. Human Rvbl/Tip49 is required for the histone acetyltransferase activity of Tip60/NuA4 and for the Downregulation of phosphorylation on H2AX after DNA damage. Molecular and Cellular Biology 28:2690-2700.

Jian, Y., and Lin, Z. 2003. NoPUMA, no death: Implications for p53-dependent apoptosis. Cancer Cell 4:248-249.

Jiricny, J. 2006. The multifaceted mismatch-repair system. Nat Rev Mol Cell Biol 7:335-346.

Kamakaka, R. T., and Biggins, S. 2005. Histone variants: deviants? Genes Dev 19:295-310.

Kamijo, T., Weber, J. D., Zambetti, G., Zindy, F., Roussel, M. F., and Sherr, C. J. 1998. Functional and physical interactions of the ARF tumor suppressor with p53 and Mdm2. Proc Natl Acad Sci U S A 95:8292-8297.

Khorasanizadeh, S. 2004. The nucleosome: from genomic organization to genomic regulation. Cell 116:259-272.

Kimura, A., and Horikoshi, M. 1998. Tip60 acetylates six lysines of a specific class in core histones in vitro. Genes to Cells 3:789-800.

Korgaonkar, C., Hagen, J., Tompkins, V., Frazier, A. A., Allamargot, C., Quelle, F. W., and Quelle, D. E. 2005. Nucleophosmin (B23) targets ARF to nucleoli and inhibits its function. Molecular and Cellular Biology 25:1258-1271.

Kortlever, R. M., Higgins, P. J., and Bernards, R. 2006. Plasminogen activator inhibitor-1 is a critical downstream target of p53 in the induction of replicative senescence. Nature Cell Biology 8:877-U155.

Kouzarides, T. 2007. Chromatin modifications and their function. Cell 128:693-705.

Kubbutat, M. H., Ludwig, R. L., Levine, A. J., and Vousden, K. H. 1999. Analysis of the degradation function of Mdm2. Cell Growth Differ 10:87-92.

Kubbutat, M. H. G., Jones, S. N., and Vousden, K. H. 1997. Regulation of p53 stability by Mdm2. Nature 387:299-303.

Kurki, S., Peltonen, K., Latonen, L., Kiviharju, T. M., Ojala, P. M., Meek, D., and Laiho, M. 2004. Nucleolar protein NPM interacts with HDM2 and protects tumor suppressor protein p53 from HDM2-mediated degradation. Cancer Cell 5:465-475.

Kusch, T., Florens, L., Macdonald, W. H., Swanson, S. K., Glaser, R. L., Yates, J. R., Abmayr, S. M., Washburn, M. P., and Workman, J. L. 2004. Acetylation by Tip60 is required for selective histone variant exchange at DNA lesions. Science 306:2084-2087.

Lane, D. P., and Crawford, L. V. 1979. T-Antigen Is Bound to a Host Protein in Sv40-Transformed Cells. Nature 278:261-263.

Li, Q., Zhou, H., Wurtele, H., Davies, B., Horazdovsky, B., Verreault, A., and Zhang, Z. G. 2008. Acetylation of histone H3 lysine 56 regulates replication-coupled nucleosome assembly. Cell 134:244-255.

Liang, Y. L., Lin, S. Y., Brunicardi, F. C., Goss, J., and Li, K. Y. 2009. DNA Damage Response Pathways in Tumor Suppression and Cancer Treatment. World Journal of Surgery 33:661-666.

Lo, W. S., Duggan, L., Emre, N. C. T., Belotserkovskya, R., Lane, W. S., Shiekhattar, R., and Berger, S. L. 2001. Snf1 - a histone kinase that works in concert with the histone acetyltransferase Gcn5 to regulate transcription. Science 293:1142-1146.

Lusser, A., and Kadonaga, J. T. 2003. Chromatin remodeling by ATP-dependent molecular machines. Bioessays 25:1192-1200.

Lohrum, M. A. E., Ludwig, R. L., Kubbutat, M. H. G., Hanlon, M., and Vousden, K. H. 2003. Regulation of HDM2 activity by the ribosomal protein L11. Cancer Cell 3:577-587.

Ma, H., and Pederson, T. 2007. Depletion of the nucleolar protein nucleostemin causes G1 cell cycle arrest via the p53 pathway. Mol Biol Cell 18:2630-2635.

Ma, J., Martin, J. D., Zhang, H., Auger, K. R., Ho, T. F., Kirkpatrick, R. B., Grooms, M. H., Johanson, K. O., Tummino, P. J., Copeland, R. A., and Lai, Z. 2006. A second p53 binding site in the central domain of Mdm2 is essential for p53 ubiquitination. Biochemistry 45:9238-9245.

Mandal, P. K., Blanpain, C., and Rossi, D. J. 2011. DNA damage response in adult stem cells: pathways and consequences. Nat Rev Mol Cell Biol 12:198-202.

McPherson, K., Steel, C. M., and Dixon, J. M. 2000. ABC of breast disease: Breast cancer-epidemiology, risk factors, and genetics. British Medical Journal 321:624-628.

Meulmeester, E., Frenk, R., Stad, R., de Graaf, P., Marine, J. C., Vousden, K. H., and Jochemsen, A. G. 2003. Critical role for a central part of Mdm2 in the ubiquitylation of p53. Molecular and Cellular Biology 23:4929-4938.

Michael, D., and Oren, M. 2003. The p53-Mdm2 module and the ubiquitin system. Semin Cancer Biol 13:49-58.

Momand, J., Zambetti, G. P., Olson, D. C., George, D., and Levine , A. J. 1992. The Mdm-2 Oncogene Product Forms a Complex with the P53 Protein and Inhibits P53-Mediated Transactivation. Cell 69:1237-1245.

Morrison, A. J., Highland, J., Krogan, N. J., Arbel-Eden, A., Greenblatt, J. F., Haber, J. E., and Shen, X. 2004. INO80 and gamma-H2AX interaction links ATP-dependent chromatin remodeling to DNA damage repair. Cell 119:767-775.

Murr, R., Loizou, J. I., Yang, Y. G., Cuenin, C., Li, H., Wang, Z. Q., and Herceg, Z. 2006. Histone acetylation by Trrap-Tip60 modulates loading of repair proteins and repair of DNA double-strand breaks. Nat Cell Biol 8:91-99.

Nampoothiri, V. K. 1998. P53 degradation by Mdm2 - A novel mechanism for regulation of p53 stability. Current Science 75:875-877.

Peng, G., Yim, E. K., Dai, H., Jackson, A. P., van der Burgt, I., Pan, M. R., Hu, R. Z., Li, K. Y., and Lin, S. Y. 2009. BRIT1/MCPH1 links chromatin remodelling to DNA damage response. Nature Cell Biology 11:865-U221.

Pestov, D. G., Strezoska, Z., and Lau, L. F. 2001. Evidence of p53-dependent cross-talk between ribosome biogenesis and the cell cycle: effects of nucleolar protein Bop1 on G(1)/S transition. Mol Cell Biol 21:4246-4255.

Peterson, C. L. 2002. Chromatin remodeling: Nucleosomes bulging at the seams. Current Biology 12:R245-R247.

Peterson, C. L., and Workman, J. L. 2000. Promoter targeting and chromatin remodeling by the SWI/SNF complex. Curr Opin Genet Dev 10:187-192.

Pharoah, P. D. P., Antoniou, A., Bobrow, M., Zimmern, R. L., Easton, D. F., and Ponder, B. A. J. 2002. Polygenic susceptibility to breast cancer and implications for prevention. Nature Genetics 31:33-36.

Pomerantz, J., Schreiber-Agus, N., Liegeois, N. J., Silverman, A., Alland, L., Chin, L., Potes, J., Chen, K., Orlow, I., Lee, H. W., Cordon-Cardo, C., and DePinho, R. A. 1998. The Ink4a tumor suppressor gene product, p19(Arf), interacts with MDM2 and neutralizes MDM2's inhibition of p53. Cell 92:713-723.

Ponder, B. A. J., Day, N. E., Easton, D. F., Pharoah, P. D. P., Lipscombe, J. M., Redman, K., Antoniou, A., Basham, V., Gregory, J., Gayther, S., Dunning, A., and Grp, A. S. 2000. Prevalence and penetrance of BRCA1 and BRCA2 mutations in a population-based series of breast cancer cases. British Journal of Cancer 83:1301-1308.

Rea, S., Eisenhaber, F., O'Carroll, D., Strahl, B., Sun, Z.W., Schmid, M. Opravil, M., Mechtler, K., Ponting, C.P., Allis, C.D., and Jenuwein, T. 2000. Regulation of chromatin structure by site-specific histone H3 methyltransferase. Nature 403:593-599.

Rogakou, E. P., Pilch, D. R., Orr, A. H., Ivanova,V. S., and Bonner, W. M. 1998. DNA double-stranded breaks induce histone H2AX phosphorylation on serine 139. J Biol Chem 273:5858-5868.

Ronai, Z. 2006. Balancing Mdm2 - a Daxx-HAUSP matter. Nat Cell Biol 8:790-791.

Rouse, J., and Jackson, S. P. 2002. Interfaces between the detection, signaling, and repair of DNA damage. Science 297:547-551.

Rubbi, C. P., and Milner, J. 2003. Disruption of the nucleolus mediates stabilization of p53 in response to DNA damage and other stresses. EMBO J 22:6068-6077.

Ryan, K. M., Phillips, A. C., and Vousden, K. H. 2001. Regulation and function of the p53 tumor suppressor protein. Current Opinion in Cell Biology 13:332-337.

Seo, Y. R., Fishel, M. L., Amundson, S., Kelley, M. R., and Smith, M. L. 2002. Implication of p53 in base excision DNA repair: in vivo evidence. Oncogene 21:731-737.

Sherr, C. J., and Weber, J. D. 2000. The ARF/p53 pathway. Current Opinion in Genetics & Development 10:94-99.

Shim, E. Y., Ma, J. L., Oum, J. H., Yanez, Y., and Lee, S. E. 2005. The yeast chromatin remodeler RSC complex facilitates end joining repair of DNA double-strand breaks. Mol Cell Biol 25:3934-3944.

Sjoblom, T., Jones, S., Wood, L. D., Parsons, D. W., Lin, J., Barber, T. D., Mandelker, D., Leary, R. J., Ptak, J., Silliman, N., Szabo, S., Buckhaults, P.,

Farrell, C., Meeh, P., Markowitz, S. D., Willis, J., Dawson, D., Willson, J. K., Gazdar, A. F., Hartigan, J., Wu, L., Liu, C., Parmigiani, G., Park, B. H., Bachman, K. E., Papadopoulos, N., Vogelstein, B., Kinzler, K. W., and Velculescu, V. E. 2006. The consensus coding sequences of human breast and colorectal cancers. Science 314:268-274.

Strahl, B. D., and Allis, C. D. 2000. The language of covalent histone modifications. Nature 403:41-45.

Stiff, T., O'Driscoll, M., Rief, N., Iwabuchi, K., Lobrich, M., and Jeggo, P. A. 2004. ATM and DNA-PK function redundantly to phosphorylate H2AX after exposure to ionizing radiation. Cancer Res 64:2390-2396.

Stommel, J. M., and Wahl, G. M. 2004. Accelerated MDM2 auto-degradation induced by DNA-damage kinases is required for p53 activation. EMBO J 23:1547-1556.

Stott, F. J., Bates, S., James, M. C., McConnell, B. B., Starborg, M., Brookes, S., Palmero, I., Ryan, K., Hara, E., Vousden, K. H., and Peters, G. 1998. The alternative product from the human CDKN2A locus, p14(ARF), participates in a regulatory feedback loop with p53 and MDM2. Embo Journal 17:5001-5014.

Thut, C. J., Goodrich, J. A., and Tjian, R. 1997. Repression of p53-mediated transcription by MDM2: a dual mechanism. Genes & Development 11:1974-1986.

Tsai, R. Y., and McKay, R. D. 2002. A nucleolar mechanism controlling cell proliferation in stem cells and cancer cells. Genes Dev 16:2991-3003.

Tsukuda, T., Fleming, A. B., Nickoloff, J. A., and Osley, M. A. 2005. Chromatin remodelling at a DNA double-strand break site in Saccharomyces cerevisiae. Nature 438:379-383.

Turner, B. M. 2002. Cellular memory and the histone code. Cell 111:285-291.

van Attikum, H., Fritsch, O., Hohn, B., and Gasser, S. M. 2004. Recruitment of the INO80 complex by H2A phosphorylation links ATP-dependent chromatin remodeling with DNA double-strand break repair. Cell 119:777-788.

van Attikum, H., and Gasser, S. M. 2009. Crosstalk between histone modifications during the DNA damage response. Trends in Cell Biology 19:207-217.

Vassilev, L. T., Vu, B. T., Graves, B., Carvajal, D., Podlaski, F., Filipovic, Z., Kong, N., Kammlott, U., Lukacs, C., Klein, C., Fotouhi, N., and Liu, E. A. 2004. In vivo activation of the p53 pathway by small-molecule antagonists of MDM2. Science 303:844-848.

Venkitaraman, A. R. 2001. Functions of BRCA1 and BRCA2 in the biological response to DNA damage. Journal of Cell Science 114:3591-3598.

Vogelstein, B., and Kinzler, K. W. 2001. Achilles' heel of cancer? Nature 412:865-866.

Vogelstein, B., and Kinzler, K. W. 2004. Cancer genes and the pathways they control. Nature Medicine 10:789-799.

Vogelstein, B., Lane, D., and Levine, A. J. 2000. Surfing the p53 network. Nature 408:307-310.

Vousden, K. H., and Lu, X. 2002. Live or let die: the cell's response to p53. Nat Rev Cancer 2:594-604.

Wallace, M., Worrall, E., Pettersson, S., Hupp, T. R., and Ball, K. L. 2006. Dual-site regulation of MDM2 E3-ubiquitin ligase activity. Molecular Cell 23:251-263.

Wood, L. D., Parsons, D. W., Jones, S., Lin, J., Sjoblom, T., Leary, R. J., Shen, D., Boca, S. M., Barber, T., Ptak, J., Silliman, N., Szabo, S., Dezso, Z., Ustyanksky, V., Nikolskaya, T., Nikolsky, Y., Karchin, R., Wilson, P. A., Kaminker, J. S., Zhang, Z. M., Croshaw, R., Willis, J., Dawson, D., Shipitsin, M., Willson, J. K. V., Sukumar, S., Polyak, K., Park, B. H., Pethiyagoda, C. L., Pant, P. V. K., Ballinger, D. G., Sparks, A. B., Hartigan, J., Smith, D. R., Suh, E., Papadopoulos, N., Buckhaults, P., Markowitz, S. D., Parmigiani, G., Kinzler, K. W., Velculescu, V. E., and Vogelstein, B. 2007. The genomic landscapes of human breast and colorectal cancers. Science 318:1108-1113.

Wooster, R., and Weber, B. L. 2003. Breast and ovarian cancer. New England Journal of Medicine 348:2339-2347.

Xirodimas, D., Saville, M. K., Edling, C., Lane, D. P., and Lain, S. 2001. Different effects of p14ARF on the levels of ubiquitinated p53 and Mdm2 in vivo. Oncogene 20:4972-4983.

Xue, L., Zhou, B., Liu, X., Heung, Y., Chau, J., Chu, E., Li, S., Jiang, C., Un, F., and Yen, Y. 2007. Ribonucleotide reductase small subunit p53R2 facilitates p21 induction of G1 arrest under UV irradiation. Cancer Res 67:16-21.

Xue, W., Zender, L., Miething, C., Dickins, R. A., Hernando, E., Krizhanovsky, V., Cordon-Cardo, C., and Lowe, S. W. 2007. Senescence and tumour clearance is triggered by p53 restoration in murine liver carcinomas. Nature 445:656-660.

Yang, X. J. 2004. The diverse superfamily of lysine acetyltransferases and their roles in leukemia and other diseases. Nucleic Acids Research 32:959-976.

Yun, J. P., Chew, E. C., Liew, C. T., Chan, J. Y. H., Jin, M. L., Ding, M. X., Fai, Y. H., Li, H. K. R., Liang, X. M., and Wu, Q. L. 2003. Nucleophosmin/B23 is a proliferate shuttle protein associated with nuclear matrix. Journal of Cellular Biochemistry 90:1140-1148.

Zhang, Y. P., Xiong, Y., and Yarbrough, W. G. 1998. ARF promotes MDM2 degradation and stabilizes p53: ARF-INK4a locus deletion impairs both the Rb and p53 tumor suppression pathways. Cell 92:725-734.

Ziv, Y., Bielopolski, D., Galanty, Y., Lukas, C., Taya, Y., Schultz, D. C., Lukas, J., Bekker-Jensen, S., Bartek, J., and Shiloh, Y.Y 2006. Chromatin relaxation in response to DNA double-strand breaks is modulated by a novel ATM- and KAP-1 dependent pathway. Nat Cell Biol 8:870-876.

VITA

Ruozhen Hu was born at Yongkang, China on March 4, 1982, the daughter of Zuying Hu and Lanying Tong. After completing her high school at The Second High School of Yongkang, Zhejiang, China in 1998, she entered College of Life Science at Zhejiang University in Hangzhou, China. She received the degree of Bachelor of Science with a major in biotechnology from Zhejiang University in July, 2002. For the next three years, she entered Dr. Jian-Zhong Shao's lab to study embryonic stem cells and received the degree of Master of Science with a major in cell biology from Zhejiang University in July 2005. Then she enrolled in the Interdisciplinary program in Biomedical Sciences at University of Florida and worked on hematopoietic stem cell research under the supervising of Dr. Edward Scott. In January 2007, she entered The University of Texas Health Science Center at Houston Graduate School of Biomedical Sciences and The University of MD Anderson Cancer Center (Advisor, Shiaw-Yih Lin, Ph.D.).

Permanent address:

Apt 402, Building 2, Lane 3,

Gongyuanli, Yongkang,

Zhejiang, China, 321300.